On the stability of the Atlantic Meridional Overturning Circulation and its climate impact during Late Neogene

Dissertation zur Erlanggung des
akademischen Grades eines Doktors
der Naturwissenschaften

Dr. rer. Nat.

im Fachbereich 5 Geowissenschaften
der Universität Bremen

vorgelegt von:

Xiao Zhang

Bremen, Juli 2014

Erklärung

Name: Xiao Zhang

Anschrift: Wilhelm Liebknecht Strasse 8, 28329 Bremen

Hiermit versichere ich, dass ich

1. die Arbeit ohne unerlaubte fremde Hilfe angefertige habe,

2. keine anderen als die von mir angegebenen Quellen und Hilfsmittel benutzt habe und

3. die den benutzten Werken wörtlich oder inhaltlich entnommenen Stellen als solche kenntlich gemacht habe.

Bremen, Juli 2014 (Unterschrift) 

Gutachter

Prof. Dr. Michael Schulz

Prof. Dr. Gerrit Lohmann

Acknowledgements

My Ph.D project was funded by the DFG (Deutsche Forschungsgemeinschaft) through the DFG-Research Center and MARUM (Zentrum für Marine Umweltwissenshaften) Project OC3. The project was carried out in department of Geoscience of University of Bremen through DFG Research Center/Excellence Cluster “The Ocean in the Earth System”.

I would like to thank professor Michael Schulz, who is also my supervisor for his consistently constructive suggestions. These ideas always open my mind, give me new angles to review the problem and inspire me to work harder and smarter. I really admire your rich knowledge of science and hard working spirit. Secondly, I want to thank Dr. Matthias Prange. You always cheer me up with your laughter (I noticed that even before I met you in person, during the phone interview) and positive attitudes. More importantly, thank you for the entire scientific brainstorm and help with my manuscripts. You always have smart ideas.

Surely I also need to thank all the members in the Geo-modeling group. Andreas, thank your for making coffee for us and thank you for all the work you have done for us as an system administrator. You are always very kind and extremely helpful. Takasumi, thanks for the Japanese lessons. You are also very patient and you know how I love Japanese songs, which colored my life. All the girls in the group, thanks for bearing with my sometimes somehow strange silence. After all I am not a talkative person but you girls can always bring me joy and support.

Thank you all the co-authors. Your contributions and suggestions for the manuscripts are necessary and constructive, which make the manuscript complete and precious.

At last, I sincerely thank my family and friends in China, in the US and in Japan for your support and unconditional love. I can always count on you and you ask for nothing back.

Lots of love

X

Abstract

This thesis focused on the Atlantic Meridional Overturning Circulation (AMOC) stability and global climate responses of an altered AMOC in the late Neogene by performing computer simulations, using both intermediate complexity climate models and state-of-the-art coupled climate models. Two time slices were studied: 1) 38 ka BP (kilo years before present), during Heinrich event 4, and 2) around 4-5 million years ago, when the Panamanian Seaway finally gradually closed.

The AMOC is one of the most important climate systems modulating the world climate due to the significant amount of oceanic transport of heat, carbon and nutrients. Understanding the AMOC stability behaviour is essential to investigate climate in the past and present as well as possible changes in the future. The circulation strength changes were suggested to have an association with observed millennial abrupt climate oscillations during Marine Isotope Stage 3 (MIS3, 57-29 ka BP and tropical Pacific thermocline variation during the Pliocene. A strong/weak circulation is related with a mild interstadial/cold stadial climate. The large amount of freshwater flux at the ocean surface provided by melted icebergs during warm interstadial in the North Atlantic has been argued to potentially be able to induce this AMOC strength change, which possibly triggered an abrupt climate oscillation process; many conceptual models have explained the occurrences of abrupt climate changes based on multiple equilibria of the AMOC. More complex models, on the other hand, produced different results in the AMOC stability property based on freshwater hosing experiments. State-of-the-art models have higher possibilities to produce a monostable AMOC, whereas most inter-complexity models have resulted in an AMOC with multiple equilibria. One of the deficiencies of these model studies has been that most of the simulations were run with the present day background climate even though the AMOC might have had different stability properties during the glacial period compared to the present day.

Therefore, this thesis firstly bridged the simulation gap of the AMOC performed by a state-of-the-art coupled climate model with 38 ka BP glacial boundary conditions. The AMOC stability and how its variation affected global climate were systematically studied in a set of freshwater forcing experiments. It was demonstrated that the AMOC is in a monostable mode during cold stadials and external freshwater forcing was essential to contain the AMOC 'off' mode. The 38 ka BP climate is unstable against a small amount of freshwater flux (±0.02 Sverdrup). Threshold behaviour was observed in both Greenland temperature and Northern Hemisphere ice cover with regard to the AMOC maximum

in the simulations, which indicates a system transition between a mild interstadial state and a cold stadial state. Experiment results suggested that the Greenland temperature was mainly controlled by Northern Hemisphere sea ice, since the simulated Greenland temperature change magnitude was in line with the observations, which was not shown in previous model studies using realistic freshwater input. Strong feedback from the sea ice and surface wind played an important role in this climate shift and a strong subsurface warming was also observed in the simulation, as indicated by proxy records. These conclusions demonstrate the importance of the background climate in glacial climate simulation, especially with regard to AMOC studies (Chapter 2). Moreover, the global imprint of the AMOC change was also investigated in detail. Applying the Analysis of Variances (ANOVA) statistical method, several locations with high sensitivity to the AMOC strength change were captured at the surface, e.g. the Southern Indian Ocean and the North Atlantic. In these areas, a linear relationship between the surface temperature or precipitation and the AMOC maximum was established, hence these locations are ideal for AMOC reconstruction. Subsurface layers of the ocean showed different sensitivities to freshwater forcing; the North Atlantic generally showed a high linear response from the surface to the deep ocean, whereas linear regression was not visible in the northern and tropical Pacific intermediate layers. More importantly, the changes in the AMOC strength between interstadial and stadial/Heinrich stadial states were also quantified based on both climate models and proxy records. It was estimated the AMOC experienced a deduction of 9.2 ±1.2 Sv of its circulation strength from warm interstadials to cold stadials and this decrease in vigour was stronger from interstadial states to Heinrich stadials, with a larger estimated uncertainty (Chapter 3).

Sediment records from the North Pacific show a shoaling of the thermocline, as well as AMOC intensification as a response to the closure of the Panamanian gateway during the early Pliocene. In order to study this process, a comparison of model results from 11 sensitivity tests performed by seven different climate models with independent setups was undertaken. The results revealed that in all models, the closure of the Panamanian Seaway could lead to an enhancement of the AMOC and also causes a shoaling of the equatorial Pacific thermocline. The change in the thermocline depth in the Equator is then preconditioned to the present Pacific cold tongue state. Wind stress feedback was able to amplify this process. With the presence of dynamic atmosphere model, a linear relationship between the AMOC change and the thermocline shoaling has been demonstrated (Chapter 4).

Zusammenfassung

Schwerpunkt der vorliegenden Dissertation ist die Stabilität der atlantischen meridionalen Umwälzzirkulation (AMOC) während des marinen Sauerstoffisotopenstadiums 3 (MIS3) und die Reaktion des globalen Klimas auf eine Änderung der AMOC während des späten Neogens unter Verwendung der numerischen Klimamodellierung, basierend auf Klimamodellen mittlerer (EMIC) und hoher Komplexität. Es werden die Ergebnisse von zwei Zeitintervallen analysiert: 1) 38 ka BP (Tausend Jahre vor heute), während des stärksten Heinrich-Ereignisses im MIS3 (Heinrich Ereignis 4) und 2) 4-5 Ma (Millionen Jahre vor heute), während der Bildung des Isthmus von Panama.
Aufgrund des bedeutenden Wärme- und Stofftransports und die damit einhergehende Beeinflussung auf das globale Klima ist die AMOC ein wichtiger Bestandteil des Klimasystems. Um die Klimaveränderungen in der Vergangenheit, Gegenwart und in der Zukunft zu verstehen, ist es notwendig die Stabilität der AMOC zu ermitteln. Es wird angenommen, dass Veränderungen in der Stärke der AMOC mit den Ereignissen abrupter Klimawechsel während des MIS 3 (57-29 ka BP) und mit der Änderung in der tropischen Thermokline des Pazifischen Ozeans im Pliozän einhergehen. Eine starke Zirkulation steht im Zusammenhang mit einem milden Interstadial, während eine schwache Zirkulation mit einem kalten Stadial in Verbindung gebracht wird. Ein großer Zufluss von Süßwasser in Form von schmelzenden Eisbergen im nordatlantischen Ozean führte vermutlich zu einer Veränderung in der Stärke der AMOC und löste somit wahrscheinlich einen abrupten Klimawechsel aus. Einerseits zeigen vereinfachte Klimamodelle, dass das Auftreten dieser abrupten Klimaschwankungen vermutlich auf die multiplen Gleichgewichtszustände der AMOC zurückgeführt werden kann. Andererseits werden in Klimamodellen höherer Komplexität mithilfe von sogenannten Süßwasser-Simulationen gegensätzliche Ergebnisse in Bezug auf die Stabilität der AMOC aufgezeigt. Die komplexeren Klimamodelle hervorbringen eine monostabile AMOC, während die Modelle mittlerer Komplexität eine multistabile AMOC aufweisen. Die größte Unzulänglichkeit dieser Simulationen ist der Zustand, dass die meisten Experimente unter Berücksichtigung verschiedener AMOC Stabilitäten im abweichenden Klima (z.B. größere Meereisbedeckung während eines kalten Klimas) mit dem heutigen Hintergrundklima durchgeführt wurden.
Daher füllte diese Dissertation diese Lücke aufgrund der Durchführung von AMOC Simulationen anhand von Klimamodellen mit den glazialen Randbedingungen vor 38 ka BP. Die AMOC Stabilität und wie ihre Veränderung sich auf das globale Klima auswirkt, wurde systematisch anhand von Süßwasser-Experimenten untersucht. Es zeigte sich, dass die AMOC sich in einem monostabilen Zustand während eines kalten Stadials befindet und dass der externe Süßwasserzufluss essentiell

war um die AMOC zu kontrollieren. Während des Klimas vor 38 ka BP war die AMOC besonders instabil gegen kleine Süßwasserzuflüsse (± 0,02 Sv). Die Beobachtung eines Grenzwertverhaltens sowohl in der Eisbedeckung auf der nördlichen Hemisphäre als auch in den Temperaturen in Grönland in Bezug auf die AMOC-Maxima deutet einen Übergang des Klimasystems zwischen einem milden Interstadial und einem kalten Stadial an. Ergebnisse verschiedener Experimente zeigten, dass die Temperatur in Grönland hauptsächlich von der Meereisbedeckung der nördlichen Hemisphäre gesteuert wird, denn die simulierte Größenordnung der Grönland-Wintertemperaturänderung ist im Einklang mit Beobachtungen, was in früheren Modellstudien mit einem realistischen Süßwassereintrag nicht gezeigt wurde. Die starke Rückkopplung des Meereises und der Oberflächenwinde spielte eine wichtige Rolle während der Klimaveränderung und es zeigte sich eine Erwärmung des tieferen Ozeans, die auch von Proxy-Daten angedeutet wird. Diese Schlussfolgerungen demonstrieren die Bedeutung des Hintergrundklimas in eiszeitlichen Klimasimulationen, insbesondere mit Hinblick auf Untersuchungen der Stabilität der atlantischen meridionalen Umwälzzirkulation (Kapitel 2).

Darüber hinaus wurde auch der globale Einfluss der AMOC-Veränderungen in allen Einzelheiten untersucht. Die Regionen mit einer hohen Empfindlichkeit gegenüber AMOC-Veränderungen wurden durch die sogenannte Varianzanalyse (ANOVA) erfasst, z.B. die Labradorsee, der südindische Ozean. In diesen Regionen konnte ein linearer Zusammenhang zwischen der Oberflächentemperatur bzw. Niederschlagsmenge und der AMOC-Maxima hergestellt werden. Daher eignen sich insbesondere diese Gebiete zur Untersuchung für die Rekonstruktion der AMOC. Tiefere Schichten des Ozeans zeigten unterschiedliche Empfindlichkeiten gegenüber einem Süßwasserzufluss. Der Nordatlantik zeigte eine generelle hohe Linearität von der Wasseroberfläche bis in den tiefen Ozean wobei diese Linearität nicht in den mittleren Ozeanschichten des nördlichen und tropischen Pazifiks beobachtet werden konnte. Noch wichtiger ist, wurden die Änderungen in der AMOC zwischen Interstadial und Stadial / Heinrich Stadial Staaten auch basierend auf beiden Klimamodelle und Proxy-Datensätze quantifiziert. Es wurde geschätzt, dass die AMOC einen Abschwächer (9.2 ± 1.2 Sv) von Interstadial bis Stadial hat und diese Abnahme stärker von Interstadial bis Heinrich Stadial war (Kapitel 3).

Es gibt eine simulierte Verstärkung der AMOC aufgrund der Schließung des Panama-Seeweges während des frühen Pliozäns hin. Um diesen Prozess näher zu untersuchen, wurden die Modellergebnisse von sieben Klimamodellen mit unabhängigen Einstellungen verglichen. Die Ergebnisse zeigten, dass die Bildung des Isthmus von Panama zu einer Verstärkung der AMOC und einer weiteren Abflachung der Thermokline im äquatorialen pazifischen Ozean führte. Die Veränderung in der Thermoklinentiefe war dann die Voraussetzung für die Bildung der heutigen ostpazifischen Kältezunge. Dieser Prozess wurde verstärkt durch die Rückkopplung des

Oberflächenwindes. Bei Abwesenheit eines dynamischen Atmosphärenmodells konnte ein linearer Zusammenhang zwischen einer AMOC-Änderung und der Abflachung der Thermokline gezeigt werden (Kapitel 4).

Table of Contents

Chapter 1

1. Introduction

Atlantic Meridional Overturning Circulation (AMOC) plays a major role in global climate manipulation and it has experienced strength alterations that are linked to abrupt climate change during the last glacial maximum. The following thesis is focused on analysing the AMOC stability and its climate impact in a fully coupled state-of-the-art climate model, during 1) the Marine Isotope Stage 3 (MIS3) induced by freshwater perturbation in the North Atlantic and 2) the early Pliocene (ca. 5 – 4 million years ago) caused by the Panamanian Seaway closure.

1.1 Stability of the AMOC --- its behaviour

The AMOC is a closed ocean circulation cell spanning both hemispheres, generally consisting of four phases: 1) deep water formation areas, where water becomes denser and sinks into the deep ocean, 2) deep currents transport denser water to low latitudes, 3) upwelling processes which bring deep water to the surface, and finally 4) the surface current closes the loop by taking water back to high latitude water sinking areas. There are two major deep water formation cells involved in the AMOC, the North Atlantic Deep Water Formation (NADW) and the Antarctic Bottom Water (AABW). The strength of the AMOC, usually defined by the maximum of the overturning stream function, is estimated to be 15±2 Sv (1Sv = $10^6 m^3/s$) (Ganaschaud and Wunsch 2000) at present and its strength is suggested to be sensitive to the surface water budget (e.g. Stocker and Wright 1991).

Previous modelling studies, from very simple box models (e.g. Stommel 1961) to general ocean circulation models (e.g. Bryan 1986; Marotzke and Willebrand 1991) and finally to coupled atmosphere-ocean models (Manabe and Stouffer 1988) have shown that the AMOC is a highly non-linearity system that shows hysteresis behaviour and might have multiple equilibrium states as a response to external forcing (e.g. Broecker et al. 1985*;* Stocker and Wright 1991; Mikolajewicz and Maier-Reimer 1994), for instance surface freshwater inflow in the North Atlantic. There is a threshold point whereby if the freshwater inflow does not reach this point, the NADW will be active and in a stable 'on' mode, whereas in the other case, if freshwater inflow passes the threshold, the NADW will be greatly reduced, and therefore in a stable 'off' mode. This bistable regime is clearly reflected in the

hysteresis graph (Fig.1, Stocker and Wright 1991). The star indicates the present day AMOC state. The upper branch of the curve represents the 'on' mode with active NADW, which can become unstable and switch abruptly to a 'off' mode when the net freshwater flux from the Atlantic to the Pacific through the atmosphere is reduced to less that 0.3 Sv. The lower branch ('off' mode), with active deep water formation only in the Southern Ocean, is also able to switch to the 'on' mode when this freshwater flux exceeds 0.36 Sv. However, it should be noted that hysteresis behaviour should not be interpreted as a sign of existence of bistable states in the AMOC; only an instant recovery of the AMOC after the freshwater flux is terminated implies a monostable circulation. Climate models could show a hysteresis response from the AMOC while it is actually in a monostable regime.

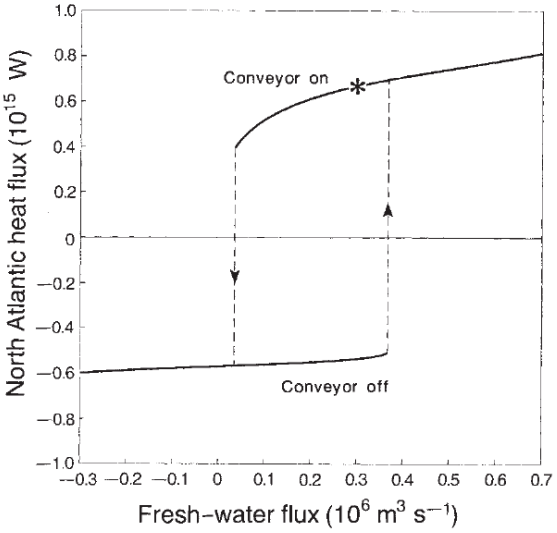

Figure. 1 Hysteresis Curve of the AMOC as a response to freshwater flux

In order to further understand the AMOC stability properties, several model inter-comparison studies have been done, reaching different conclusions. Rahmstorf et al. (2005) compared model results from eleven different atmosphere-ocean coupled climate models, including intermediate complexity models, ocean models coupled with intermediate complexity atmosphere models, general ocean circulation (GCM) models coupled with simplified atmospheric models and coarse-resolution ocean GCMs coupled with simplified atmosphere models. All of these models have shown similar hysteresis behaviour when freshwater perturbation is added at the North Atlantic and the AMOC was found to be in a bistable mode in seven of the models, whereas in the other four models it is in a mono-stable regime. Stouffer et al. (2006) extended the stability study of the AMOC by comparing model results in a set of coupled climate models, including fully coupled atmosphere-ocean general circulation models

(AOGCMs), which were not included by Rahmstorf et al. (2005). They concluded that there was no significant difference in the AMOC activity and climate changes as a response to freshwater flux between Earth system Models of Intermediate Complexity (EMICs) and AOGCMs. Though the AMOC response time varied in the different models, they all demonstrated a reduced AMOC and it recovered instantly after the freshwater perturbation was eliminated, implying that the 'off' mode of the AMOC is not stable and therefore the AMOC is in a monostable state. Most recently, half (15 out of 30) of the models in the 5th phase of the Coupled Model Inter-comparison Project (CMIP5, Taylor et al. 2012) as well as an inter-comparison project among EMICs showed that the AMOC was in a bistable or multiple stable mode and it is unlikely the AMOC will experience abrupt changes due to global warming (Weaver et al. 2012). However, Weaver et al. (2012) did not include the effects of external freshwater forcing via ice sheet melting, which occurred during abrupt climate change during the last glacial and is closely related to AMOC strength change (e.g. Bond et al. 1992; Hemming 2004). Instead, they examined the AMOC response to different Representative Concentration Pathways.

These experiments were all concentrated on the present day AMOC and, though many models have shown hysteresis response and multiple equilibria, large uncertainties still exist in these model studies. As Ganopolski and Rahmstorf (2001) speculated, the AMOC might have different stability behaviours during the cold glacial compared to the present day. In other words, the AMOC reacted differently to freshwater flux during the last glacial. They concluded that the AMOC was more sensitive to freshwater discharge in the North Atlantic during the last glacial than under present day conditions due to the different configuration of the convection sites. In addition, Bitz et al. (2007) showed that the AMOC recovery following a freshwater input was slower during the last glacial maximum than for modern climates. Furthermore, current models have been argued to be too stable to simulate the AMOC stability (e.g. Hofmann and Rahmstorf 2009; Drijfhout et al. 2011), resulting in a monostable AMOC. Owing to these controversies, it is necessary to extend AMOC stability model study to include the glacial background climate.

1.2 Stability of the AMOC --- its controlling mechanisms

In order to further investigate the AMOC stability properties, it is essential to understand the driving process of the AMOC in the first place. There are two main candidates for the circulation driver; the first one is the traditional thermohaline driven process and the other is wind-induced Ekman upwelling.

The traditional thermohaline driven theory was firstly tested in a two box model (representing the pole and the Equator) by Stommel (1961) who also speculated that the AMOC might have two stable states. The solution of this box model showed that water flow in the system depends either on temperature (thermo) or density (hacline) gradient. In the first stable mode, water flows from cold boxes to warm boxes, indicating that temperature differences dominate density differences and deep water formation occurs in polar areas. On the other hand, the other stable mode is density dominated, water flows from warm vessels to cold vessels, featuring equatorial deep water formation. This theory, however, was not further investigated until twenty years later; Rooth (1982) improved Stommel's model by adding another polar box in the model and suggesting that an equatorial symmetric circulation was not stable and would eventually develop into a single pole-to-pole cell with asymmetric surface forcing. These box models were not tested in general circulation models until the work of Bryan (1986). He confirmed in his experiments that, driven by symmetric forcing with symmetrical geometry, it is still possible to have three equilibrium solutions with small asymmetric salinity perturbations in either the northern polar box or the southern polar box. However, it should be mentioned that when Stommel (1961) and Bryan (1986) conceptually analysed the stability of the thermohaline circulation, it was still not understood that the original source of the North Atlantic Deep Water formation is the Southern Ocean. It is Gorden (1986) who theoretically proposed that warm thermocline layer water, which compensated the loss of surface water in the North Atlantic due to deep water formation, was mainly formed in the Southern Ocean due to upwelling.

In order to sustain a stable circulation, an extra energy source is required to compensate for energy loss in the friction process. However, solar forcing and geothermal heating are not able to provide enough energy (Huang and Wang 2003; Huang 1999). In thermohaline driven theory, diapycnal mixing (turbulent mixing across equal density surfaces) generated by surface wind stress, tides and heat flux from the atmosphere and the ocean floor provides energy sources for the circulation. Internal ocean waves are generated by both surface buoyancy fluxes due to surface heat flux and interaction between tidal forces and the ocean floor. These internal waves then create turbulent mixing that raises deep-water mass in the low latitudes to the surface. Afterwards, upper layer water is advected towards the North Atlantic, where it again sinks into the deep ocean due to atmospheric cooling and vertical mixing (Munk and Wunsch 1998). Interior heat flux is required in this diapycnal mixing process and stronger vertical mixing could enhance the overturning rate and transportation of heat to the poles (Bryan 1986).

Motivated by this mechanism, freshwater flux by the AMOC into the South Atlantic (Fov) at around 35°S was suggested to be an indicator of AMOC stability in many of the model studies (e.g. de Vries and We 2005; Huisman et al. 2010). If Fov > 0, the AMOC exports salt and the system is in a monstable state, whereas if Fov < 0 the AMOC exports freshwater and it is in a multiple equilibrium state. However, studies have also argued that Fov is not always a good indicator (Sijp et al. 2012). Model bias could have a large impact on the AMOC sensitivity to freshwater flux (Jackson 2013) and state-of-the-art GCMs have different Fov signs in present day simulations (Weaver et al. 2012); this issue again demonstrates the importance of the mean climate state in the simulation. Liu et al. (2013) proposed another stability indicator for the AMOC based on both Fov and the AMOC strength, since paleo-observations have shown that the AMOC is never in a perfect equilibria (e.g. McManus et al. 2004) and it is a slowly evolving circulation. They suggested that the AMOC is in a monostable state at both present day and the last glacial maximum by performing simulations in a state-of-the-art climate model. In their simulations, strong hysteresis behaviour from the AMOC was presented in response to freshwater forcing. A similar Bering Strait effect was also shown by Hu et al. (2012).

The thermohaline driven theory was challenged by the 'Drake Passage effect' (Toggweiler and Samuels 1995; Kuhlbrodt et al. 2007), which argues that the magnitude of NADW outflow from the Atlantic basic is dictated by the wind stress in the Drake Passage latitude band. In this case, surface winds directly transfer large scale kinetic energy into the circulation. The surface wind stress induced by Ekman divergence in the Drake Passage latitude band (app. 50°S) forces approximately 15 Sv deep water to the surface and transports it north to low latitudes (Hellerman and Rosenstein 1983); the only place in the Northern Hemisphere where this large amount of surface water can be returned to the deep ocean is the North Atlantic, where the NADW is formed. Later, Toggweiler and Samuels (1998) applied formal energy analysis to their general circulation models and showed that a wind-driven overturning circulation linked with the Antarctic Circumpolar Current could exist without vertical mixing and a lack of energy from the surface buoyancy forces. Thus, an AMOC controlled by 'Drake Passage effect' is solely wind-controlled and independent of vertical mixing as well as upwelling to the thermocline. Such results implied that stronger westerly circumpolar winds would result in more deep water formation in the Northern Hemisphere. This wind-driven theory does not involve diapycnal mixing but only isopycnal upwelling and was supported by both model study and observations. For instance, upwelling in the Southern Ocean was shown in model simulations (e.g Döös and Coward 1997) and radiocarbon data (Toggweiler and Samuels 1993; Gnanadesikan and Toggweiler 1999),

while an asymmetric distribution of $\Delta^{14}C$ due to this hemisphere coupling was also proposed (Toggweiler and Samuels 1993).

In reality, it is possible that both of these two mechanisms play a role in the AMOC driving process (e.g. Sloyan and Rintoul 2001). If only considering the first possibility, a larger turbulent diffusion coefficient is required in the ocean interior, and there is significant uncertainty about the estimated value of available energy from turbulent mixing to keep an active circulation. On the other hand, in extreme cases without turbulent mixing, water mass transport from the Southern Ocean to the North Atlantic also largely depends on the Southern Ocean density structure and a large volume of water mass from the Southern Ocean does not reach the North Atlantic. However, the most important aspect of this thesis is to explore different AMOC sensitivities to surface forcing, which could be led by distinctive driving mechanisms as discussed in the next chapter.

1.3 Stability of the AMOC --- its climate signal

1.3.1 Observations of abrupt climate changes

Ice-rafted detritus (IRD) data recorded several lithic fragment percentage peaks in the sediment cores from the North Atlantic (e.g. Heinrich 1988; Labeyrie et al. 1999; Hemming and Hajdas 2003) during the last glacial. Six anomalous peaks in these drops of IRD events were entitled Heinrich Events (HEs) between 60 – 16 kyr. By locating the margin of Heinrich layers in the IRD belt based on these records, Bond et al. (1992) suggested that HEs have a cycle of app. 7000 years. The other clear evidence of abrupt changes was shown in the Greenland ice cores (e.g. Dansgaard et al. 1993; Grootes et al. 1993) from Greenland Ice Sheet Projects 1 and 2 (GISP and GISP2). These so called Dansgaard-Oeschger (D-O) events were suggested to have a cycle of app. 1500 years and they were characterised by an abrupt 8-16°C warming (mild interstadials) within a decade followed by slower cooling over centuries (North Greenland Ice Core Project Members 2004) back to a cold state (cold stadials). Despite the fact that HEs and D-O events have different climate fingerprints and timescales, they clearly cannot be separated from each other. One clear linkage reflected in proxy data is that HEs always occur during the cold stadials of the D-O events and are followed by a particularly warm D-O event (Bond et al. 1992).

These abrupt climate oscillations were closely related to the AMOC strength and NADW reduction was shown during the colder period in independent approaches. For instance, grainsize data from the Northeast Atlantic showed a weaker deep flow during HE1 (McCave et al. 1995), which also indicated surface cooling. Carbon isotopes from benthic foraminifera data in Keigwin and Lehman (1994) as well as Elliot et al. (2002) presented the lowest NADW production rate during H1. Although $^{231}Pa/^{230}Th$ data has a high uncertainty, it also indicated that NADW decreased during HEs (e.g. McManus et al. 2004; Gherardi et al. 2005). Both horizontal heat/salt advective and vertical convective feedbacks were involved in this AMOC strength variation (Rahmstorf and Willebrand 1995). An interruption of vertical convection induced by surface freshwater reduces surface heat loss and accumulated freshwater at the ocean surface; hence, the convection remains stopped and the AMOC possibly collapses. While convective feedback occurs mostly at the high latitude of the North Atlantic, advective feedback has a larger spatial scale. In these circumstances, a small amount of surface freshwater flux (e.g. increased precipitation), can reduce the AMOC slightly and a weakened AMOC further favours this freshening since precipitation always exceeds evaporation at the high latitude of the North Atlantic. The AMOC will only decrease to zero when freshwater input exceeds the threshold in the system; otherwise, it will remain active.

As the AMOC strength change greatly affects the heat transport between the two hemispheres, abrupt oscillations signals are mostly visible in polar ice and North Atlantic records. The clearest records are the previously mentioned GISP and GISP2 datasets. Other examples include: $\delta^{18}O$ and the dramatic drop in the abundance of planktonic foraminiferal species during the HEs inside the IRD zone, indicating a decrease in both sea surface temperature and salinity (e.g. Maslin et al. 1995; Zahn et al. 1997) due to melted sea ice. The same conclusion has also drawn by de Vernal et al. (2000), who further showed that the coldest period during the last glacial corresponded to HEs with extensive sea ice at the North Atlantic. A strong resemblance between GISP2 data and the $\delta^{18}O$ record from Irminger Sea cores was shown by van Kreveld et al. (2000); this could also be interpreted as an AMOC strength change.

The fingerprint of these abrupt changes is not constrained to Greenland and the North Atlantic but is present worldwide. However, HEs signals only stand out in a few of these records, for instance in the Northern Hemisphere, temperature records from pollen data at Lake Tulane (Grimm et al. 1993; 2006), C37 alkenone from the Alaboran Sea (Cacho et al. 1999), and median grain sizes from the Chinese loess plateau (Porter and An 1995). There are also several tropical records showed HEs

fingerprints, e.g. Ti–Ca and Fe–Ca ratios from a sediment core at the Brazil margin (Arz et al. 1998) and organic carbon data from the Arabian Sea (Schulz et al. 1998).

D-O events signals are more widespread signals and have more correspondence than HEs. Derived SST data from the Bermuda Rise record shows high correspondence with Greenland core records (Sachs and Lehman 1999). The Greenland record was also suggested to have a link with deep North Atlantic temperatures (Skinner and Elderfield 2007) and the Santa Barbara Basin (Hendy et al. 2002), which is related to the last deglaciation. Peterson et al. (2000) showed drier conditions during the cold stadials and they argued that ITCZ in the tropical Pacific moved southward and is related to an El-Nino pattern of sea surface temperature change. Several records have connected Greenland temperature with the Asian monsoon system; for instance, the Hulu Cave record (Wang et al. 2001) demonstrates a positive relationship between summer/winter precipitation ratio and Greenland temperatures in Eastern China. Arabian Sea sediment records (Schulz et al. 1998) show higher productivity due to stronger upwelling and stronger monsoons during mild interstadials. The variation in the monsoon system as a response to the AMOC strength change has also been investigated in other modelling and proxy studies, showing that a reduction of the AMOC results in a weaker wind system (e.g. Lachniet et al. 2013; Sun et al. 2011). Voelker (2002) provided an overview of 183 terrestrial, oceanic and ice records with different resolutions spanning MIS3; most of these records are located in the Northern Hemisphere and half of them show D-O type oscillations.

Although data from the Southern Hemisphere is quite sparse, it still shows a strong one-to-one coupling between Antarctica warming and Greenland cooling (e.g. EPICA Community Members 2006; Blunier and Brook 2001). Benthic $\delta^{18}O$ from Greenland strongly resembled temperature records from the Antarctica, which changed as a function of ice volume (Shackleton et al. 2000). This inter-hemisphere coupling is argued to be due to a weakened AMOC that transports less heat to the North. This pattern is recognised as a bipolar seesaw (e.g. Stocker 1998; Broecker 1998), which has also been observed in many modelling studies. It should also be mentioned that alongside surface temperature the NADW and AABW also have a 'seesaw' effect (Seidov and Maslin 2001). A collapsed NADW corresponds with a stronger AABW, leading to southward heat transpiration and vice versa.

1.3.2 Mechanisms of abrupt climate changes

Many attempts have been made to explore the mechanisms of these abrupt changes. The first process suggested to produce abrupt climate scenario is related to the AMOC strength change, e.g. a weak/strong circulation is related to cold stadials/mild interstadials. However, there are different hypothesis about how this change occurs.

Since observations have shown surface melting events at the North Atlantic occurred before abrupt climate changes as previously stated, direct freshwater discharge from the Lawrence ice sheet is the most commonly discussed trigger for the AMOC strength change; this might also be accompanied by an AMOC mode exchange (e.g. Rahmstorf 1995; Alley et al. 1999). This external freshwater inflow reduces surface water density, slows down the vertical branch of the AMOC and later the whole circulation, decreases vertical and horizontal heat and water mass transport and eventually leads to sea surface cooling in the North Atlantic and Greenland. In order to investigate this hypothesis, numerous freshwater hosing experiments were done with different climate model classes and as shown in Chapter 1 the results are largely model dependent. Many of these models have shown a rapid change of the AMOC as response to freshwater perturbation (e.g. Stouffer et al. 2006; Rind et al. 2001a). However, whether the AMOC wound recovers after the freshwater forcing is terminated remains in doubt due to the fact that individual models have distinctive AMOC stability properties. Greenhouse Gas concentration alone could also lead to AMOC strength change; Gregory et al. (2005) compared AMOC responses to climate change caused by increasing atmospheric CO2 concentration from 11 different climate models. All the models in the project, including both AOGCMs and EMICs, showed a weakened (but not collapsed) AMOC as a response to surface heat flux change caused by atmospheric CO_2 concentration increase other than surface water flux and there was evidence of no significant surface cooling.

As Wunsch (2006) argued, the AMOC change alone cannot explain these abrupt climate oscillations. The second potential mechanism of the abrupt climate swings is Northern Hemisphere sea ice. Gildor and Tziperman (2003) argued that abrupt climate changes could occur even without AMOC variations; it is the sea ice cover change which induces strong albedo feedback and affects evaporation, and storm tracking in the North Atlantic results in abrupt climate oscillations. Kaspi et al. (2004) later used a box model to explain that sea ice in the North Atlantic has three distinctive states during the HEs cycle. Initiated as a moderate cold state, ice sheets kept growing gradually. When a temperature threshold was reached, the ice sheets started melting and discharged freshwater into the North Atlantic, which weakened the AMOC. A decreased AMOC drew less heat to the North Atlantic and the

sea ice grew to its maximum extension due to higher albedo and less heat exchange between the atmosphere and the ocean. However, there is another internal limit in the ice system that ended the melting process. When the melting stopped, higher sea surface salinity resulted in stronger vertical mixing, which caused a subsurface warming. This subsurface warming again lead to ice sheet collapses and thus another new cycle began. Based on this theory, the observed abrupt warming at Greenland was explained by retreating sea ice in the North Atlantic and the length of the mild interstadial was determined by the duration of the sea ice reforming process (Li et al. 2005; Peterson et al. 2013).

This process could be primarily a winter behaviour (Li et al. 2010). The subsurface warming was not necessarily related to a strong reduction of the AMOC (Brady and Otto-Bliesner 2011; Mahajan et al. 2011) and it is not only visible in climate models but also in marine isotope records; for example, Rasmussen et al. (1996); Rasmussen and Thomsen (2004) showed depletions of $\Delta^{18}O$ during the cold stadials, implying a higher intermediate water mass temperature. However, some other studies have argued that this isotope signal was due to brine rejection before the occurrence of the HEs (e.g. Dokken and Jansen 1999; Labeyrie et al. 2005). Recently, Marcott et al. (2011) showed agreement of subsurface warming between state-of-the-art climate model results and proxy signal from intermediate depth and the bottom of the North Atlantic, which again supported this ice threshold theory.

Seager and Battisti (2007) provided another alternative theory to explain the AMOC weakening based on tropical high latitude teleconnections through the atmosphere circulation in the Atlantic, since climate models showed strong tropical responses to AMOC strength change (Zhang and Delworth 2005; Vellinga and Wood 2002; Wang et al. 2004). They proposed a positive feedback process as follows: tropical Atlantic ITCZ moves southward during the cold stadials due to heat flux change as the AMOC weakens; a relatively northern jet in the Atlantic storm track turns eastward, moving from southern North America to the Mediterranean. This more zonal surface wind field is able to produce surface cooling in the North Atlantic since less warm and salty water is transposed to the high ocean latitudes. In the mean time, heat flux in the atmosphere was also reduced. As a result, the sea ice expands and the NADW shifts southward or even shuts down. Meanwhile, in addition to the Atlantic thermocline, the Pacific thermocline is affected by this change in mid latitude storm track (Hazeleger et al. 2004) and the reduction of the AMOC. It has been suggest that the tropical Pacific thermocline is shallower and the El Niño-like condition is terminated as a response to the AMOC strengthening

(Timmermann et al. 2005). The linkage between Pacific thermocline and the AMOC strength is discussed in detail in 1.4.

Although Muscheler and Beer (2006) did not find convincing evidence of solar influence on D-O events, recently it has been suggested that solar activities are also able to trigger D-O events. A small change of irradiance, which was not detectable in proxy records, was able to affect sea ice cover and further resulted in abrupt changes (van de Berg et al. 2011; Wollez et al. 2012). Using a highly simplified model, Braun et al. (2008) not only suggested a threshold crossing process in D-O events, but also that Greenland temperature was in phase with solar activity.

1.3.3 Model uncertainties in the AMOC simulation

Though climate models are broadly used to study the AMOC and abrupt climate change related issues, limitations do exist. For instance, the simulated cooling in Greenland and Europe is less significant than in actual observations (Huber et al. 2006; Denton et al. 2005), even with a larger amount of freshwater inflow than the estimated value (e.g. Zhang and Delworth 2005; Stouffer et al. 2006). In addition, though many climate models have indeed shown a southward shift of the ITCZ, the AMOC variation cannot fully explain the reduction in monsoon strength (e.g. Marzin et al. 2013). Many possibilities can lead to these deficiencies in model simulations. One important speculation is the background climate (e.g. ice sheets, greenhouse gas concentrations, bathymetry etc.) applied in the model. The AMOC itself might have different stability properties during the cold stadials compared to mild interstadials, or its sensitivity to freshwater perturbation may be background climate dependent (e.g. Ganopolski and Rahmstorf 2001; Schmittner and Clement 2002; Prange et al. 2002; Knorr and Lohmann 2007). Most recently, Gong et al. (2013) performed hosing experiments using a fully coupled ocean-atmosphere-sea ice-land model to investigate the dependence of abrupt AMOC change on the background climate. They showed that there was no overshoot of the AMOC after freshwater injection and ocean intermediate warming in 32 ka BP experiments in the preindustrial case. A closed Bering Strait could also lead to a slower AMOC recovery and a merged hysteresis curve since it inhibits throughflow between the Pacific and the Arctic (Hu et al. 2010).

Freshwater injection properties could also affect model behaviour, e.g. the amount of freshwater input, its duration in model simulation and its location. Based on observations, the average surface water discharge rate stayed at around 0.1 Sv, assuming melting event lasting 500 years as the amount of

this freshwater could depend on the duration of the melting (Hemming 2004). However, such an amount of freshwater flux in the model induced weaker climate responses than the observations. A larger freshwater flux was required to shut down the AMOC in some of the climate models (e.g. Stouffer et al. 2006), which implies that the models were too stable to simulate abrupt climate changes (e.g. Valdes 2011). Otto-Bliesner and Brady (2010) studied this freshwater injection magnitude and location issue in a Last Glacial Maximum environment. They found that freshwater injection in the Labrador Sea could directly affect ocean convection, while injection in the Gulf of Mexico affected water transportation to the convection sites more significantly. They also showed that different AMOC recovery characteristics and threshold freshwater hosing rates affected the subtropics and the tropics. Furthermore, Kleinen et al. (2009) showed that although the AMOC weakened in all their experiments, different locations of freshwater injection could still alter water transportation from Greenland to the Norwegian Sea.

Model dynamical parameterisation also potentially has an influence on AMOC stability behaviour. As demonstrated earlier by Bryan (1986), the overturning strength was suggested to be very sensitive to vertical mixing. It has further been shown that the AMOC multiple equilibria depends on mixing parameterisation (Knutti et al. 2000), and vertical diffusion could determine the stability of an 'off' NADW (Manabe and Stouffer 1999). If vertical diffusivity crosses a threshold, the bistability behaviour will disappear. Later model studies showed contradicting results with regards to diffusivity; simulations from a simple coupled model in Schmitter and Weaver (2001) showed that the diffusivity change would only cause a shift in the hysteresis curve; the intensity of hysteresis was not affected. This hypothesis is challenged by results in Prange et al. (2003) from a Hamburg large-scale geostrophic ocean model. They found that large diffusivity would always result in significant hysteresis behaviour. However, if the diffusivity decreases to a very small value, two branches of the hysteresis curve will merge with each other and the AMOC is in a monostable state. The advection schemes in the model could also affect the stability property of the AMOC. Nof et al. (2007) investigated how model diffusivities affect the AMOC multiple equilibria by using both a wind controlled box model and the ocean component from Uvic-ESCM, concluding that multiple equilibria was artificially introduced in the model because 1) unrealistic strong upwelling and horizontal cross-isopycnal flows were produced in the Atlantic due to high cross-isopycnal diffusivity, and 2) the origin of the returning flow to the North Atlantic from the Southern Ocean was ignored in earlier model studies.

1.4 AMOC reconstruction

Despite the fact that the AMOC is a crucial component in the climate system, it is not easy to measure its present day strength and is even more difficult to estimate how active the circulation was during the last glacial.

For the present situation, the mean AMOC is estimated to be about 19 Sv based on observations at Northern hemisphere mid latitudes (e.g. Cunningham et al. 2007; Kanzow et al. 2010). As for the glacial condition, the most commonly used proxy record to reconstruct the circulation strength is $^{231}Pa/^{230}Th$ ratio (Yu et al. 1996). Since ^{231}Pa has a longer residence time than ^{230}Th in the North Atlantic water column, a higher ratio would suggest a more active circulation and a lower ratio corresponds to a more inactive AMOC. There are also other proxies used for the glacial AMOC reconstruction, such as $^{143}Nd/^{144}Nd$ (Piotrowski et al. 2005), $^{18}O/^{16}O$ (Lynch-Stieglit et al. 2006), $^{13}C/^{12}C$ (Curry and Oppo 2005). However, results from these studies were controversial; both a weak and a stronger AMOC during the last glacial maximum compared to present day were suggested since sediment records are very sparse and have particularly high uncertainties. There has also been debate about the AMOC strength deduction during the Heinrich events. It is commonly argued that the circulation was reduced during these freshwater discharge events, however recent studies have proposed that some of the Heinrich events showed little change in the ventilation strength since it is already weakened before the onset of these cold events (Lynch-Stieglitz et al. 2014).

Climate model were surely used to aid reconstruction work too; as stated in the previous section, AMOC strength is closely coupled with abrupt climate changes during MIS3, hence one way to investigate the AMOC variations is to conduct freshwater forcing sensitivity tests. Such tests could provide global climate responses to the AMOC change and thus suggest preferable locations for AMOC reconstruction (e.g. Heslop and Paul 2011) and compare the existing proxy records with model results. However most model simulations have focused on the last glacial maximum and also have deficiencies due to their present day boundary conditions and low complexity. In this sense, it is ideal to combine both model experiments and proxy records to estimate AMOC variations; MIS3 is a favourable period since pronounced and regular abrupt climate changes were observed. Most recently, Ritz et al. (2013) estimated approximately 12 Sv in AMOC deduction from the interstadial to the stadial state by combining model results and sediment records. They also concluded that the North Atlantic surface temperatures are highly sensitive to AMOC change, implying that this location is

suitable for AMOC reconstruction. However, their uncertainty regarding the AMOC variation was quite high. Inspired by this work, the AMOC deduction between interstadial and stadial states was also estimated in this thesis based on model results and high-resolution records during MIS3.

1.5 Closure of the Panamanian Seaway during early Pliocene and its climate impacts

The final closure of Panamanian Seaway during the early pliocene (about 4-5 million years ago; e.g. Keigwin 1982; Bartoli et al. 2005) was accompanied with significant climate change, since it altered the ocean circulation pattern (e.g. Haug and Tiedemann 1998; Lear et al. 2003) and reduced water transport from the Pacific to the Atlantic. Observations show that during this period, global temperature was about 3°C warmer and average sea level was ~25m higher than the present day. The Northern Hemisphere Greenland ice sheet was also absent due to the higher global temperature (e.g. Dowsett et al. 1999; Ravelo et al. 2004; Mudelsee and Raymo 2005).

Arguments exist about NADW production rate as response to the seaway closure based on sediment observations, e.g. Wright et al. (1992) and Delaney (1990) demonstrated that NADW was significant when the seaway was open, while Billups et al. (1999) and Haug and Tiedemann (1998) showed a stronger NADW after the seaway was closed. Molnar (2008) speculated this controversy might due to deep water formation site shifts. Contradictions were also observed in climate model simulations. Most model studies showed an enhanced AMOC when the seaway was closed due to the lack of freshwater transport to the Atlantic from the Pacific (e.g. Prange and Schulz 2004; Klocker et al. 2005; Schneider and Schmittner 2006; Lunt et al. 2008). However, Mikolajewicz and Crowley (1997) did find a weaker AMOC with an open seaway.

In the low latitudes, the eastern equatorial Pacific cold tongue was also absent and the thermocline was deeper than the present day in this region (e.g. Fedorov et al. 2006; Lawrence et al. 2006). By analyzing Mg/Ca temperatures from deep-dwelling planktonic foraminifers, Steph et al. (2010) reconstructed the Pliocene evolution of the thermocline in the eastern equatorial Pacific. They confirmed that shoaling of the thermocline between 4.8 and 4 million years ago occurred synchronously with the progressive closure of the Panamanian seaway, as well as an increase in the AMOC. They also performed model simulations and further suggested the following mechanisms regarding how the closure of the seaway affected the global climate and the modern equatorial Pacific cold tongue was formed: when the seaway gradually closed, shallow layer water mass transportation

from the Pacific to the Atlantic was greatly reduced; the AMOC was then intensified due to higher vertical temperatures and salinity gradient, and strengthened western boundary currents were present as well. Stronger NADW formation lead to an increase in the volume of the cold water sphere and further caused a shoaling of global thermocline (e.g. Huang et al. 2000*;* Timmermann et al. 2005). At the eastern equatorial Pacific region, shallowed thermocline eventually led to the formation of the present day Pacific cold tongue.

Surface wind system feedback was also involved in this thermocline shoaling process. Sediment records suggest that the seaway closure resulted in an intensification of upwelling in Southwest Africa. This increased upwelling at eastern boundaries promoted atmosphere CO_2 sinking, and as a result the polar-equator temperature gradient increased and Northern Hemisphere glaciation intensified. Meanwhile, cooling temperatures at coastal areas decreased precipitation, favoured nutrition supply to the ocean and resulted in stronger ocean carbon pumping (e.g. Marlow et al. 2000; Steph et al. 2010). Such footprints were shown in climate models as well. Prange and Schulz (2005) performed model experiments showing that compared to the present day, with an open Panamanian Seaway, the AMOC was weaker and surface wind between the North and South Atlantic showed a seesaw pattern – more upwelling was shown in the Northern Hemisphere and less upwelling was shown in the South. Temperatures in the North Atlantic decreased and the Northern Hemisphere subtropical high was weakened due to the reversed meridional heat transportation between the South and North Atlantic. This decreased AMOC induced upwelling seesaw effect was also observed during the HEs, for example Little et al. (1997) showed reduced upwelling at Benguela-Namibia during Heinrich events and Zhao et al. (2000) showed enhanced upwelling at Cap Blanc, which is located in the North Atlantic.

1.6 Objective of this thesis

The AMOC stability behaviour and its strength change are closely related to abrupt climate oscillations in the past and might have significant climate influences to global climate in the future but such mechanisms are still poorly understood based on both climate records and climate models. Hence, it is necessary to simulate such climate events in more complex climate models.

As it is stated in 1.1 and 1.2, MIS3 is particularly preferable time period to study the AMOC stability and abrupt climate changes. So far, there is no state-of-the-art climate model simulations of HE4

applying 38 ka BP background climate. As a result, the highlight of this thesis is to explore the following scientific questions by systematically analysing the AMOC stability and its climate impact under MIS3 conditions using a fully coupled state-of-the-art general circulation model. The subsequent scientific questions were stressed in chapters 2 and 3:

1) Is the AMOC in a multiple equilibrium state or a monostable state if we apply glacial boundary conditions in a state-of-the-art coupled model through freshwater hosing/extraction experiments?

2) How does global climate system response to North Atlantic freshwater perturbation in such model setups? Is glacial background climate able to improve the model results compare to observations?

3) By applying statistical test, is it possible to locate areas, which are sensitive or even have linear temperature responses to the AMOC strength variation, since such information is helpful for the AMOC reconstruction? Are these statistical results consistent with observations?

4) Is it possible to estimate the AMOC strength variations between cold stadial and warm interstadial based on the simulations? Was the AMOC greatly deducted during the Heinrich statial compare to interstadial?

Since Panamanian Seaway closure greatly affected the AMOC strength and the global climate, chapter 4 focused on this geological change and its climate impact by comparing different model results. The following scientific questions are intend to be answered:

5) How does the AMOC response to closure of the Panamanian Seaway?

6) Does the Pacific thermocline show shoaling or deepening as response to the Seaway closure? Is this shoaling/deepening model dependent?

7) How was the wind system involved to this process, especially at upwelling areas?

1.7 Models and experiment setups

1.7.1 CCSM3

In order to explore questions above, the Community Climate System Model Version 3 (CCSM3) performed most of the simulations in this thesis.

CCSM3 (Collins et al. 2006*)* is a state-of-the-art coupled climate model developed at National Center for Atmospheric Research (NCAR). It consists of four components, Community Atmosphere Model (CAM), Community Land Model (CLM), Parallel Ocean Program (POP) and Community Sea Ice Model (CSIM). These four components communicate with each other through a central coupler. The model has been previously used for both present day simulation and glacial climate modelling (e.g. Merkel et al. 2010; Otto-Bliesner and Brandy 2006).

CCSM3 has several different resolution versions. The version used in this thesis is the lower resolution version as follows: POP and CSIM: gx3x5 in horizontal (100 longitudinal grid points and 116 latitudinal grid points) with 25 vertical levels. The depth of the layer varies from 8 meters at the surface to 500 meters in the deep ocean. The longitude resolution keeps at constant with 3.6° and the latitude resolution varies from 0.9° at the equator to 1.5° towards the pole. The North Pole in POP and CSIM is placed over Greenland to avoid time-step constraints due to grid convergence; CAM: T31 version with 26 vertical levels, which follow the sigma coordinates and 3.75° resolution in both latitudinal and longitudinal direction (96x48 grid points); CLM: same horizontal resolution as CAM with 10 soil layers.

Model biases do exist in CCSM3 if one compare model results to modern observations. These biases are attributable to either single model component or coupling processes between different components. These systematic biases are generated due to integration imbalance and can be quite significant with long model integration (Large and Danabasoglu 2006)

In the polar area, CCSM3 produced a stronger Antarctic Circumpolar Current due to stronger eastward extropical wind stress. At the Arctic Ocean, the model underestimates downward shortwave radiation but overestimates 2 meter temperature during boreal winter (Collins et al. 2006). In the tropical area, due to lack of rainfall, higher Sea Surface Salinity (SSS) than observed in tropical Eastern Pacific was shown, whereas in central Southern Pacific showed lower SSS as response to

excessive rainfall was presented. This abundant precipitation produced a positive bias zone at southern equatorial Pacific, which usually refereed as double ITCZ figure and commonly observed in many other climate models (Lin 2007). Accompanied with double ITCZ pattern, stronger trade winds, more latent heat flux and less shortwave heat flux were observed. Recently, it is suggested that this bias could be related to cloud feedback in the Southern Ocean and Southern Hemisphere atmosphere energy flux (Hwang and Frierson 2012). It could be avoided by applying new convection scheme, which affects SST related energy feedback and produces less precipitation in the tropics (Zhang and Song 2010).

An artificial semiannual cycle of the SST and underestimates SST variability at Nino 3.4 region (5°S-5°N, 120°W-170°W) in the tropical Pacific (Large and Danabasoglu 2006). Chang et al. (2007) studied CCSM3 bias focusing on the tropical Atlantic. They showed that there is a cold/warm annual SST bias in the tropical Northern/Southern Atlantic. This SST bias results in a southward shift of the trade wind as well as the ITCZ. Meanwhile, positive sea level pressure was related to Amazonian draught and intensified the westerlies, which lead to a deeper thermocline in eastern Atlantic than the observations though the year. At the eastern boundaries, large positive SST bias was observed, especially at southwest Africa as a result of both ocean upwelling and coastal topography. In western boundaries, strong SST and SSS biases associated with stronger western boundary currents were also shown (Large and Danabasoglu 2006). Model resolution does not have great effect to these model biases and these deficiencies could be found in many other general circulation climate models as well (e.g. Guilyardi et al. 2009).

In this thesis, along with one MIS3 control run, twelve freshwater sensitivity experiments addressing the abrupt climate changes were performed using CCSM3 (Chapter 2 and 3) and two more experiments concentrating on the effects of Panamanian Seaway closure were performed (Chapter 4). The detailed model setups were provided in each chapter.

1.7.2 Other models

In order to investigate the climate effects of Panamanian Seaway closure, simulations performed by six other climate models were included in this thesis. A brief description of these models is provided below.

1.7.2.1 CCSM2

Community Climate System Model Version 2 (CCSM2, Kiehl and Gent 2004; Prange 2008) is the previous version of CCSM3. The model also includes the same four components running in parallel, atmosphere, land, ocean and sea ice. The same resolution version of each component as CCSM3 was used to simulate a(n) closed/open Panamanian Seaway.

1.7.2.2 UVic model

The University of Victoria Earth System Climate Model (UVic) is an intermediate complexity coupled climate-marine ecosystem model, which contains an ocean general circulation model, a single layer vertical integrated energy-moisture balanced atmosphere model and a thermodynamic sea ice model. The ocean component has 19 vertical layers of 50-500 meters thickness and the horizontal resolution of all the components is the same, which is 1.8°×3.6° (lat × lon). The ocean model is based on MOM-2 (Pacanowski 1990) and no flux correction is applied. Further model descriptions can be found at Weaver et al. (2001).

1.7.2.3 LSG model

The Large Scale Geostrophic ocean circulation model (LSG) has 22 vertical layers with horizontal resolution of 3.5° on E grid type (Mesinger and Arakawa 1976). The ocean model integrates the momentum equations (excludes nonlinear advection) using an implicit scheme. For ocean temperature and salinity calcaulation, a new tracer advection scheme adopted from Farrow and Stevens (1995) was implemented. The ocean model is less diffusive and dispersive than the standard version of LSG by introducing such scheme.

1.7.2.4 MIT model

The Massachusetts Institute of Technology Ocean General Circulation Model (MIT) was built on the incompressible Navier Stokes equations (Marschall et al. 1997). The model put more focus on studying the ocean circulation at vertical direction other than at horizontal direction. The simulation case performed for this thesis (Nisancioglu et al. 2003) has a horizontal resolution of constant at about 2.8 °x2.8°. There are 15 levels in the vertical, with the thickness increasing from 50 m at the ocean

surface to 690 m at the bottom (around 5000 m deep). The detailed model description can be found at Marschall et al. (1997).

1.7.2.5 HadCM3 model

The Hardly Centre coupled model (HadCM3) is one of the major models that used for the IPCC forth report. An atmosphere component, an ocean component and a sea ice model with different horizontal resolutions are couple in the model. There are 19 vertical levels in the atmosphere component, following hybrid vertical coordinate and the horizontal resolution is about 2.5°x3.75° on latitude and longitude grids, which produces a global grid of 96 x 73 grid cells. Several new schemes were applied in the atmosphere model compare to the previous version, including a new radiation scheme, a new land surface scheme and a new gravity wave drag scheme (Edwards and Slingo 1996; Cox et al. 1999). The time step of the atmosphere model is 30 min. The ocean component has 20 vertical layer and horizontal resolution is 1.25°x1.25° (Gordan et al. 2000). These two components are coupled once a day in the model. The sea ice model is Genie land ice model with multipy-enabled regions (GLIMMER). It uses a simple thermodynamic scheme and the core of the model is based on the ice sheet model described by Payne (1999).

1.7.2.6 ECBILT-CLIO

ECBILB is a three-layer global quasi-geostrophic atmosphere model, which has T21 horizontal resolution (5.6° × 5.6°) (Opsteegh et al. 1998). The atmosphere boundary layer is not resolved in the model. Thus prescribed boundary layer conditions are necessary to calculate the heat, momentum and moisture flux between the atmosphere component and the ocean component. There are four types of land type to determine the surface albedo, land, snow, ocean and sea-ice. CLIO represents the ocean/sea-ice model. It has a higher horizontal resolution than ECBILB, which is about 3° and 20 uniformed depth vertical layers until 4000m in the ocean. It is discretized on B grid and the atmosphere forcing is only added to the first two layers of the model. There are also no heat and salt fluxes at the boundary and the bottom topography is absent. The sea ice model, which defined at the scalar points of the ocean model, would form sea ice in the ocean if the ocean temperature drops below 2° in the coupled thermodynamic sea ice model. The thickness of the sea ice is computed based on the thermodynamic balance between the top and the bottom of the ice.

1.8 Outline of the Chapters

Chapter 2

Instability of the Atlantic overturning circulation during Marine Isotope Stage 3

[Xiao Zhang[1], Matthias Prange[1], Ute Merkel[1], Michael Schulz[1]]

(Published at Geophysical Research Letters)

(Object 1 and 2)

Pronounced millennial-scale climate variability was observed during MIS3. The most regular occurrence of these climate oscillations events was refereed as D-O events, featuring transitions between cold stadias and mild interstadials in the Greenland ice core. The origin of these events is still unknown but the strength change of the AMOC is suggested to be closely associated with their occurrence. E.g. the AMOC strength variation resulted in a switch of different AMOC modes and further triggered the abrupt climate events. One possible process leads to the AMOC strength change is freshwater injection observed during the other type of abrupt climate change – Heinrich Events at the North Atlantic. In order to understand the AMOC stability and its relation to abrupt climate changes, a lot of efforts have been put on modelling studies among different model classes. The results are quite controversial and so far in the AMOC stability study, there is no attempt applied 38 ka BP boundary conditions, during when the biggest Heinrich Event, H4 occurred. Hence, this chapter focus on systematic stability analysis of the AMOC and its associated global climate effects using a comprehensive state-of-the-art coupled atmosphere-ocean general circulation model forced with MIS3 boundary conditions. Twelve freshwater sensitivity tests with different amount of freshwater perturbation were performed to investigate the AMOC stability behaviour and its association with abrupt climate mechanisms.

Chapter 3

Spatial fingerprint and magnitude of changes in the Atlantic overturning circulation during Marine Isotope Stage 3

[Xiao Zhang[1], Matthias Prange[1], Ute Merkel[1], Michael Schulz[1]]

(Will submitted to Geophysical Research Letters)

(Object 2, 3 and 4)

This chapter firstly highlighted a general picture of how global ocean responded to the AMOC strength change. Secondly, since previous study showed there is a possible linear relationship between ocean temperature and the AMOC changes, ANOVA statistical test was applied to all ocean model grids to locate areas, which are sensitive or even have a linear relationship of ocean temperature to the AMOC strength. Such approach is able to aid the AMOC reconstruction since locations did not show strong linear relationship could be avoided. Lastly, by combining proxy data and model simulation, the AMOC strength variation between warm interstadial and cold stadial state was estimated.

Chapter 4

Changes in equatorial Pacific thermocline depth in response to Panamanian Seaway closure: Insights from a multi-model study

[Xiao Zhang[a,*], Matthias Prange[a,b], Silke Steph[b], Martin Butzin[a], Uta Krebs[c], Daniel J. Lunt[d], Kerim H. Nisancioglu[e], Wonsun Park[f], Andreas Schmittner[g], Birgit Schneider [c], Michael Schulz[a,b]]

(Published at Earth and Planetary Science Letters)

(Object 5, 6 and 7)

Chapter 4 is a model inter-comparison project. It compared model simulations between a closed Panamanian Seaway and an open Panamanian Seaway among eight different climate models with distinctive model complexity. By comparing model results, we at first aimed at investigating possible effects of Panamanian Seaway closure to the AMOC strength as well as tropical Pacific thermocline depth. Secondly, the robustness among different models was also explored. Last but not the least, how strong wind-stress feedback would influence the Pacific thermocline was also stressed.

References

Alley, R., P. U. Clark, L. D. Keigwin, and R. S. Webb, (1999), Making sense of millennial-scale climate change, in Mechanisms of Global Climate Change at Millennial Time Scales, Geophys. Monogr. Ser., 112, 385–394.

Bartoli, G., M. Sarnthein, M. Weinelt, H, Erlenkeuser, D, Garbe-Schonberg and W, Lea, (2005), Final closure of Panama and the onset of Northern Hemisphere glaciation, Earth Planet Sci. Lett., 237, 33–44.

Billups, K., A. C. Ravelo, J. C. Zachos, and R. D. Norris, (1999), Link between oceanic heat transport, thermohaline circulation, and the Intertropical Convergence Zone in the early Pliocene Atlantic, Geology, 27(4), 319–322.

Bitz, C. M., J. C. H. Chiang, W. Cheng, and J. J. Barsugli, (2007), Rates of thermohaline recovery from freshwater pulses in modern, Last Glacial Maximum, and greenhouse warming climates, Geophys. Res. Lett., 34, L07708, doi:10.1029/2006GL029237.

Blunier, T., and E. J. Brook, (2001), Timing of millennial-scale climate change in Antarctica and Greenland during the last glacial period, Science, 291, 109–112.

Bond, G. et al. (1992), Evidence for massive discharges of icebergs into the North Atlantic ocean during the last glacial period, Nature, 360, 245−249.

Brady, E. C., and B.L. Otto-Bliesner, (2011), The role of meltwater-induced subsurface ocean 520 warming in regulating the Atlantic meridional overturning in glacial climate simulations, Clim. Dynam., doi: 10.1007/s00382-010-0925-9.

Braun, H., Ditlevsen, P., Chialvo, D. R., (2008), Solar forced Dansgaard-Oeschger events and their phase relation with solar proxies, Geophys. Res. Lett. 35, L06703.

Broecker, W. S., D. M. Peteet, and D. Rind, (1985), Does the ocean-atmosphere system have more than one stable mode of operation? Nature, 315, 21–25, doi:10.1038/315021a0.

Broecker, W. S., (1998), Paleocean circulation during the last deglaciation: A bipolar seesaw? Paleoceanography, 13, 119–121.

Bryan, F., (1986), High-latitude salinity effects and interhemispheric thermohaline circulations, Nature, 323, 301–304.

Cacho, I. et al., (1999), Dansgaard-Oeschger and Heinrich event imprints in the Alboran Sea paleotemperatures, Paleoceanography, 14, 698–705.

Chang, Ching-Yee, James A. Carton, Semyon A. Grodsky, Sumant Nigam, (2007), Seasonal Climate of the Tropical Atlantic Sector in the NCAR Community Climate System Model 3: Error Structure and Probable Causes of Errors, J. Climate, 20, 1053–1070.

Collins D. W., M. L. Blackmon, G. B. Bonan, J. J. Hack, T. B. Henderson, J. T. Kiehl, W. G. Large, and D. S. McKenna, (2006), The Community Climate System Model Version 3 (CCSM3), J. Climate, 19, 2122-2143.

Cox, P., R. Betts, C. Bunton, R. Essery, P.R. Rowntree, and J. Smith, (1999), The impact of new land surface physics on the GCM simulation of climate and climate sensitivity, Clim. Dynam., 15, 183-203.

Cunningham et al., (2007), Temporal Variability of the Atlantic Meridional Overturning Circulation at 26.5°N, Science, 31, 935-938.

Curry,W. B. and D. W. Oppo, (2005), Glacial water mass geometry and the distribution of 13C of 6CO2 in the western Atlantic Ocean, Paleoceanography, 20, PA1017, doi:10.1029/2004PA001021.

Dansgaard, W., et al., (1993), Evidence for general instability of past climate from a 250-kyr ice core record, Nature, 364, 218–220, doi:10.1038/364218a0.

Delaney, L. M., (1990), Miocene benthic foraminiferal Cd/Ca records: South Atlantic and western equatorial Pacific, Paleoceanography, 5, 743–760.

Denton, G. H., Alley, R. B., Comer, G. C. and W. S. Broecker, (2005), The role of seasonality in abrupt climate change, Quat. Sci. Rev., 24, 1159–1182.

de Vernal, A., Hillaire-Marcel, C., Turon, J.L., and J. Matthiessen, (2000), Reconstruction of sea-surface temperature, salinity, and sea-ice cover in the northern North Atlantic during the last glacial maximum based on dinocyst assemblages, Can. J. Earth Sci., 37(5), 725-750, doi:10.1139/cjes-37-5-725

de Vries, P., and S. L. Weber, (2005), The Atlantic freshwater budget as a diagnostic for the existence of a stable shut down of the meridional overturning circulation, Geophys. Res. Lett., 32, L09606, doi:10.1029/2004GL021450.

Dokken, T.M., and E. Jansen, (1999), Rapid changes in the mechanism of ocean convection during the last glacial period, Nature, 401, 458–461.

Dowsett, H.J., J.A. Barron, R. Z. Poore, R. S. Thompson., T. M. Cronin, S. E. Ishman, D. A. Willard, (1999), Middle Pliocene paleoenvironmental reconstruction: PRISM2, USGS Open File Report, 99-535.

Döös, K. and D. J. Webb, (1994), The deacon cell and the other meridional cells of the southern ocean. J. Phys. Oceanogr., 24, 429–442.

Döös K. and A.C. Coward, (1997), The Southern Ocean as the major upwelling zone of the North Atlantic Deep Water, WOCE Newsletter, 27, 3-17.

Drijfhout, S.S., S.L. Weber and E. van der Swaluw, (2011), The stability of the MOC as diagnosed from model projections for pre-industrial, present and future climates, Clim. Dyn., 37, 1575-1586, doi:10.1007/s00382-010-0930-z.

Edwards, J. M. and A. Slingo, (1996), Studies with a flexible new radiation code I: choosing a configuration for a large-scale model, Q. J. R. Meteorol. Soc., 122, 689-719.

Elliot, M., L. Labeyrie, and J. C. Duplessy, (2002), Changes in North Atlantic deep-water formation associated with the Dansgaard-Oeschger temperature oscillations (60–10 ka), Quat. Sci. Rev., 21(10), 1153–1165.

EPICA Community Members, (2006), One-to-one coupling of glacial climate variability in Greenland and Antarctica, Nature, 444, 195–198.

Farrow, D. E. and D. P. Stevens, (1995), A new tracer advection scheme for Bryan and Cox type ocean general circulation models, J. Phys. Oceanogr., 25, 1731–1741.

Fedorov, A.V., P. S. Dekens, M. McCarthy, A. C. Ravelo, P. B. deMenocal, M. Barreiro, R. C. Pacanowski and S. G. Philander, (2006), The Pliocene Paradox (Mechanisms for a Permanent El Niño), Science, 312, 1485–1489, doi:10.1126/science.1122666.

Ganopolski, A., and S. Rahmstorf, (2001), Rapid changes of glacial climate simulated in a coupled climate model, Nature, 409, 153–158.

Ganachaud, A., and C. Wunsch, (2000), Improved estimates of global ocean circulation, heat transport and mixing from hydrographic data, Nature, 408, 453–457.

Gherardi, J.M., L. Labeyrie, J.F. McManus, R. François, L.C. Skinner and E. Cortijo, (2005), Evidence from the Northeastern Atlantic basin for variability in the rate of the meridional overturning circulation through the deglaciation, Earth Planet. Sci Lett., 240, 710-723.

Gildor, H., and E. Tziperman, (2003), Sea-ice switches and abrupt climate change, Philos. Trans. R. Soc. London, Ser. A, 361, 1935–1942, doi:10.1098/rsta.2003.1244.

Gnanadesikan, Anand, and J Robert Toggweiler, (1999), Constraints placed by silicon cycling on vertical exchange in general circulation models, Geophys. Res. Lett., 26(13), 1865-1868.

Gordan, A.L., (1986), Interocean exchange of thermocline water, J. Geophys. Res., 91, doi: 10.1029/0JGREA0000910000C4005037000001, issn: 0148-0227.

Gordan, C., C. Cooper, C.A. Senior, H. Banks, J.M. Gregory, T.C. Johns, J.F.B. Mitchell and R.A. Wood, (2000), The simulation of SST, sea ice extents and ocean heat transports in a version of the Hadley Centre coupled model without flux adjustments, Clim. Dynam., 16, 147-168.

Gregory, J. M., et al., (2005), A model intercomparison of changes in the Atlantic thermohaline circulation in response to increasing atmospheric CO2 concentration, Geophys, Res. Lett., 32, L12703, doi:10.1029/2005GL023209.

Grimm E.C., G. L. Jacobson, W. A. Watts, B.C.S. Hansen and K.A. Maasch, (1993), A 50,000 year record of climatic oscillations from Florida and its temperal correlation with the Heinrich events, Science, 261, 198–200.

Grimm, E. C., W. A. Watts, G. L. Jacobsen Jr., B. C. S. Hansen, H. R. Almquist, and A. C. Dieffenbacher-Krall, (2006), Evidence for warm wet Heinrich events in Florida, Quat. Sci. Rev., 25, 2197–2211, doi:10.1016/j.quascirev.2006.04.008.

Grootes, P. M., M. Stuiver, J. W. C. White, S. Johnsen, and J. Jouzel, (1993), Comparison of oxygen isotope records from the GISP2 and GRIP Greenland ice cores, Nature, 366, 552–554, doi:10.1038/366552a0.

Guilyardi, E., A. Wittenberg, A. Fedorov, M. Collins, C. Wang, A. Capotondi, G. J. van Oldenborgh, T. Stockdale, (2009), Understanding El Niño in Ocean–Atmosphere General Circulation Models - progress and challenges, B. Am. Meteorol. Soc. 90 (No. 3), 325–340.

Haug, G.H., and R. Tiedemann, (1998), Effect of the formation of the Isthmus of Panama on Atlantic Ocean thermohaline circulation, Nature, 393, 673–676.

Hazeleger,W., R. Seager, M. A. Cane, and H.H. Naik, (2004), How can tropical Pacific ocean heat transport vary, J. Phys. Oceanogr., 24, 320–333.

Heinrich, H., (1988), Origin and consequences of cyclic ice rafting in the Northeast Atlantic Ocean during the past 130,000 years, Quat. Res., 29, 142–152.

Hellerman, Sol, and Mel Rosenstein, (1983), Normal Monthly Wind Stress Over the World Ocean with Error Estimates, J. Phys. Oceanogr., 13, 1093–1104.

Hemming, S.R., and I. Hajdas, (2003), Ice-rafted detritus evidence from Ar-40/Ar-39 ages of individual hornblende grains for evolution of the eastern margin of the Laurentide ice sheet since 43 C-14 ky, Quaternary International., 99, 29-43.

Hemming, S. R., (2004), Heinrich events: massive late Peistocene detrius layers of the North Atlantic and their global climate imprint, Rev. Geophys, 42:RG1005, doi:10.1029/2003RG000128.

Hendy, I. L., J. P. Kennett, E. B. Roark, and B. L. Ingram, (2002), Apparent synchroneity of submillennial scale climate events between Greenland and Santa Barbara Basin, California from 30–10 ka, Quat. Sci. Rev., 21, 1167–1184.

Heslop, D and A. Paul, (2011), Fingerprinting of the Atlantic Meridional Overturing Circulation in climate models to aid in the design of proxy investigations, Clim. Dyn., 38:1047-1064, doi: 10.1007/s00382-011-1042-0.

Hofmann, M. and S. Rahmstorf, (2009), On the stability of the Atlantic meridional overturning circulation, Proc. Natl. Acad. Sci. U. S. A. 106, 20584–20589.

Hu, A., et al., (2010), Influence of Bering Strait flow and North Atlantic circulation on glacial sea level changes, Nat. Geosci., 3,118–121, doi:10.1038/ngeo729.

Hu, A., et al., (2012), Role of the Bering Strait on the hysteresis of the ocean conveyor belt circulation and glacial climate stability, Proc. Natl. Acad. Sci. USA, www.pnas.org/cgi/doi/10.1073/pnas.1116014109.

Huang, R. X., M. A. Cane, N. Naik, and P. Goodman, (2000), Global adjustment of the thermocline in response to deepwater formation, Geophys. Res Lett., 27(6), 759–762.

Huber, C., M. Leuenberger, R. Spahni, J. Flückiger, J. Schwander, T. F. Stocjer, S. Johnsen, A. Landais, and J. Jouzel, (2006), Isotope calibrated Greenland temperature record over Marine Isotope Stage 3 and its relation to CH_4, Earth Planet. Sci. Lett., 243, 504–519.

Huisman, S. E., M. den Toom, H. A. Dijkstra, and S. Drijfhout, (2010), An indicator of the multiple equilibria regime of the Atlantic meridional overturning circulation, J. Phys. Oceanogr., 40, 551–567, doi:10.1175/2009JPO4215.1.

Hwang, Y.-T. and D. M. W. Frierson, (2013), Link between the double-Intertropical Convergence Zone problem and cloud bias over Southern Ocean, Proc. Nat. Acad. Sci., 110, 4935-4940.

Jean Lynch-Stieglitz et al., (2014), Muted change in Atlantic overturning circulation over some glacial-aged Heinrich events, nature, 7, 144–150.

Jackson, L.C., (2013), Shutdown and recovery of the AMOC in a coupled global climate model: The role of the advective feedback, Geophys. Res. Lett., doi:10.1002/grl.50289.

Kanzow et al., (2010), Seasonal variability of the Atlantic meridional overturning circulation at 26.5°N, J. Climate, 23, 5678–5698.

Kaspi, Y., R. Sayag, and E. Tziperman, (2004), A “triple sea-ice state” mechanism for the abrupt warming and synchronous ice sheet collapses during Heinrich events, Paleoceanography, 19(3), PA3004, doi:10.1029/2004PA001009.

Keigwin, L. D., Jr., (1982), Isotope paleoceanography of the Caribbean and east Pacific: Role of Panama uplift in late Neogene time, Science, 217, 350–353.

Keigwin, L.D. and S. J. Lehman, (1994), Deep circulation change linked to HEINRICH event 1 and Younger Dryas in a middepth North Atlantic core, Paleoceanography, 9, doi: 10.1029/94PA00032.

Kiehl J. T. and P. R. Gent, (2004), The Community Climate System Model, Version 2, J. Climate, 17,3666-3682.

Kleinen, T., T. J. Osborn, and K. R. Briffa, (2009), Sensitivity of climate response to variations in freshwater hosing location, Ocean Dynam., 59, 509–521.

Klocker, A., M. Prange, and M. Schulz, (2005), Testing the influence of the Central American Seaway on orbitally forced Northern Hemisphere glaciation, Geophys. Res. Lett., 32, L03703, doi:10.1029/2004GL021564.

Knorr, G., and G. Lohmann, (2007), Transitions in the Atlantic thermohaline circulation by global deglacial warming and melt-water pulses, Geochem. Geophys. Geosyst., doi:10.1029/2007GC001604.

Knutti, R., T. F. Stocker, and D. G. Wright, (2000), The effects of sub-gridscale parameterizations in a zonally averaged ocean model, J. Phys.Oceanogr., 30, 2738– 2752.

Kuhlbrodt, T., A. Griesel, M. Montoya, A. Levermann, M. Hofmann, and S. Rahmstorf, (2007), On the driving processes of the Atlantic meridional overturning circulation, Rev. Geophys., 45, RG2001, doi:10.1029/2004RG000166.

Labeyrie, L., H. Leclaire, C.Waelbroeck, E. Cortijo, J.-C. Duplessy, L. Vidal, M. Elliot, B. Le Coat, and G. Auffret, (1999), Temporal variability of the surface and deep waters of the North West Atlantic Ocean at orbital and millennial scales, in Mechanisms of Global Climate Change at Millennial Time Scales, Geophys. Monogr. Ser., vol. 112, edited by P. U. Clark, R. S. Webb, and L. D. Keigwin, pp. 77–98, AGU, Washington D. C.

Labeyrie, L., et al., (2005), Changes in deep water hydrology during the Last Deglaciation, C.R. Geosciences, 337, 919-927.

Lachniet, M.S., Y. Asmerom, J. P. Bernal, V. Polyak, and L. Vazquéz-Selem, (2013), Orbital pacing and ocean circulation-induced collapses of the Mesoamerican monsoon over the past 22,000 y, Proc. Natl. Acad. Sci., doi:10.1073/pnas.1222804110.

Large, W. G., and G. Danabasoglu, (2006), Attribution and impacts of upper-ocean biases in CCSM3, J. Climate, 19, 2325–2346.

Lawrence, K.T., Z. H. Liu, and T. D. Herbert, (2006), Evolution of the eastern tropical Pacific through Plio-Pleistocene glaciation, Science, 312, 79–83, doi:10.1126/science.1120395.

Lear C.H., Y. Rosenthal, J. D. Wright, (2003), The closing of a seaway:ocean water masses and global climate change, Earth Planet Sci. Lett., 210, 425–436.

Li, C., D. S. Battisti, D. P. Schrag, and E. Tziperman, (2005), Abrupt climate shifts in Greenland due to displacements of the sea ice edge, Geophys. Res. Lett., 32, L19702, doi:10.1029/2005GL023492.

Li, C., D. S. Battisti, and C. M. Bitz, (2010), Can North Atlantic sea ice anomalies account for Dansgaard-Oeschger climate signals?, J. Climate, 23, 5457–5475.

Lin, J.L., (2007), The doubble-ITCZ problem in IPCC AR4 coupled GCMs:Ocean-atmoshpere feedback analysis, J.Climate, 20, 4497-4525.

Little, M. G., R. R. Schneider, D. Kroon et al. (1997), Trade wind forcing of upwelling, seasonality, and Heinrich events as a response to sub-Milankovitch climate variability, Paleoceanography, 12, 568– 576.

Liu, W., Z. Liu, and A. Hu, (2013), The stability of an evolving atlantic meridional overturning, Geophys. Res. Lett., 40, 1-7, doi:10.1002/grl.50365.

Lunt, D. J., P. J. Valdes, A. Haywood, and I. C. Rutt, (2008), Closure of the Panama Seaway during the Pliocene: Implications for climate and Northern Hemisphere glaciation, Clim. Dyn., 30, 1–18, doi:10.1007/s00382-007-0265-6.

Lynch-Stieglitz, J. et al., (2006), Meridional overturning circulation in the South Atlantic at the last glacial maximum, Geochem. Geophy. Geosys., 7, Q10N03, doi:10.1029/2005GC001226.

Maier-Reimer, E., U. Mikolajewicz, and K. Hasselmann, (1993), Mean circulation of the Hamburg LSG OGCM and its sensitivity to the thermohaline surface forcing, J. Phys. Oceanogr., 23, 731– 757.

Mahajan, S., R. Zhang, T. L. Delworth, S. Zhang, A. J. Rosati, and Y.-S. Chang, (2011), Predicting Atlantic meridional overturning circulation (AMOC) variations using subsurface and surface fingerprints, Deep-Sea Res. II, 58, 1895–1903.

Manabe, S., and R. J. Stouffer, (1988), Two stable equilibria of a coupled ocean-atmosphere model, J. Clim., 1, 841–866.

Manabe, S., and R. J. Stouffer, (1999), Are two modes of thermohaline circulation stable? Tellus A, 51A(3), 400-411.

Marotzke, J., and J. Willebrand, (1991), Multiple equilibria of the global thermohaline circulation, J. Phys. Oceanogr., 21, 1372–1385.

Marcott ,S.A, et al. (2011), Ice-shelf collapse from subsurface warming as a trigger for Heinrich events, Proc. Natl. Acad. Sci. U.S.A., 108, 13415–13419.

Marlow, J. R., C. B. Lange, G. Wefer, and A. Rosell-Mele, (2000), Upwelling intensification as part of the Pliocene-Pleistocene climate transition, Science, 290, 2288–2291.

Marshall, J., A. Adcroft, C. Hill, L. Perelman, and C. Heisey, (1997), A finite-volume, incompressible Navier-Stokes model for studies of the ocean on parallel computers, J. Geophys. Res., 102(C3), 5753–5766.

Marzin C, N. Kallel, M. Kageyama, J-C. Duplessy, P. Braconnot, (2013), Glacial fluctuations of the Indian monsoon and their relationship with North Atlantic climate: new data and modelling experiments, Clim. Past, 9,2135–2151.

Maslin, M.A., N.J. Shackleton, and U. Pflaumann, (1995), Surface water temperature, salinity, and density changes in the northeast Atlantic during the last 45,000 years: Heinrich events, deep water formation, and climatic rebounds, Paleoceanography 10, doi: 10.1029/94PA03040.

McCave, I.N., B. Manighetti, and S.G. Robinson, (1995), Sortable silt and find sediment size/composition slicing: Parameters for paleocurrent speed and paleoceanography, Paleoceanography 10: doi: 10.1029/94PA03039.

McManus, J. F., R. Francois, J-M. Gherardi, L. Keigwin, and S. Brown-Leger, (2004), Collapse and rapid resumption of Atlantic meridional circulation linked to deglacial climate changes, Nature, 428, 834–837.

Merkel, U., M. Prange, and M. Schulz, (2010), ENSO variability and teleconnections during glacial climates, Quaternary Science Reviews, 29, 86-100.

Mesinger, F., and A. Arakawa, (1976), Numerical methods used in atmospheric models, volume I. GARP Publications Series 17,WMO, 64 pp.

Mikolajewicz, U. and E. Maier-Reimer, (1994), Mixed boundary conditions in ocean general circulation models and their influence on the stability of the model's conveyor belt, J. Geophys. Res., 99, doi: 10.1029/94JC01989.

Mikolajewicz, U., and T. J. Crowley, (1997), Response of a coupled ocean/energy balance model to unrestricted flow through the Central American isthmus, Paleoceanography, 12(3), 429– 441.

Molnar, P., (2008), Closing of the Central American Seaway and the Ice Age: A critical review, Paleoceanography, 23, PA2201, doi:10.1029/2007PA001574.

Mudelsee, M., and M. E. Raymo, (2005), Slow dynamics of the Northern Hemisphere glaciation, Paleoceanography, 20, PA4022, doi:10.1029/2005PA001153.

Muscheler, R., and Beer, J., (2006), Solar forced Dansgaard/Oeschger events ?Geophys. Res. Lett.33 (L20706).

Munk, W., and C. Wunsch, (1998), Abyssal recipes, II, Energetics of tidal and wind mixing, Deep Sea Res., Part I, 45, 1977–2010.

Nisancioglu, K. H., M. E. Raymo, and P. H. Stone, (2003), Reorganization of Miocene deep water circulation in response to the shoaling of the Central American Seaway, Paleoceanography, 18(1), 1006, doi:10.1029/2002PA000767.

Nof, D., S. Van Gorder, A. M. De Boer, (2007), Does the Atlantic meridional overturning cell really have more than one stable steady state? Deep-Sea Res. I 54 (11), 2005–2021.

North Greenland Ice Core Project members, (2004), High-resolution record of Northern Hemisphere climate extending into the last interglacial period, Nature, 431, 147–151.

Opsteegh, J.D., R.J. Haarsma, and F.M. Selten, (1998), ECBilt: A dynamic alternative to mixed boundary conditions in ocean models, Tellus, 50A, 348-367.

Otto-Bliesner, Bette L., E. C. Brady, G. Clauzet, R. Tomas, S. Levis, and Z. Kothavala, (2006), Last Glacial Maximum and Holocene Climate in CCSM3, J. Climate, 19, 2526–2544, doi: http://dx.doi.org/10.1175/JCLI3748.1

Otto-Bliesner B.L., and E.C. Brady, (2010), The sensitivity of the climate response to the magnitude and location of freshwater forcing: last glacial maximum experiments, Quat. Sci. Rev., 29, 56-73.

Pacanowski, R.C., (1990), MOM2 Documentation, User's Guide and Reference Manual, Tech.Rep.3, Geophys. Fluid Dyn. Lab. Ocean Group, Princeton, N.J.

Payne, A.J., (1999), A thermomechanical model of ice flow in West Antarctica, Clim. Dyn., 15, 115-125.

Peterson, L. C., G. H. Haug, K. A. Hughen, and U. Röhl, (2000), Rapid changes in the hydrologic cycle of the tropical Atlantic during the last glacial, Science, 290, 1947–1951, doi:10.1126/science.290.5498.1947.

Petersen, S. V., D. P. Schrag, and P. Clark, (2013), A new mechanism for Dansgaard-Oeschger cycles, Paleoceanography, 28, 24–30, doi:10.1029/2012PA002364.

Piotrowski, A. M., S. L. Goldstein, S. R. Hemming and R.G. Fairbanks, (2006), Temporal Relationships of Carbon Cycling and Ocean Circulation at Glacial Boundaries, Science, 307, 1933–1938.

Prange, M., V. Romanova, and G. Lohmann, (2002), The glacial thermohaline circulation: Stable or unstable? Geophys. Res. Lett., 29(21), 2028, doi:10.1029/2002GL015337.

Prange, M., G. Lohmann, and A. Paul, (2003), Influence of vertical mixing on the thermohaline hysteresis: Analyses of an OGCM, J. Phys. Oceanogr., 33(8), 1707-1721.

Prange, M., and M. Schulz, (2004), A coastal upwelling seesaw in the Atlantic Ocean as a result of the closure of the Central American Seaway, Geophys. Res. Lett., 31, L17207, doi:10.1029/2004GL020073.

Prange, M., (2008), The low-resolution CCSM2 revisited: new adjustments and a present-day control run, Ocean Science, 4, 151-181.

Rahmstorf, S., (1995), Bifurcations of the Atlantic thermohaline circulation in response to changes in the hydrological cycle, Nature, 378, 145-149.

Rahmstorf, S. and J. Willebrand, (1995), The role of temperature feedback in stabilizing the thermohaline circulation, J. Phys. Oceanogr., 25, 787-805.

Rahmstorf, S., M. Crucifix, A. Ganopolski, H. Goosse, I. V. Kamenkovich, R. Knutti, G. Lohmann, R. Marsh, L. A. Mysak, Z. Wang, and A. J. Weaver, (2005), Thermohaline circulation hysteresis: a model intercomparison, Geophys. Res. Lett., 32, L23605, doi:10.1029/2005GL023655.

Rasmussen, T. L., E. Thomsen, T. C. E. Veering and L. Labeyrie, (1996), Rapid changes in surface and deep water conditions at the Faeroe margin during the last 58,000 years, Paleoceanography, 11(6), 757-771, doi:10.1029/96PA02618

Rasmussen, T.L. and E. Thomsen, (2004), The role of the North Atlantic Drift in the millennial timescale glacial climate fluctuations, Palaeogeography, Palaeoclimatology, Palaeoecology, 210, 101–116.

Ravelo, A. C., D. H. Andreasen, M. Lyle, A. O. Lyle, and M. W. Wara, (2004), Regional climate shifts caused by gradual global cooling in the Pliocene epoch, Nature, 429, 263–267, doi:10.1038/nature02567.

Redi, M.H., (1982), Isopycnal mixing by coordinate rotation. J. Phys. Oceanogr. 12, 1154–1158.

Rind, D., P. Demenocal, G.L. Russell, S. Sheth, D. Collins, G.A. Schmidt, and J. Teller, (2001), Effects of glacial meltwater in the GISS Coupled Atmosphere-Ocean Model: Part I: North Atlantic Deep Water response, J. Geophys. Res., 106, 27335-27354, doi:10.1029/2000JD000070.

Rooth, C., (1982), Hydrology and ocean circulation, Prog. Oceanogr., 11, 131–149, doi: 10.1016/0079-6611(82)90006-4.

Ritz et al., (2013), Estimated strength of the Atlantic overturning circulation during the last deglaciation, Nature Geosci., 6, 208–212.

Sachs, J.P. and S.J. Lehman, (1999), Subtropical North Atlantic Temperatures 60,000 to 30,000 Years Ago, Science, 286, 756-759

Schmittner, A., and A. C. Clement, (2002), Sensitivity of the thermohaline circulation to tropical and high latitude freshwater forcing during the last glacial-interglacial cycle, Paleoceanography, 17(2), 1017, doi:10.1029/2000PA000591.

Schmittner, A., and A. J. Weaver, (2001), Dependence of multiple climate states on ocean mixing parameters, Geophys. Res. Lett., 28, 1027-1030.

Schneider, B., and A. Schmittner, (2006), Simulating the impact of the Panamanian seaway closure on ocean circulation, marine productivity and nutrient cycling, Earth Planet. Sci. Lett., 246, 367– 380.

Schulz, H., U. von Rad, and H. Erlenkeuser, (1998), Correlation between Arabian Sea and Greenland climate oscillations of the past 110,000 years, Nature, 393, 54–57.

Seidov, D., and M. Maslin, (2001), Atlantic Ocean heat piracy and the bipolar climate see-saw during the Heinrich and Dansgaard–Oeschger events, J. Quat. Sci., 16, 321–328.

Shackleton, N. J., M. A. Hall, and E. Vincent, (2000), Phase relationships between millennial-scale events 64,000–24,000 years ago, Paleoceanography, 15(6), 565–569, doi:10.1029/2000PA000513.

Sijp, W.P., M. H. England, and J.M. Gregory, (2012), Precise calculations of the existence of multiple AMOC equilibria in coupled climate models, Part I: equilibrium states, J. Climate, 25, 282-298.

Skinner, L. C., and H. Elderfield, (2007), Rapid fluctuations in the deep North Atlantic heat budget during the last glacial period, Paleoceanography, 22, PA1205, doi:10.1029/2006PA001338.

Sloyan, B. M., and S. R. Rintoul, (2001), The Southern Ocean limb of the global deep overturning circulation, J. Phys. Oceanogr., 31, 143–173.

Steph, S., R. Tiedemann, M. Prange, J. Groeneveld, M. Schulz, A. Timmermann, D. Nürnberg, C. Rühlemann, C. Saukel, and G. H. Huang, (2010), Early Pliocene increase in thermohaline overturning: A precondition for the development of the modern equatorial Pacific cold tongue, Paleoceanography, 25, PA2202, doi:10.1029/2008PA001645.

Stocker, T. F., and D. G. Wright, (1991), Rapid transitions of the ocean's deep circulation induced by changes in surface water fluxes, Nature, 351, 729–732.

Stocker, T. F., (1998), The seesaw effect, Science, 282, 61–62.

Stouffer, R.J., Yin J, Gregory, J.M, Dixon, K.W, Weaver, A.J, Spelman, M.J, Hurlin, W, participating groups, (2006), Investigating the causes of the response of the thermohaline circulation to past and future climate changes, J. Clim. 19,1365–1387.

Stommel, H., (1961), Thermohaline convection with two stable regimes of flow, Tellus, 13, 224–230.

Sun, B., Y. Zhu, and H. Wang, (2011), The recent interdecadal and interannual variation of water vapor transport over eastern China, Adv. Atmos. Sci., 28, 1039–1048.

Taylor, K. E., R. J. Stouffer, and G. A. Meehl., (2012), An overview of CMIP5 and the experiment design, Bull. Am. Meteorol. Soc., 90, 485–498, doi:10.1175/BAMS-D-11-00094.1.

Timmermann, A., S.I. An, U. Krebs, and H. Goosse, (2005), ENSO suppression due to weakening of the North Atlantic Thermohaline Circulation, J. Clim., 18, 3122–3139.

Toggweiler, J.R., and B. L. Samuels, (1993), New radiocarbon constraints on the upwelling of abyssal water to the ocean's surface, In The Global Carbon Cycle, NATO ASI Series - Vol. 115. Heidelberg, Germany, Springer-Verlag, 333-366.

Toggweiler, J.R., and B. L. Samuels, (1995), Effect of Drake Passage on the global thermohaline circulation, Deep-Sea Research, Part I, 42(4), 477-500.

Toggweiler, J.R., and B. L. Samuels, (1998), On the ocean's large-scale circulation near the limit of no vertical mixing, J. Phys. Oceanogr., 28(9), 1832-1852.

Valdes, P., (2011), Built for stability, Nat. Geosci., 4(7), 414–416, doi:10.1038/ngeo1200.

van deBerg,W., van de Broeke, M., Ettema, J., van Meijgaard, E., Kaspar, F., (2011), Significant contribution of insolation to Eemian melting of the Greenlandice
sheet, Nat .Geosci. 4, 679–683.

Vellinga, M. and R. A. Wood, (2002), Global climatic impacts of a collapse of the Atlantic thermohaline circulation, Clim. Change, 54, 251–267.

Voelker, A.H.L., and Workshop Participants, (2002), Global distribution of centennial-scale records for Marine Isotope Stage (MIS) 3: A database, Quaternary Sci. Rev., 21,1185–1212, doi: 10.1016/S0277–3791(01)00139–1.

Wang, Y. J., H. Cheng, R. L. Edwards, Z. S. An, J. Y. Wu, C.C. Shen, and J. A. Dorale, (2001), A high-resolution absolute-dated late Pleistocene monsoon record from Hulu Cave, China, Science, 294, 2345–2348, doi:10.1126/science.1064618.

Wang, X., A. S. Auler, R. L. Edwards, H. Cheng, P. S. Cristalli, P. L. Smart, D. A. Richards, and C.-C. Shen, (2004), Wet periods in northeastern Brazil over the past 210 kyr linked to distant climate anomalies, Nature, 432, 740–743, doi:10.1038/nature03067.

Weaver, A. J., and Coauthors, (2001), The UVic Earth System Climate Model: Model description, climatology and application to past, present and future climates, Atmos.–Ocean, 39, 361–428.

Weaver, A. J. et al. (2012), Stability of the Atlantic meridional overturning circulation: A model intercomparison, Geophys. Res. Lett., 39, L20709.

Woillez, M.N., Krinner, G., Kageyama, M., Delaygue, G., (2012), Impact of solar forcing on the surface mass balance of northern ice sheets for glacial conditions, Earth Planet. Sci. Lett. 335–336, 18–24.

Wright, J. D., K. G. Miller, and R. G. Fairbanks, (1992), Early and middle Miocene stable isotopes: Implications for deepwater circulation and climate, Paleoceanography, 7, 357–389.

Wunsch, C., (2006), Abrupt climate change: An alternative view, Quat. Res., 65, 191–203, doi:10.1016/j.yqres.2005.10.006.

Yu, E.-F., R. Francois, and M. P. Bacon, (1996), Similar rates of modern and last-glacial ocean thermohaline circulation inferred from radiochemical data, Nature, 379, 689–694.

Zahn, R., J. Shönfeld, H.R. Kudrass, M.H. Park, H. Erlenkeuser, and P. Grootes, (1997), Thermohaline instability in the North Atlantic during meltwater events: Stable isotope and ice-rafted detritus records from core SO75-26KL, Portuguese margin, Paleoceanography, 12(5), 696–710.

Zhao, M., G. Eglinton, S. K. Haslett, R. W. Jordan, M. Sarnthein, and Z. Zhang, (2000), Marine and terrestrial biomarker records for the last 35,000 years at ODP site 658C off NW Africa, Organ. Geochem., 31, 919– 930.

Zhang, R., and T. L. Delworth, (2005), Simulated Tropical Response to a Substantial Weakening of the Atlantic Thermohaline Circulation, J. Climate, 18, 1853–1860.

Zhang, G. J., and X. Song, (2010), Convection parameterization, tropical Pacific double ITCZ, and upper-ocean biases in the NCAR CCSM3. Part II: Coupled feedback and the role of ocean heat transport, J. Climate, 23, 800–812.

Chapter 2

Instability of the Atlantic overturning circulation during Marine Isotope Stage 3

Xiao Zhang[1], Matthias Prange[1], Ute Merkel[1], Michael Schulz[1]

[1]MARUM – Center for Marine Environmental Sciences and Faculty of Geosciences, University of Bremen, Klagenfurter Str., 28334 Bremen, Germany

Key Points:

Hosing experiments with CCSM3 under Marine Isotope Stage 3 conditions
A highly unstable AMOC is simulated in a state-of-the-art climate model
Minor freshwater fluxes trigger Dansgaard-Oeschger type climate shifts

Abstract:

Variations in the strength of the Atlantic meridional overturning circulation (AMOC) were involved in the occurrences of Dansgaard-Oeschger (D-O) events during Marine Isotope Stage 3 (MIS3). The stability of the AMOC to North Atlantic freshwater perturbations is studied using a comprehensive climate model under MIS3 boundary conditions. An AMOC stability diagram constructed from a series of equilibrium freshwater perturbation experiments reveals a highly non-linear dependence of AMOC strength on freshwater forcing. The MIS3 baseline state is remarkably unstable with respect to minor perturbations. The global climate signal associated with a change in AMOC strength is consistent with a transition from an interstadial to a stadial state including an annual-mean surface air temperature drop of ~8 K in central Greenland. We suggest that minor freshwater perturbations in the hydrologic cycle, e.g. related to ice-sheet processes, had the potential to trigger D-O-type climate shifts associated with a threshold in the atmosphere-ocean system.

Key Words:

Atlantic Meridional Overturning Circulation, Marine Isotope Stage 3, Dansgaard-Oeschger (D-O) events, Climate modeling

1. Introduction

Marine Isotope Stage 3 (MIS3, 57-29 ka BP) was a period of pronounced millennial-scale climate variability, associated with the most regular occurrence of Dansgaard-Oeschger (D-O) events [Schulz, 2002]. Characterized by rapid transitions between cold stadials and warm interstadials at northern latitudes [Dansgaard et al., 1993, Bond et al., 1993], the significance of D-O events is substantiated by global-scale climate variations that can be correlated to the Greenland temperature record [Broecker, 2000, Voelker et al., 2002, EPICA community members, 2006]. The origin of D-O events is still a matter of controversy [Timmermann et al., 2003], but there is strong evidence that variations in the strength of the Atlantic meridional overturning circulation (AMOC) and its associated heat transport were involved, where strong (weak) overturning is related to interstadial (stadial) climate, although these D-O-type AMOC variations were probably much smaller than those associated with Heinrich events [Keigwin and Boyle, 1999, van Kreveld et al., 2000, Sarnthein et al., 2001, Elliot et al., 2002, Clement and Peterson, 2008]. A widely held view of D-O dynamics involves switches between two stable states of different AMOC strength. Accordingly, numerous conceptual models have been suggested to explain the millennial-scale climate oscillations based on the concept of oceanic bi-stability [e.g. Stocker and Wright, 1991, Timmermann et al., 2003, Sarnthein et al., 2001, Clement and Peterson, 2008, Colin de Verdière et al., 2006]. Meltwater injections into the Nordic Seas associated with internal northern ice-sheet dynamics have been suggested as a potential pacemaker for AMOC state transitions and associated D-O climate oscillations [van Kreveld et al., 2000]. Understanding the stability properties of the glacial ocean circulation to freshwater perturbations is therefore key towards an understanding of D-O climate variability.

Important insights into the potential dynamics of D-O events were provided by simulations with the Earth system model of intermediate complexity (EMIC) CLIMBER-2 [Ganopolski and Rahmstorf, 2001]. It has been shown that the stability properties of the AMOC under glacial boundary conditions may differ fundamentally from the interglacial case. In particular, CLIMBER-2 suggested the existence of two modes of the AMOC in close proximity to the unperturbed glacial state and that minor freshwater perturbations can trigger transitions between these two modes causing D-O-type climate variations. It is known, however, that AMOC stability properties are model-dependent [e.g. Rahmstorf et al., 2005, Stouffer et al., 2006], and it is therefore unclear to which extent the EMIC-based results are robust in the framework of more complex models. While various EMICs have been employed to

study abrupt climate change associated with AMOC stability properties specific to the last glaciation [Prange et al., 2002, Schmittner et al., 2002, van Meerbeeck et al., 2009, Montoya and Levermann, 2008, Knorr and Lohmann, 2003, Banderas et al., 2012], so far no attempts have been made to systematically examine AMOC stability in a comprehensive coupled general circulation model under MIS3 boundary conditions. Here, we present results from a series of quasi-equilibrium freshwater-hosing/extraction experiments using the Community Climate System Model version 3 (CCSM3) forced with MIS3 boundary conditions and varying North Atlantic freshwater perturbations to assess the stability properties of the ocean circulation and its potential role in D-O climate variability.

2. Experimental design

NCAR's (National Center for Atmospheric Research) CCSM3 is a fully-coupled comprehensive general circulation model, composed of four separate components representing atmosphere, ocean, land and sea-ice [Collins et al., 2006]. In our simulations, the resolution of the atmospheric component is given by T31 (3.75° transform grid) with 26 layers in the vertical, while the ocean has a nominal resolution of 3° with equatorial grid refinement in meridional direction (down to 0.9°) and 25 levels in the vertical [Yeager et al., 2006]. The land model is defined on the same horizontal grid as the atmosphere and includes components for biogeophysics, biogeochemistry, the hydrologic cycle as well as an interactive dynamic global vegetation model [Oleson et al., 2004, Levis et al., 2004]. In order to improve the simulation of the land surface hydrology and vegetation cover, new parameterizations for canopy interception and soil evaporation have been implemented into the land component [Oleson et al., 2008], identical to the model design used in a previous study [Handiani et al., 2013].

Along with a 1000-year integrated pre-industrial control run, we performed a MIS3 baseline simulation applying 38 ka BP orbital forcing [Berger, 1978] and corresponding greenhouse gas concentrations of CO_2 (215 ppmv), CH_4 (501 ppbv), and N_2O (234 ppbv) [Flückiger et al., 2004, Spahni et al., 2005, Ahn and Brook, 2007, Bereiter et al., 2012]. In addition, the 38 ka BP ICE-5G continental ice-sheet distribution has been implemented [Peltier, 2004], and the correspondingly reduced sea level results in a modified land-sea distribution (e.g. closing of the Bering Strait). The MIS3 baseline simulation was initialized with the final state of a 1500 years long simulation with LGM (Last Glacial Maximum, 21 ka BP) boundary conditions and integrated for another 2170 years. Note that this MIS3 simulation differs from a previous CCSM3 MIS3 experiment with the same resolution [Merkel et al., 2010] by the choice of the time slice, the implementation of a dynamic vegetation module, changes in the parameterizations for canopy interception and soil evaporation, and the integration length. The 38 ka

time slice was chosen because it lies right in the middle of a rather regular sequence of D-O-cycles and coincides with Heinrich event 4 [Hemming, 2004].

Branching off from year 1670 of the MIS3 simulation, we performed twelve freshwater-hosing/extraction experiments with different rates of continuous, unbalanced freshwater surface flux (treated as a virtual salinity flux [e.g. Prange and Gerdes, 2006] in CCSM3) homogeneously distributed over the Nordic Seas [cf. van Kreveld et al., 2000], ranging from ± 0.005 Sv to ± 0.2 Sv (1 Sv = 10^6 m^3/s). The integration time for these experiments was long enough for the AMOC to reach a new equilibrium (500 years or longer if necessary, Fig. S1), which has been assessed by means of a t-test.

In order to study the potential for bi-stability, the experiment with the strongest freshwater input of +0.2 Sv was subsequently continued after removing the freshwater perturbation. Recovery of the AMOC hints at a mono-stable MIS3 baseline AMOC [Prange et al., 2002]. All results presented in this paper refer to the last 100-year mean climate of each experiment, representing quasi-equilibrium conditions. In all simulations, ozone and aerosol distributions were kept at pre-industrial levels [Otto-Bliesner et al., 2006].

3. Results

The 38 ka BP baseline simulation results in a climate that is significantly colder than PI with a maximum cooling of more than 24 K in annual-mean surface temperature over the Laurentide ice-sheet in North America (Fig. 1a). The annual global mean surface temperature is 3.3 K lower than in the PI run. As shown in Figure 1a, the high latitudes generally experience a stronger temperature decrease compared to lower latitudes. However, a region of positive surface temperature anomalies in the Nordic Seas indicates intense inflow of Atlantic water from the south in the MIS3 simulation. This supply of warm and salty water keeps large parts of the Nordic Seas ice-free (Fig. 1a) and maintains convection and deep-water formation during winter. As a result, CCSM3 simulates a vigorous AMOC in the MIS3 baseline run with a North Atlantic overturning-maximum of 15.4 Sv, which is ~1.5 Sv stronger than in the PI control run (Fig. 2). The southward flow of North Atlantic deep-water occurs at shallower levels in the MIS3 run than under PI conditions.

We perturbed the AMOC in a series of freshwater-hosing/extraction experiments as described above. In almost all experiments, an integration time of 500 years was long enough for the meridional overturning streamfunction to reach a new equilibrium, only in one case the

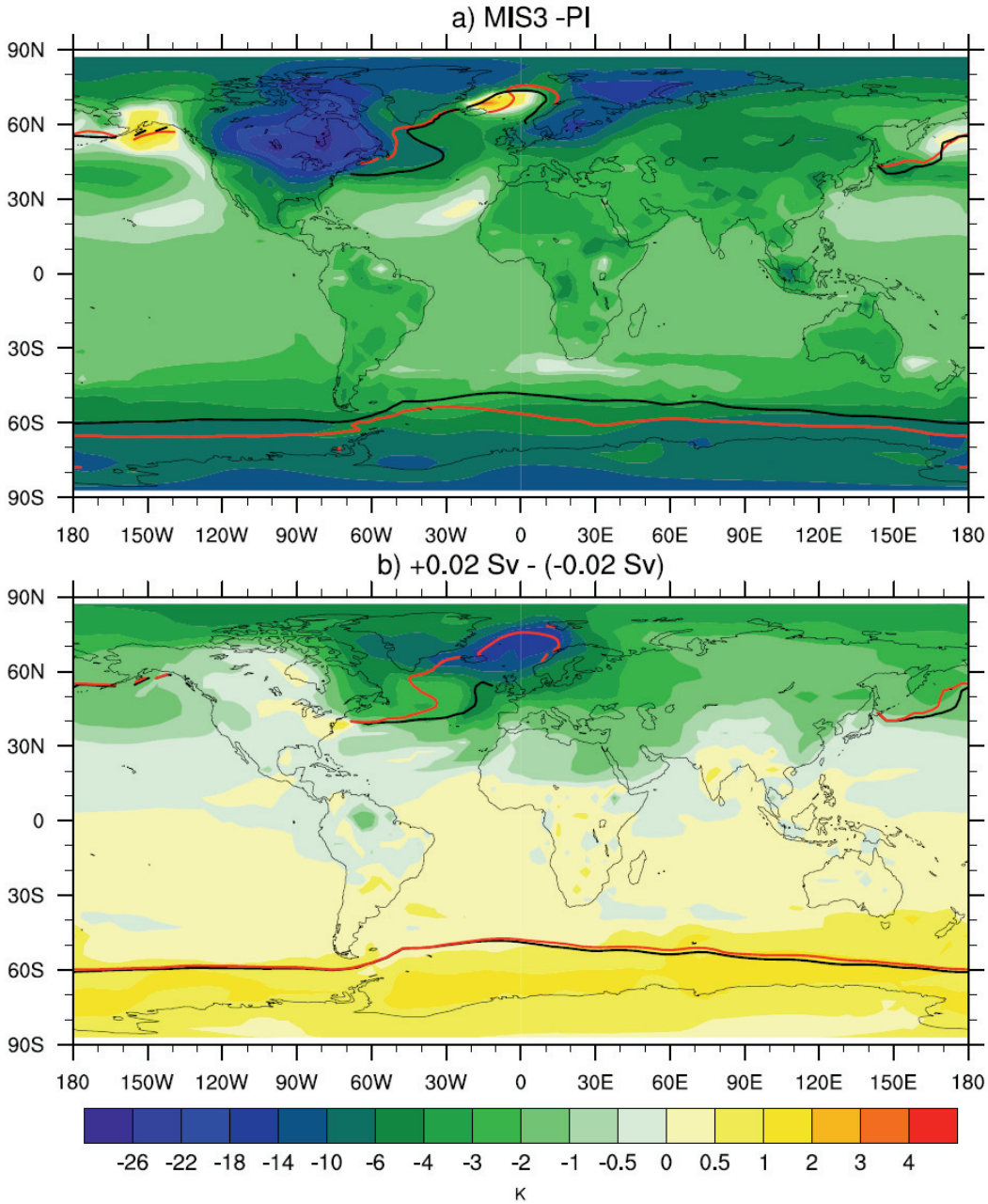

Fig. 1. Annual-mean surface temperature differences with winter (Dec-Feb mean) sea ice margins. a, Difference between the MIS3 baseline simulation with 38 ka BP boundary conditions and the pre-industrial control run. Black and red contour lines mark the winter sea ice margins (with 10% sea ice concentration) for the MIS3 and pre-industrial simulations, respectively. **b**, difference between the MIS3 freshwater perturbation experiments with +0.02 Sv and -0.02 Sv forcing interpreted as stadial-interstadial climate difference. Black and red contour lines mark the winter sea ice margins for the +0.02 Sv and -0.02 Sv experiments, respectively. Note the irregular contour intervals.

integration had to be extended (Fig. S1). The AMOC equilibrium response to freshwater forcing in our set of experiments reveals the existence of a threshold by an abrupt drop in AMOC strength for North Atlantic freshwater forcing between -0.02 Sv and +0.02 Sv, with a particularly sensitive behaviour between +0.01 Sv and +0.02 Sv (Fig. 3a). Comparing the climatic states just above (+0.02 Sv perturbation; Fig. 2c) and below (-0.02 Sv perturbation; Fig. 2d) the threshold reveals a maximum cooling in the +0.02 Sv experiment over the Nordic Seas (Fig. 1b) associated with an expansion of sea ice resulting in an increase of surface albedo and a decrease in ocean-atmosphere surface heat flux. In boreal winter, the sea-ice margin in the North Atlantic is dramatically displaced to mid-latitudes in response to the small positive freshwater forcing (Fig. 1b). While the surface ocean experiences strongest cooling in the northern North Atlantic, subsurface temperatures increase in these regions (Fig. S2).

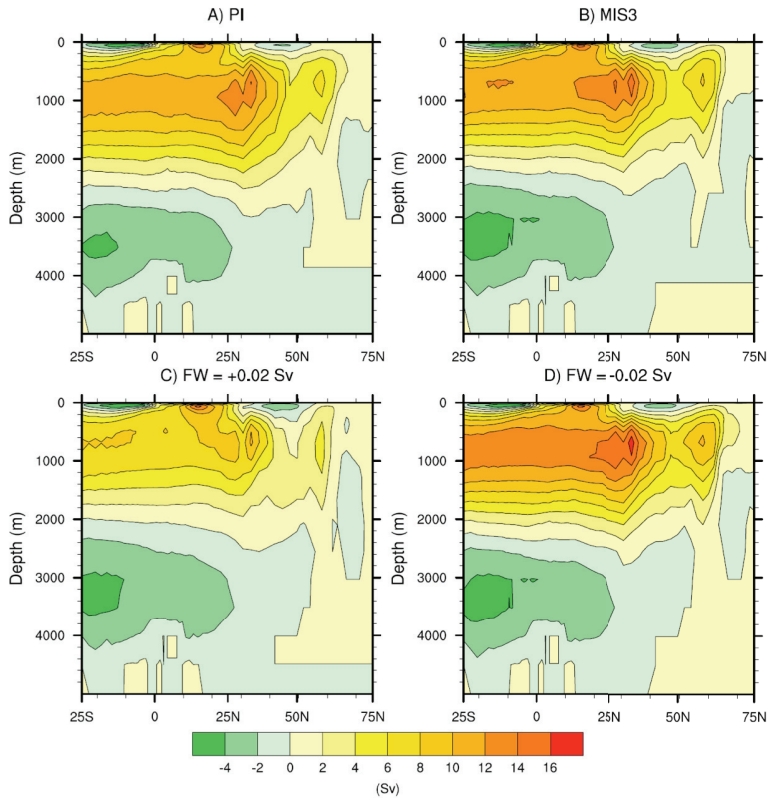

Fig. 2. Meridional overturning streamfunction of the Atlantic Ocean (annual mean) in different experiments. a, Pre-industrial control run. **b**, MIS3 baseline simulation. **c**, MIS3 freshwater-hosing experiment with +0.02 Sv perturbation. **d**, freshwater extraction experiment with -0.02 Sv forcing. Positive values indicate clockwise circulation.

In order to examine the AMOC for multiple equilibria, the +0.2Sv experiment was continued without anomalous freshwater forcing (see Experimental design). Upon removal of the freshwater perturbation the AMOC fully recovers, suggesting mono-stability of the MIS3 baseline AMOC (Fig. S3).

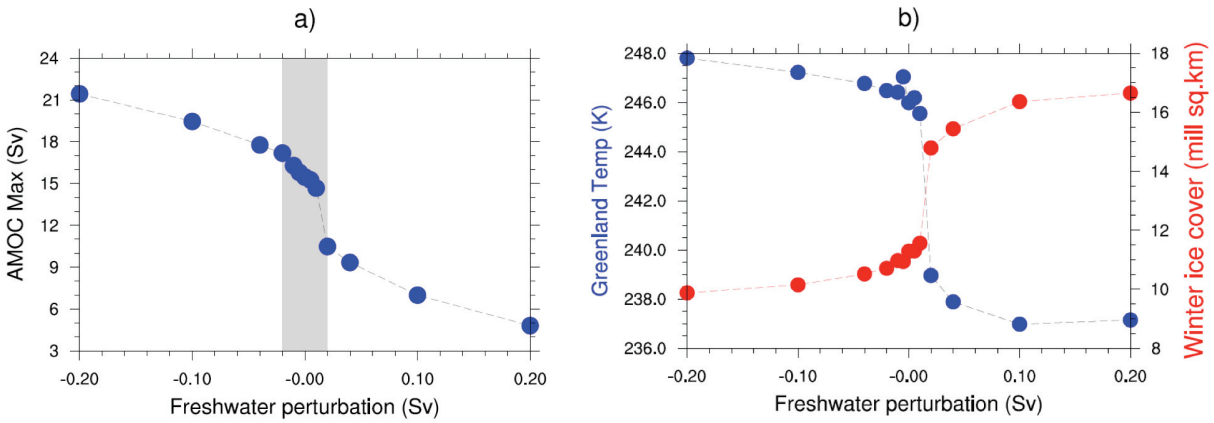

Fig. 3. Modelled climate changes as a function of freshwater perturbation. a, Strength of the equilibrated AMOC as a function of freshwater perturbation. The AMOC strength was defined as the maximum value of the overturning streamfunction below 300 m depth in the North Atlantic. Positive perturbations correspond to freshwater input to the Nordic Seas, whereas negative perturbations correspond to freshwater removal. The threshold between -0.02 Sv and +0.02 Sv is highlighted. **b**, annual-mean central Greenland surface temperature (blue) and winter (Dec-Feb mean) sea-ice area over the North Atlantic/Arctic Ocean (red) as a function of freshwater perturbation.

In summary, the MIS3 baseline state is very sensitive with respect to minor freshwater perturbations. A decrease (increase) to 10.6 Sv (17.2 Sv) of the AMOC strength in response to a weak positive (negative) freshwater forcing of 0.02 Sv is simulated (Fig. 3a). The associated difference in oceanic heat transport between these two states with reduced and intensified AMOC leads to a pronounced interhemispheric “seesaw pattern” [Stocker, 1998, Stocker and Johnsen, 2003] in surface temperature (Fig. 1b). More specifically, the annual-mean surface temperature over central Greenland is about 8 K lower in the +0.02 Sv experiment compared to the -0.02 Sv run, while Antarctica warms by about 0.5-1 K, consistent with the difference between an interstadial and a stadial climate state [EPICA community members, 2006, Huber et al., 2006].

4. Implications

Previous freshwater-hosing studies with comprehensive coupled climate models run under modern (interglacial) or Last Glacial Maximum (LGM; 21 ka BP) boundary conditions suggested a rather linear response of the AMOC to increasing freshwater perturbations without any obvious threshold effects [e.g. Rind et al., 2001, Otto-Bliesner and Brady, 2010]. By contrast, the MIS3 AMOC stability diagram constructed from the set of our freshwater perturbation experiments reveals a pronounced threshold for anomalous freshwater forcing between -0.02 Sv and +0.02 Sv (Fig. 3a). Consequently, the MIS3 baseline climate state is remarkably unstable with respect to minor freshwater perturbations which are an order of magnitude smaller than what is generally necessary to induce a substantial weakening of

the AMOC and associated Greenland cooling in climate models under modern or glacial boundary conditions [Rahmstorf et al., 2005, Stouffer et al., 2006, Valdes, 2011, Kageyama et al., 2013, Gong et al., 2013, Hopcroft et al., 2011], or what has been estimated as meltwater input during Heinrich events [Hemming, 2004].

In our MIS3 experiments, climate states below the freshwater perturbation threshold, with an AMOC strength of 16 Sv and more, are consistent with interstadial conditions, while climate states above the threshold, with an AMOC weaker than 11 Sv, correspond to stadial conditions. Our MIS3 baseline simulation yields an AMOC transport of about 15 Sv which is slightly stronger than in the PI control run. Previous MIS3 simulations using CCSM3 by Merkel et al. [2010] and Brandefelt et al. [2011] provided climate states with weaker North Atlantic overturning circulation of ~8 and ~11 Sv, respectively, and fully ice-covered Nordic Seas in winter, which have been interpreted as stadial climates in the absence of freshwater perturbations. Given the proximity of the MIS3 baseline climate to the AMOC stability threshold (Fig. 3a) we conjecture that minor differences in the modeled hydrologic cycles compared to our baseline experiment resulted in the simulation of stadial MIS3 equilibrium states in these earlier studies. Such minor differences in the hydrologic cycles may be caused not only by the use of different MIS3 boundary conditions (including ice-sheet distribution, greenhouse gas concentrations and orbital parameters) and CCSM3 grid resolutions [Brandefelt et al., 2011] but also by our modifications in the land model component including the implementation of interactive dynamic vegetation. Indeed, applying a negative freshwater forcing of -0.1 Sv to the MIS3 simulation of Merkel et al. [2010] resulted in a strengthening of the North Atlantic overturning to ~18 Sv [Merkel et al., 2010], which is similar to the AMOC intensity in our -0.1 Sv freshwater-extraction experiment (Fig. 3a). As such, our new results are consistent with the earlier MIS3 simulations using CCSM3. However, due to the proximity of the MIS3 baseline climate state to the AMOC stability threshold, we infer that the unperturbed “typical near-equilibrium” [Van Meerbeeck et al., 2009] MIS3 climate cannot unequivocally be assigned to a stadial [Merkel et al., 2010, Brandefelt et al., 2011], or interstadial [Van Meerbeeck et al., 2009] state.

For central Greenland, the simulated annual-mean surface temperature difference between stadial and interstadial climates is 8-11 K(Fig. 3b), in line with reconstructions from ice cores [Huber et al., 2006, Landais et al., 2004]. This temperature change over Greenland along with a concurrent anomaly in Antarctica of opposite sign is accomplished by relatively moderate changes in the AMOC in our CCSM3 experiments and lends further support to the bipolar seesaw concept as a characteristic of D-O events [Stocker and Johnsen, 2003]. Under modern boundary conditions, Greenland cooling larger than 6 K can usually only be achieved with a complete AMOC shutdown that often requires strong

freshwater forcing in the order of 1 Sv in coupled atmosphere-ocean models [Stouffer et al., 2006]. Atmosphere general circulation model experiments [Li et al., 2010] suggest that central Greenland surface temperature anomalies during D-O cycles are mainly controlled by winter sea-ice coverage in the Nordic Seas. Our experiments strongly corroborate this finding (Fig. 3b). Relatively warmer, interstadial conditions over Greenland are associated with reduced sea-ice cover in the northern North Atlantic, with major ice-free areas in the Nordic Seas even during winter. By contrast, during cold, stadial conditions over Greenland, the winter sea-ice margin shifts into the mid-latitude North Atlantic.

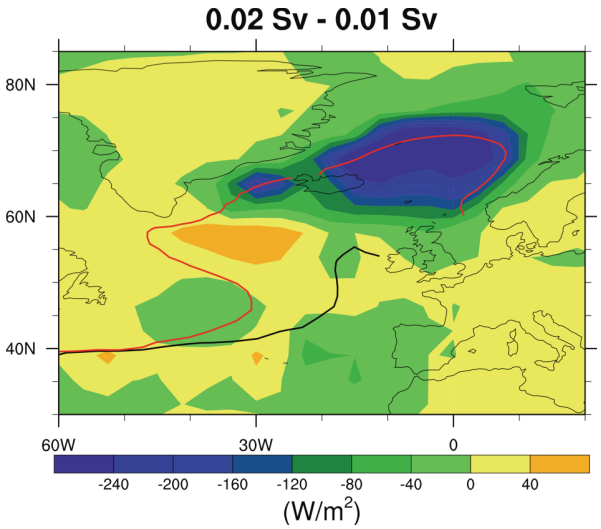

Fig. 4. Winter (December–February mean) surface heat flux anomaly. Shown is the heat flux difference between the MIS3 freshwater-hosing experiment with +0.02 Sv forcing and the one with +0.01 Sv forcing. Positive values indicate upward heat flux into the atmosphere. Black and red contour lines mark the Northern Hemisphere winter sea ice margins for the +0.02 Sv and +0.01 Sv experiments, respectively.

The most dramatic temperature drop over Greenland is found for freshwater perturbations between +0.01 Sv and +0.02 Sv accompanied by a substantial winter sea-ice expansion (Fig. 3b). A closer inspection of these two climate states reveals that the expansion of the winter sea-ice cover in the experiment with +0.02 Sv freshwater forcing results in a reduction of the surface heat flux from the Nordic Seas to the overlying atmosphere by more than 240 W m^{-2} compared to the +0.01 Sv experiment (Fig. 4), leading to a strong atmospheric cooling in that region during the winter months. The diabatic change is effectively distributed by wind and mixing around the Icelandic low, thereby affecting winter temperatures over the Greenland ice-sheet [cf. Li et al., 2010]. During winter, surface temperatures in central Greenland differ by ~10 K between the two experiments (not shown), whereas the difference in summer temperatures is minor (~2 K).

The close relationship between Nordic Seas' winter sea-ice cover and central Greenland temperature is also evident from the transient behavior in the AMOC recovery experiment (Fig. S3). More specifically, Greenland temperature rise (and fall) can occur at a much faster rate than changes in the AMOC strength (Fig. S3). Once the AMOC strength and its associated heat transport become large enough to substantially melt the sea ice, Greenland temperature-increase follows the sea-ice decline. However, the rise in Greenland temperature occurs on a centennial scale, which is significantly longer

than the multi-decadal timescale suggested by ice core temperature reconstructions [e.g. Ahn and Brook, 2007]. Whether this difference in timescales points to deficient (i.e. missing negative) freshwater forcing in the AMOC recovery experiment or to unresolved or missing processes in the climate model is beyond the scope of our study.Paleoceanographic data from the Nordic Seas indeed suggest ice-covered conditions during MIS3 stadials, while open-ocean convection requiring ice-free conditions has been inferred for MIS3 interstadials [Dokken and Jansen, 1999, Rasmussen and Thomsen, 2004]. Once the AMOC is weak enough (~10 Sv, i.e. above the freshwater flux threshold) and the Nordic Seas are fully ice-covered, further weakening of the AMOC has little effect on additional Greenland cooling (Fig. 3b), similar to results found by Ganopolski and Rahmstorf [2001] in their CLIMBER-2 experiments. This behavior is consistent with paleoceanographic and paleoclimatic evidence suggesting that an equivalent degree of cooling over Greenland was obtained during MIS3 stadials with different perturbations of deep-water formation [Elliot et al., 2002].

The sea-ice coverage in the northern North Atlantic, in turn, is linked to the strength of the AMOC. With weaker AMOC, less heat is transported by the ocean towards the north resulting in a southward displaced sea-ice margin. A larger sea-ice cover, on the other hand, inhibits convection and deep-water formation, thus acting as a positive feedback to the slow-down of the AMOC as pointed out by Lohmann and Gerdes [1998]. Coverage of convective sites by expanding sea ice may therefore induce non-linearity in the relationship between AMOC strength and freshwater perturbation. Shutdown of convection in the ice-covered Nordic Seas is the principle cause for the AMOC weakening in the stadial climate (cf. Fig. S4), similar to the key process in the EMIC study by Ganopolski and Rahmstorf [2001]. An important role for sea ice in abrupt millennial-scale climate change has also been suggested in previous studies [Broecker, 2000, Timmermann et al., 2003, Clement and Peterson, 2008, Montoya and Levermann, 2008, Banderas et al., 2012, Li et al., 2010, Gildor and Tziperman, 2003, Loving and Vallis, 2005, Oka et al., 2012].

In line with paleoceanographic evidence from the northern North Atlantic [Rasmussen and Thomsen, 2004, Marcott et al., 2011], our simulated stadial states exhibit large-scale subsurface oceanic warming in high northern latitudes (Fig. S2). It has been suggested that such subsurface warming during surface cold phases, in particular in the northwestern Atlantic, may have destabilized adjacent ice shelves, thus triggering ice-stream surges and producing massive iceberg discharge from the Laurentide ice sheet, referred to as Heinrich events, which would have led to further weakening of the AMOC [Marcott et al., 2011, Shaffer et al., 2004, Álvarez-Solas et al., 2011]. This scenario may provide a plausible mechanism for the coincidence of Heinrich events with D-O stadial phases.

Despite the existence of a distinct threshold in the AMOC stability diagram (Fig. 3a), we did not find evidence for the existence of multiple stable states under MIS3 boundary conditions in our simple AMOC recovery experiment. However, the existence of a narrow hysteresis, as in the EMIC study by Ganopolski and Rahmstorf [2001], cannot be ruled out. Whether the AMOC can generally possess multiple equilibria is an open question. It has been argued that bi-stability and associated irreversibility may be model-dependent [e.g. Ferreira et al., 2011, Hu et al., 2013] or model artifacts due to missing atmospheric feedbacks [Yin et al., 2006] or erroneous subgrid-scale parameterizations in the ocean [Prange et al., 2003, Nof et al., 2007].

Ice sheets have often been considered an important component of D-O dynamics. Records of ice-rafted debris indicating enhanced iceberg and hence freshwater fluxes into the Nordic Seas during each D-O stadial [Elliot et al., 2002, Dokken and Jansen, 1999, Voelker et al., 1998] – possibly related to internal coastal ice-sheet dynamics in east Greenland [van Kreveld et al., 2000] and/or Fennoscandia [Elliot et al., 2001] – support the notion that ice sheets played a role in producing the small positive freshwater flux anomalies that are required for crossing the AMOC stability threshold and thus to trigger D-O climate shifts. During interstadials, accumulation rates on continental ice-sheets increased [Anderson et al., 2006], possibly leading to a positive ice-sheet mass balance and net freshwater removal from the high-latitude northern ocean causing a negative freshwater forcing to the AMOC [Jackson et al., 2010].

5. Conclusions

The stability properties of the AMOC and associated climate impacts have been investigated systematically using a coupled general circulation model under MIS3 boundary conditions. We found that the MIS3 baseline climate is remarkably unstable such that minor North Atlantic freshwater perturbations in the order of 0.02 Sv can trigger dramatic changes in the strength of Atlantic overturning, leading to stadial-interstadial climate anomalies. The close linkage between North Atlantic sea-ice area and AMOC strength suggests a key role for sea ice in the instability of the AMOC. In addition, strong variations in Nordic Seas winter ice extent appear crucial for large D-O-type temperature anomalies (8-11 K in the annual average) in central Greenland, which is difficult to simulate when inappropriate (e.g. modern) boundary conditions are used in freshwater-hosing experiments. According to our model results, minor perturbations in the hydrologic cycle – possibly connected with ice-sheet dynamics – could have triggered substantial global D-O climate transitions. Even though the CCSM3 results are to a large extent consistent with earlier findings from an EMIC

study [Ganopolski and Rahmstorf, 2001] further MIS3 climate stability experiments with different state-of-the-art coupled general circulation models are required in order to assess the robustness of these results.

Acknowledgments

The authors thank Stefan Rahmstorf, Andrey Ganopolski and an anonymous reviewer for helpful comments that substantially improved the manuscript. This work has received funding through the DFG Research Center/Cluster of Excellence “The Ocean in the Earth System” at the University of Bremen. The CCSM3 climate model experiments were run on the SGI Altix Supercomputer of the “Norddeutscher Verbund für Hoch- und Höchstleistungsrechnen” (HLRN). Data are available at PANGAEA.

References:

Ahn, J., and E.J. Brook (2007), Atmospheric CO_2 and climate from 65 to 39 ka B.P., Geophys. Res. Lett., 34, L10703.

Álvarez-Solas, J., et al. (2011), Heinrich event 1: an example of dynamical ice-sheet reaction to oceanic changes, Clim. Past, 7, 1297–1306.

Andersen, K.K., et al. (2006), The Greenland Ice Core Chronology 2005, 15-42 ka. Part 1: constructing the time scale, Quat. Sci. Rev., 25, 3246–3257.

Banderas, R., J. Álvarez-Solas and M. Montoya (2012), Role of CO_2 and Southern Ocean winds in glacial abrupt climate change, Clim. Past, 8, 1011-1021, doi:10.5194/cp-8-1011-2012.

Bereiter et al., (2012), Mode change of millennial CO_2 variability during the last glacial cycle associated with a bipolar marine carbon seesaw, Proc. Natl. Acad. Sci. U. S. A., 109, 9755–9760.

Berger, A., (1978), Long term variations of daily insolation and Quaternary climatic changes, J. Atmos. Sci., 35(2), 2362–2367.

Bond, G., et al. (1993), Correlations between climate records from North Atlantic sediments and Greenland ice, Nature, 365,143–147.

Brandefelt, J., et al. (2011), A coupled climate model simulation of Marine Isotope Stage 3 stadial climate, Clim. Past, **7**, 649–670.

Broecker, W.S. (2000), Abrupt climate change: causal constraints provided by the paleoclimate record, Earth Sci. Rev., 51, 137–154.

Clement, A.C., and L.C. Peterson (2008), Mechanisms of abrupt climate change of the last glacial period, Rev. Geophys., 46(4), RG4002.

Colin de Verdière. A.M., J. Ben, and F. Sévellec (2006), Bifurcation structure of thermohaline millennial oscillations, J. Clim., 19, 5777–5795.

Collins, D.W., et al. (2006), The Community Climate System Model Version 3 (CCSM3), J. Clim., 19, 2122–2143.

Dansgaard, W., et al. (1993), Evidence for general instability of past climate from a 250-kyr ice-core record, Nature, 364, 218−220.

Dokken, T.M., and E. Jansen (1999), Rapid changes in the mechanism of ocean convection during the last glacial period, Nature, 401, 458–461.

Elliot, M., et al. (2001), Coherent patterns of ice-rafted debris deposits in the Nordic regions during the last glacial (10-60 ka), Earth Planet. Sci. Lett., 194,151-163.

Elliot, M.L., L. Labeyrie, and J.C. Duplessy (2002), Changes in North Atlantic deep-water formation associated with the Dansgaard-Oeschger temperature oscillations (60–10 ka), Quat. Sci. Rev., 21(10), 1153–1165.

EPICA Community Members, (2006), One-to-one coupling of glacial climate variability in Greenland and Antarctica, Nature, 444, 195–198.

Ferreira, D., J. Marshall, and B. Rose (2011), Climate determinism revisited: Multiple equilibria in a complex climate model, J. Clim., 24(4), 992–1012.

Flückiger, J., et al. (2004), N_2O and CH_4 variations during the last glacial epoch: Insight into global processes, Global Biogeochem. Cycles, 18, doi: 10.1029/2003GB002122.

Ganopolski, A., and S. Rahmstorf (2001), Rapid changes of glacial climate simulated in a coupled climate model, Nature, 409, 153–158.

Gildor, H., and E. Tziperman (2003), Sea-ice switches and abrupt climate change, Philos. Trans. R. Soc. London Ser. A 361, 1935–1942.

Gong, X., et al. (2013), Dependence of abrupt Atlantic meridional ocean circulation changes on climate background states, Geophys. Res. Lett., 40, 3691-3704.

Handiani, D., et al. (2013), Tropical vegetation response to Heinrich Event 1 as simulated with the UVic ESCM and CCSM3, Clim. Past, 9, 1683-1696, doi:10.5194/cp-9-1683-2013.

Hemming, S.R., (2004), Heinrich events: massive late Peistocene detrius layers of the North Atlantic and their global climate imprint, Rev. Geophys., 42, RG1005, doi:10.1029/2003RG000128.

Hopcroft, P.O., P.J. Valdes and D.J. Beerling (2011), Simulating idealized Dansgaard-Oeschger events and their potential impacts on the global methane cycle, Quat. Sci. Rev., 30, 3258-3268.

Hu, A., G.A. Meehl, W. Han, J. Lu, W.G. Strand (2013), Energy balance in a warm world without the ocean conveyor belt and sea ice, Geophys. Res. Lett., 40(23), 6242-6246, doi:10.1002/2013GL058123.

Huber, C., et al. (2006), Isotope calibrated Greenland temperature record over Marine Isotope Stage 3 and its relation to CH_4, Earth Planet. Sci. Lett., 243, 504–519.

Jackson, C.S., et al. (2010), A box model test of the freshwater forcing hypothesis of abrupt climate change and the physics governing ocean stability, Paleoceanography, 25, PA4222, doi:10.1029/2010PA001936.

Kageyama, M., et al. (2013), Climatic impacts of fresh water hosing under Last Glacial Maximum conditions: a multi-model study, Clim. Past, 9, 935-953.

Keigwin, L.D., and E.A. Boyle (1999), Surface and deep ocean variability in the northern Sargasso Sea during marine isotope stage 3, Paleoceanography, 14, doi:10.1029/1998PA900026.

Knorr, G., and G. Lohmann (2003), Southern ocean origin for the resumption of Atlantic thermohaline circulation during deglaciation, Nature, 424, 532-536.

Landais, A., et al. (2004), Quantification of rapid temperature change during DO event 12 and phasing with methane inferred from air isotopic measurements, Earth Planet. Sci. Lett., 225, 221-232.

Levis, S., et al. (2004), The community land model's dynamic global vegetation model (CLM-DGVM): technical description and user's guide, NCAR Technical Note NCAR/TN-459+STR, National Center for Atmospheric Research, Boulder, CO, 50 pp.

Li, C., et al. (2010), Can North Atlantic Sea Ice Anomalies Account for Dansgaard–Oeschger Climate Signals? J. Clim., 23, 5457–5475.

Lohmann, G., and R. Gerdes (1998), Sea ice effects on the sensitivity of the thermohaline circulation in simplified atmosphere-ocean-sea ice models. J. Climate 11, 2789-2803.

Loving, J.L., and G.K. Vallis (2005), Mechanisms for climate variability during glacial and interglacial periods, Paleoceanography, 20, PA4024, doi:10.1029/2004PA001113.

Marcott, S.A., et al. (2011), Ice-shelf collapse from subsurface warming as a trigger for Heinrich events, Proc. Natl. Acad. Sci. U.S.A., 108, 13415–13419.

Merkel, U., M. Prange and M. Schulz (2010), ENSO variability and teleconnections during glacial climates, Quat. Sci. Rev., 29, 86-100.

Montoya, M., and A. Levermann (2008), Surface wind-stress threshold for glacial Atlantic overturning, Geophys. Res. Lett., 35, L03608, doi:10.1029/2007GL032560.

Nof, D., S. Van Gorder and A.M. De Boer (2007), Does the Atlantic meridional overturning cell really have more than one stable steady state? Deep-Sea Res., I 54(11), 2005–2021.

Oka, A., H. Hasumi and A. Abe-Ouchi (2012), The thermal threshold of the Atlantic meridional overturning circulation and its control by wind stress forcing during glacial climate, Geophys. Res. Lett., 39, L09707, doi:10.1029/2012GL051421.

Oleson, K.W. et al. (2004), Technical description of the Community Land Model (CLM), NCAR Technical Note NCAR/TN-461+STR, National Center for Atmospheric Research, Boulder, CO, 173 pp.

Oleson, K.W., et al. (2008), Improvements to the Community Land Model and their impact on the hydrological cycle, J. Geophys. Res., 113, G01021, doi:10.1029/2007JG000563.

Otto-Bliesner, B., et al. (2006), Last Glacial Maximum and Holocene Climate in CCSM3, J. Clim., 19, 2526–2544.

Otto-Bliesner, B.L., and E.C. Brady (2010), The sensitivity of the climate response to the magnitude and location of freshwater forcing: last glacial maximum experiments, Quat. Sci. Rev., 29, 56-73.

Peltier, W.R., (2004), Global glacial isostasy and the surface of the ice-age Earth: The ICE-5G (VM2) model and GRACE, Annu. Rev. Earth Planet. Sci., 32, 111-149.

Prange, M., V. Romanova, and G. Lohmann (2002), The glacial thermohaline circulation: Stable or unstable? Geophys. Res. Lett., 29(21), 2028, doi:10.1029/2002GL015337.

Prange, M., G. Lohmann and A. Paul (2003), Influence of vertical mixing on the thermohaline hysteresis: Analyses of an OGCM, J. Phys. Oceanogr., 33(8),1707-1721.

Prange, M., and R. Gerdes (2006), The role of surface freshwater flux boundary conditions in Arctic Ocean modelling, Ocean Modelling, 13, 25-43.

Rahmstorf, S., et al. (2005), Thermohaline circulation hysteresis: A model intercomparison, Geophys. Res. Lett., 32, L23605, doi:10.1029/2005GL023655.

Rasmussen, T.L., and E. Thomsen (2004), The role of the North Atlantic Drift in the millennial timescale glacial climate fluctuations, Palaeogeogr. Palaeoclimatol. Palaeoecol., 210, 101–116.

Rind, D., et al. (2001), Effects of glacial meltwater in the GISS coupled atmosphere-ocean model: Part I: North Atlantic Deep Water response, J. Geophys. Res., 106, 27335-27353, doi:10.1029/2000JD000070.

Sarnthein, M., et al. (2001), Fundamental modes and abrupt changes in North Atlantic circulation and climate over the last 60 ky—Concepts, reconstructions and numerical modeling, The Northern North Atlantic: A Changing Environment, edited by P. Schäfer et al., pp. 365–410, Springer-Verlag, New York.

Schmittner, A., M. Yoshimori, and A.J. Weaver (2002), Instability of glacial climate in a model of the ocean-atmosphere-cryosphere system, Science, 295, 1489-1493.

Schulz, M. (2002), On the 1470-year pacing of Dansgaard-Oeschger warm events, Paleoceanography, 17(2), doi:10.1029/2000PA000571.

Shaffer, G., S.O. Malskaer and C.J. Bjerrum (2004), Ocean subsurface warming as a mechanism for coupling Dansgaard-Oeschger climate cycles and ice-rafting events, Geophys. Res. Lett., 31, L24202, doi:10.1029/2004GL020968

Spahni, R., et al. (2005), Atmospheric methane and nitrous oxide of the late Pleistocene from Antarctic ice cores, Science, 310, 1317–1321.

Stocker T.F., and D.G. Wright (1991), Rapid transitions of the ocean's deep circulation induced by changes in the surface water fluxes, Nature, 351, 729-732.

Stocker, T.F., (1998), The seesaw effect, Science, 282, 61-62.

Stocker, T. F., and S. J. Johnsen (2003), A minimum thermodynamic model for the bipolar seesaw, Paleoceanography, 18(4), 1087.

Stouffer, R.J., et al. (2006), Investigating the causes of the response of the thermohaline circulation to past and future climate changes, J. Clim., 19, 1365–1387.

Timmermann, A., et al. (2003), Coherent resonant millennial-scale climate oscillations triggered by massive meltwater pulses, J. Clim., 16, 2569–2585, doi:10.1175/1520-0442(2003)016<2569:CRMCOT>2.0.CO;2.

Valdes, P., (2011), Built for stability, Nat. Geosci., 4(7), 414–416.

van Kreveld, S.A., et al. (2000), Potential links between surging ice sheets, circulation changes, and the Dansgaard-Oeschger cycles in the Irminger Sea, 60-18 kyr, Paleoceanography, 15, doi:10.1029/1999PA000464.

Van Meerbeeck, C.J., H. Renssen, and D.M. Roche (2009), How did Marine Isotope Stage 3 and Last Glacial Maximum climates differ? – perspectives from equilibrium simulations, Clim. Past, 5, 33–51.

Voelker, A.H.L., et al. (1998), Correlation of marine ^{14}C ages from the Nordic Seas with the GISP2 isotope record: implications for ^{14}C calibration beyond 25 ka BP, Radiocarbon, 40(1), 517–34.

Voelker, A.H.L., and workshop participants (2002), Global distribution of centennial-scale records for marine istope state (MIS) 3: a database, Quat. Sci. Rev., 21, 1185–1214.

Yeager, S.G., et al. (2006), The low-resolution CCSM3, J. Clim., 19, 2545–2566.

Yin, J., et al (2006), Is a shutdown of the thermohaline circulation irreversible? J. Geophys. Res., 111, D12104, doi:10.1029/2005JD006562.

Supplementary Figures

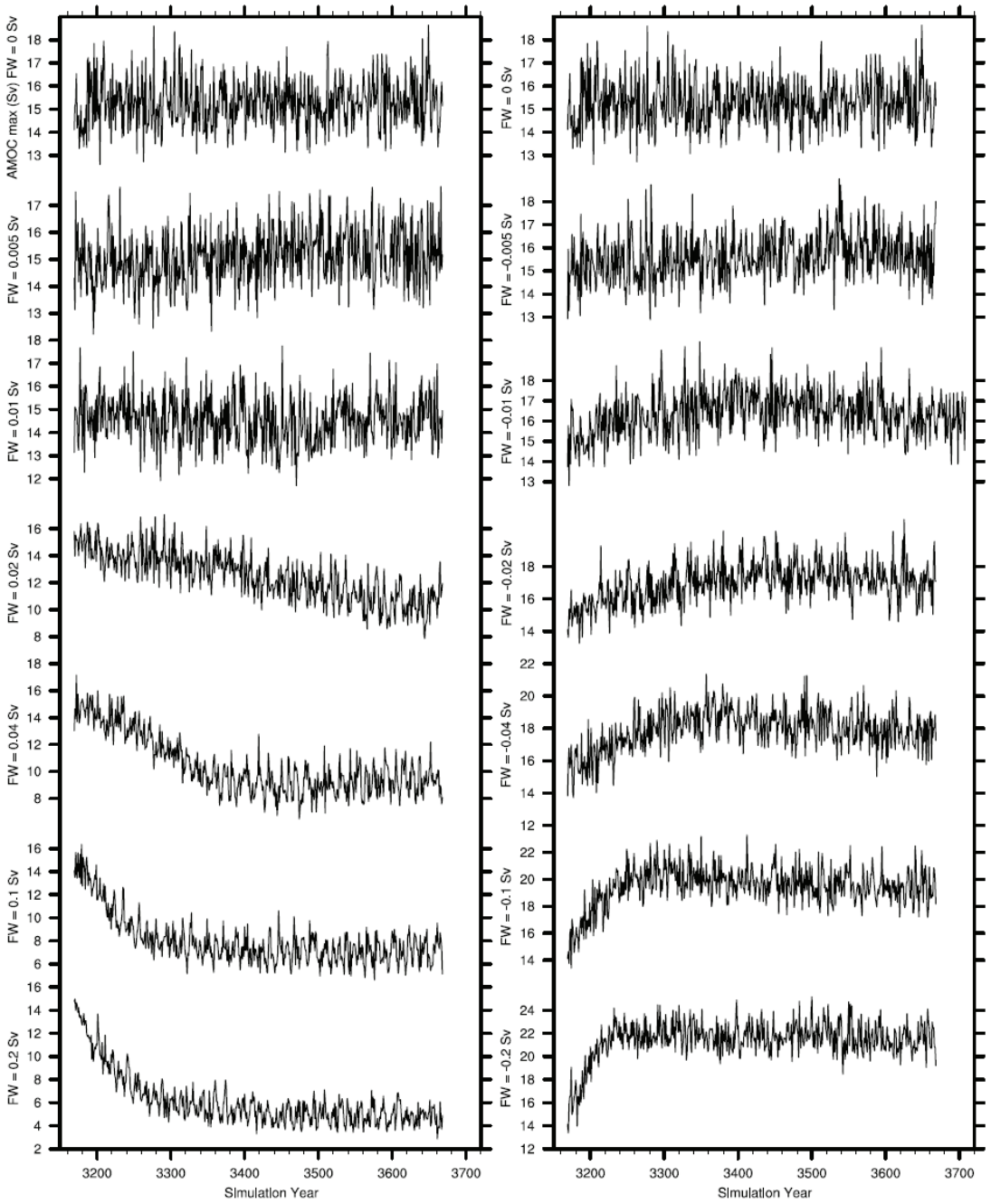

Fig. S1. Time series of the maximum in the annual-mean North Atlantic overturning streamfunction (below 300 m) from the last 500 years of the MIS3 control run (top) and the twelve freshwater hosing (left) and extraction (right) experiments. Starting at model year 3170 (see Methods) each experiment was run for 500 years. From the last 100 years of each experiment, the trend in the overturning time series was calculated based on linear regression and statistical significance at the 0.05 level was assessed via a Student t-test. Only in case the null hypothesis (being that there is no trend) was rejected the experiment was continued until the trend disappeared (again assessed by a t-test based on 100 years linear regression). A continuation was only necessary for the -0.01 Sv experiment

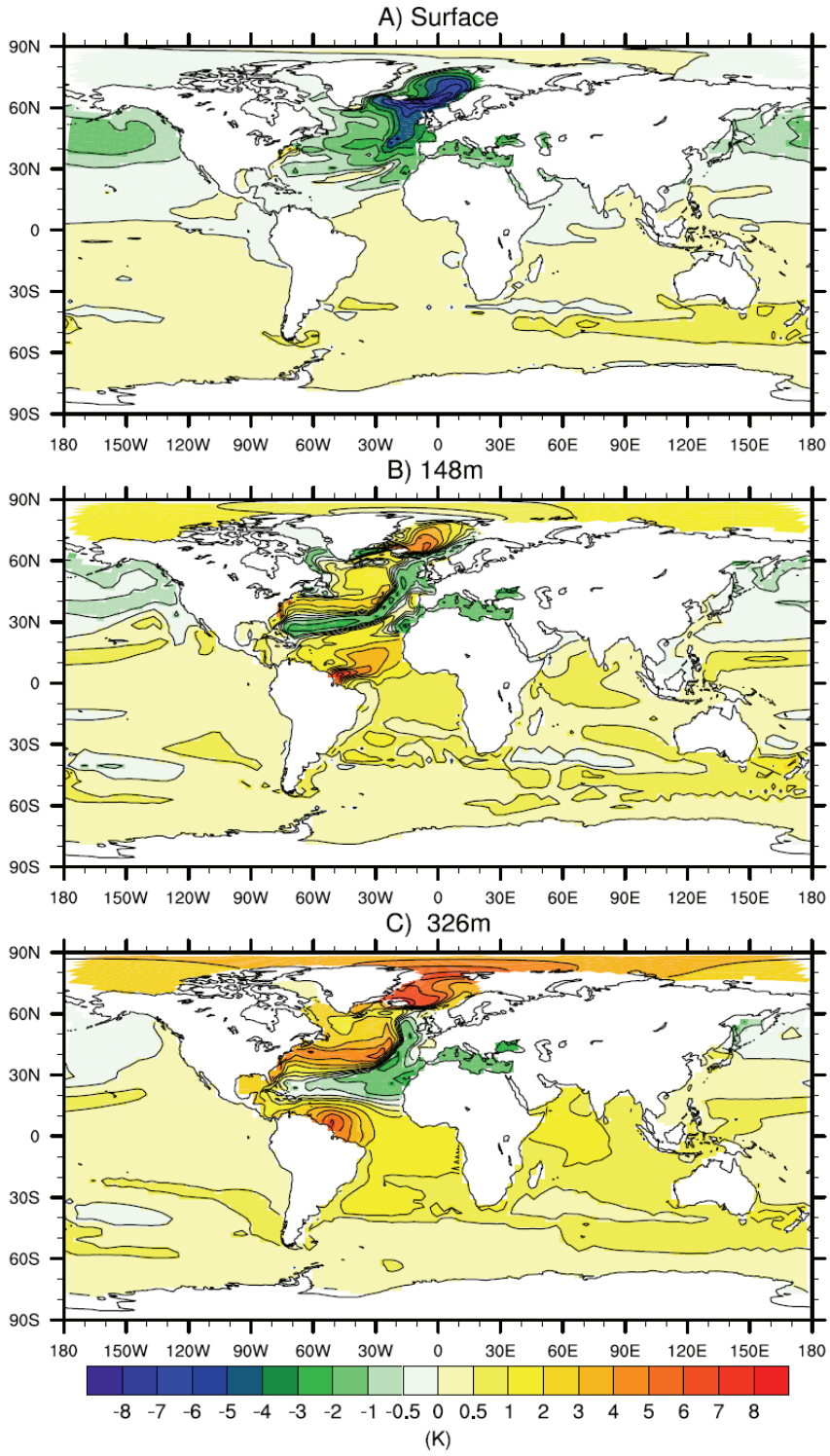

Fig. S2. Annual-mean ocean temperature differences between the MIS3 freshwater perturbation experiments with +0.02 Sv and -0.02 Sv forcing. a, Sea surface. **b**, 148 m depth. **c**, 326 m depth. The differences are interpreted as stadial-interstadial climate anomalies.

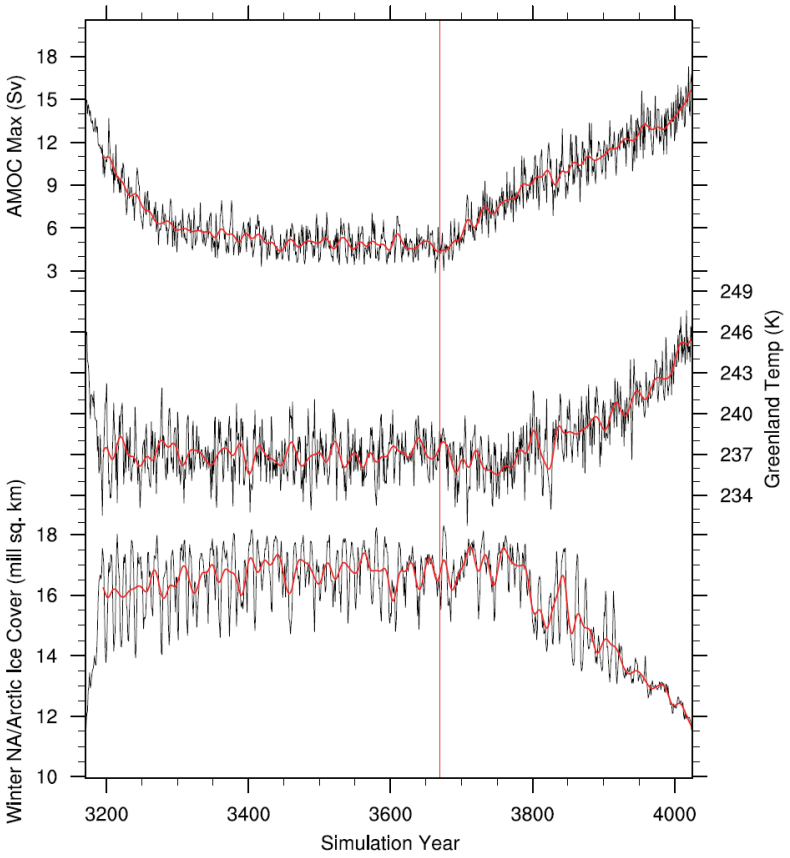

Fig. S3. Continuation of the 500-year long +0.2 Sv freshwater-hosing experiment after removal of the freshwater perturbation. Shown is the time series of the maximum in the annual-mean North Atlantic overturning streamfunction (below 300 m) along with annual-mean central Greenland surface temperature and winter sea-ice area over the North Atlantic/Arctic Ocean. The red line marks the end of the water hosing.

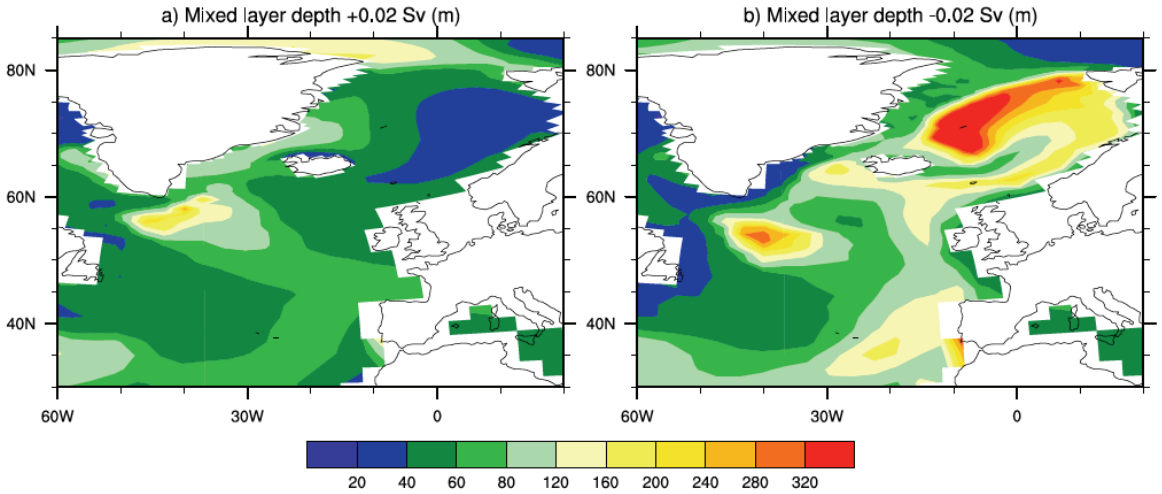

Fig. S4. Annual-mean mixed layer depths. a, MIS3 freshwater perturbation experiment with +0.02 Sv forcing (stadial climate). **b,** MIS3 freshwater perturbation experiment with -0.02 Sv forcing (interstadial climate). The mixed layer depths reveal shutdown of convection in the Nordic Seas in the stadial climate state

Chapter 3

Spatial fingerprint and magnitude of changes in the Atlantic meridional overturning circulation during Marine Isotope Stage 3

Xiao Zhang, Matthias Prange, Ute Merkel, Michael Schulz

MARUM - Center for Marine Environmental Sciences and Faculty of Geosciences,
University of Bremen
Leobener Str., 28359 Bremen, Germany

Email: xzhang@marum.de

Key points

Global footprint of MIS3 ocean temperature anomalies to AMOC changes

Combination of model results with SST records to estimate MIS3 AMOC changes

About 9 Sv change in AMOC strength between stadial and interstadial states

Key Words:

Atlantic Meridional Overturning Circulation, Marine Isotope Stage 3, Dansgaard-Oeschger cycles, Global climate modeling

Abstract

Pronounced millennial-scale climate variability during Marine Isotope Stage 3 (MIS3) is considered to be linked to changes in the state of the Atlantic meridional overturning circulation (AMOC), i.e. a warm interstadial/cold stadial state corresponds to a strong/weak AMOC. Based on a series of freshwater hosing/extraction experiments with the state-of-the-art climate model CCSM3, we construct a global spatial fingerprint of oceanic temperature anomalies in response to AMOC changes under MIS3 boundary conditions. Highest sensitivity to AMOC changes, especially in summer, is found in northeastern North Atlantic sea surface temperature, but a characteristic temperature fingerprint is also found at subsurface levels. After testing significance of the linear SST-AMOC regressions, the model results are combined with paleo-SST records to estimate the magnitude of millennial-scale Dansgaard-Oeschger AMOC variations during MIS3. The results suggest a difference in AMOC strength between interstadial and (non-Heinrich) stadial states of 9.2 ± 1.2 Sv (1σ).

1. Introduction

The Atlantic meridional overturning circulation (AMOC) is a major component of the global climate system regulating the distribution of heat as well as the cycling of carbon and other nutrients [e.g. Ganachaud and Wunsch, 2000; Johns et al., 2011]. Due to its high relevance for the climate system, many studies attempted to quantify changes in AMOC strength during the last glacial and deglaciation based on proxy records and climate models [e.g. LeGrand and Wunsch, 1995; Winguth et al., 2000; Gebbie and Huybers, 2006; Lynch-Stieglitz et al., 2007; Ritz et al., 2013]. Pronounced millennial-scale climate variability during Marine Isotope Stage 3 (MIS3; 57-29 thousand years before present [ka B.P.]), characterized by transitions between cold stadials and warm interstadials at northern latitudes [Dansgaard et al., 1993; Bond et al., 1993] and termed Dansgaard-Oeschger (D-O) cycles, are most likely related to changes in AMOC strength [e.g. Keigwin and Boyle, 1999; Broecker, 2000; Sarnthein et al., 2001; *Elliot et al., 2002*; Rahmstorf, 2002; EPICA community members, 2006]. A warm interstadial state corresponds to a strong circulation, while a cold stadial state is characterized by a weak circulation. Probably the most dramatic disruptions of the glacial AMOC are associated with massive layers of ice-rafted debris in the North Atlantic during so-called Heinrich stadials [e.g. Broecker et al., 1992; Grousset et al., 1993; Hemming, 2004; McManus et al., 2004].

Despite the importance of AMOC changes in shaping millennial-scale climate variability during MIS3, the magnitude of changes in circulation strength necessary to cause stadial-interstadial climate transitions is not known. Combining climate model simulations with marine proxy records, Ritz et al. [2013] recently presented an estimate for AMOC variations during the last deglaciation based on a linear relationship between Atlantic sea surface temperatures (SST) and AMOC strength. Their results suggest millennial-scale reductions in AMOC strength of ~14 Sv (1 Sv = 10^6 m^3/s) and ~12 Sv during Heinrich event 1 and the Younger Dryas stadial, respectively. Here, we adopt the strategy of combining SST reconstructions with climate model experiments to estimate the magnitude of differences in AMOC strength between MIS3 stadial states and interstadial states. To this end, we use a set of MIS3 freshwater hosing/extraction experiments using the comprehensive coupled climate model CCSM3 [Xiao Zhang et al., 2014] to construct a global spatial fingerprint of oceanic temperature anomalies in response to AMOC changes. After testing the significance of linear temperature-AMOC regressions, we identify optimal locations for temperature reconstructions for an estimate of MIS3 AMOC variability.

2. Model Descriptions and Experimental Design

The Community Climate System Model version 3 (CCSM3) is a global coupled general circulation model (CGCM) consisting of the four components atmosphere, land, ocean and sea ice [Collins et al., 2006; Yeager et al., 2006]. We use the atmospheric component (Community Atmosphere Model version 3) with T31 horizontal resolution (3.75° transform grid) and 26 levels in the vertical. The Community Land Model (version 3) has the same horizontal resolution as the atmosphere and contains 10 subsurface soil levels. New parametrizations of canopy interception and soil evaporation have been applied to the land model [Oleson et al., 2008], and the Dynamic Global Vegetation Model [Levis et al., 2004] was activated in our simulations [cf. Handiani et al., 2013; Mohtadi et al., 2014]. The ocean component (Parallel Ocean Program) has 25 layers with layer thickness increasing from 8 m at the surface to around 500 m at the ocean bottom. The nominal horizontal resolution is 3° with latitudinal grid refinement of 0.9° around the equator and the North Pole displaced over Greenland [cf. Smith et al., 1995]. The Community Sea Ice Model shares the same horizontal resolution with the ocean component.

A MIS3 baseline simulation centered at 38 ka B.P. (time slice right in the middle of a rather regular sequence of D-O cycles) was performed with 38 ka B.P. orbital forcing [Berger, 1978], corresponding greenhouse gas concentrations of CO_2 (215 ppmv), CH_4 (501 ppbv), and N_2O (234 ppbv) [Flückiger et al., 2004; Spahni et al., 2005; Ahn and Brook, 2007; Bereiter et al., 2012], the 38 ka B.P. ICE-5G continental ice sheet distribution [Peltier, 2004] as well as a correspondingly modified land-sea distribution (e.g., closed Bering Strait due to a reduced sea level). Under these boundary conditions, 12 freshwater hosing/extraction experiments were carried out which all branched off from the equilibrated MIS3 baseline simulation [Xiao Zhang et al., 2014]. Different rates of continuous, unbalanced surface freshwater fluxes (homogeneously distributed over the Nordic Seas and treated as virtual salinity fluxes [e.g. Prange and Gerdes, 2006], ranging from ± 0.005 Sv to ± 0.2 Sv, were applied in these hosing (positive freshwater flux into the ocean) and extraction (negative freshwater flux) experiments. Although there is evidence from records of ice-rafted debris for enhanced iceberg and hence freshwater fluxes into the Nordic Seas during D-O stadials [e.g. Dokken and Jansen, 1999; van Kreveld et al., 2000; Elliot et al., 2002], we note that other potential forcing mechanisms for D-O climate transitions may exist and have been discussed in the literature [e.g., Xu Zhang et al., 2014; Peltier and Vettoretti, 2014, and references therein]. Independent of the real D-O trigger mechanism,

freshwater forcing in the present study can be considered a pragmatic way of creating a set of different MIS3 stadial and interstadial climate states.

Integration times were 500-550 years for each hosing/extraction experiment. For further details on the initialization of model simulations and integration lengths the reader is referred to Xiao Zhang et al. [2014]. Analyses of the 13 (quasi-)equilibrium states are based on the last 100-year mean climatologies of each experiment.

3. AMOC response to freshwater forcing

In the 38 ka B.P. baseline run, the strength of the AMOC (defined as the maximum of the meridional streamfunction below 300 m in the North Atlantic Ocean) is around 15.4 Sv, which is ~1.5 Sv stronger than in a modern (pre-industrial) control run, with a southward flow of North Atlantic deep water occuring at shallower levels compared to modern [Xiao Zhang et al., 2014]. The inflow of warm and salty Atlantic water from the south keeps large parts of the Nordic Seas ice free and maintains convection and deep water formation during winter. The MIS3 baseline state is very sensitive with respect to minor freshwater perturbations. The AMOC equilibrium response to freshwater forcing in our set of experiments reveals the existence of a threshold by an abrupt drop in AMOC strength for North Atlantic freshwater forcing between -0.02 Sv and +0.02 Sv. A decrease to ~11 Sv of the AMOC strength in response to a weak positive freshwater forcing of 0.02 Sv was simulated. In contrast, AMOC strength increases to ~17 Sv upon a negative forcing of 0.02 Sv. The surface air temperature difference in central Greenland between these two climate states is about 8 K in the annual mean [Xiao Zhang et al., 2014]. With the maximum freshwater forcing in our experiments of +0.2 Sv, the AMOC drops to 4.9 Sv within ~150 model years. We note that this magnitude of freshwater forcing is consistent with estimates of the order of magnitude of meltwater influx during Heinrich stadials [Hemming, 2004].

4. Ocean equilibrium temperature response to AMOC change

Relative to the 38 ka B.P. baseline experiment, SST anomalies exhibit a bipolar seesaw pattern in all freshwater hosing (extraction) experiments, featuring a general cooling (warming) in the Northern

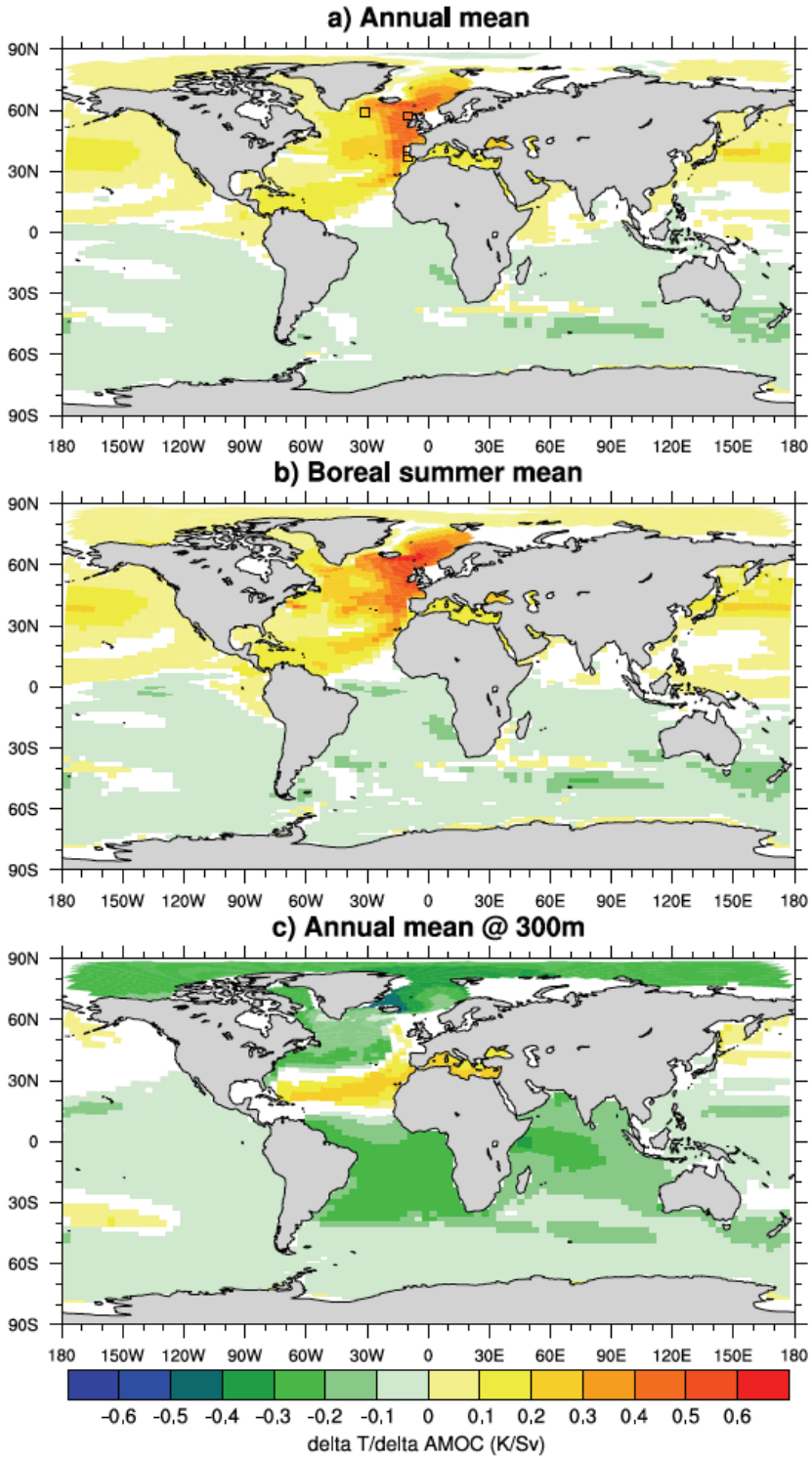

Figure 1. Ocean temperature changes in response to changes in annual mean AMOC strength as given by the least-squares regression slopes calculated from the equilibrium states of the set of MIS3 freshwater hosing/extraction experiments for (a) annual mean SST, (b) boreal summer (June-July-August; JJA) SST, and (c) 300 m depth annual mean. Locations which do not show significant ($p<0.05$) linear temperature-AMOC regression according to an ANOVA F-test are white. Frames in panel (a) show the locations of marine sediment cores providing high-resolution MIS3 temperature reconstructions (see text; Table 1).

and a warming (cooling) in the Southern Hemisphere due to a reduced (enhanced) northward heat transport in the Atlantic Ocean [Crowley, 1992; Stocker and Johnsen, 2003]. We determine the global fingerprint of ocean temperature anomalies in response to AMOC changes by linear least-squares regression analysis using the 13 MIS3 equilibrium climate states. Significance of the linear temperature-AMOC (i.e. temperature on AMOC) regressions is tested by an ANOVA (Analysis of variance) F-test [e.g. Li, 1964; Davis, 1986].

At the surface, the strongest response (i.e. the largest regression coefficient or slope) occurs in the northeastern North Atlantic (Fig. 1a; annual mean). Here, SST increases more strongly with increasing AMOC strength than in any other region of the Northern Hemisphere. The signal is advected towards the tropics along the eastern margin of the North Atlantic via the Canary Current as already described in earlier freshwater hosing model studies [e.g. Lohmann, 2003; Prange et al., 2004]. Despite the use of different models and boundary conditions, maximum sensitivities of SST upon AMOC change in the northern North Atlantic and along the eastern North Atlantic margin have also been found in previous studies [e.g. Heslop and Paul, 2012; Ritz et al., 2013].

During boreal summer, the SST sensitivity to AMOC change is even larger in the northern North Atlantic region than in the annual mean (Fig. 1b), which can mainly be attributed to sea-ice effects in winter. For a weak AMOC (i.e. smaller than ~11 Sv), large areas in the northern North Atlantic are ice-covered in winter [Xiao Zhang et al., 2014] such that further reduction in AMOC strength does not lead to further sea surface cooling once the freezing point is reached. This leads to a smaller SST-AMOC regression slope in winter and, hence, in the annual mean. Apart from the North Atlantic realm, differences between the annual mean and the boreal summer SST response are small (Fig. 1a,b). For instance, in both cases the zero line of the regression slope (i.e. the “seesaw’s fulcrum”) resides between 10°N and 20°N in the eastern North Atlantic, consistent with proxy evidence [Zarriess et al., 2011].

At subsurface levels the ocean temperature response pattern to AMOC changes is very different compared to the surface. As an example, Fig. 1c shows the linear regression coefficients at 300 m depth. Except for the subtropical North Atlantic region, where the subsurface temperature response resembles the surface signal due to advection of water masses from the northeastern North Atlantic by the subtropical gyre, subsurface temperatures decrease (increase) with increasing (decreasing) AMOC strength everywhere in the Atlanic Ocean. Subsurface and deep ocean warming in response to past AMOC slowdowns is evidenced by several proxy records from the Atlantic realm [*Rasmussen and Thomsen, 2004; Rühlemann et al., 2004; Lopes dos Santos et al., 2010; Marcott et al., 2011;*

Schmidt et al., 2012]. In the northern North Atlantic/Nordic Seas the subsurface warming can be attributed to heat accumulation in these ocean layers as vertical mixing by convection is reduced or even shut down. The subsurface signal is transmitted globally due to a global thermocline adjustment by baroclinic waves [Huang et al., 2000; Goodman, 2001; Cessi et al., 2004; Zhang et al., 2012], though the subsurface temperature response becomes relatively small in the Pacific Ocean. We note that subsurface warming in high northern latitudes during stadials has been suggested to destabilize adjacent ice shelves and, thus, to trigger ice stream surges producing Heinrich events [Marcott et al., 2011; Shaffer et al., 2004; Álvarez-Solas et al., 2011].

5. Estimating the magnitude of AMOC variations during MIS3

Having constructed the spatial fingerprint of ocean temperature anomalies with respect to AMOC changes, we attempt to estimate the magnitude of AMOC variations during MIS3 using SST reconstructions from sites of highest temperature sensitivities (i.e. largest regression slopes) to AMOC changes. Apart from being obtained in regions of highest SST sensitivity, the proxy records need to cover a substantial part of MIS3 (with a sufficient number of stadial and interstadial intervals for a reasonable statistical analysis) and must be of sufficiently high resolution such that D-O stadials and interstadials can unambiguously be identified and are captured by several data points each.

We identified four high-resolution records that fulfill the required criteria, clearly showing D-O cycles during MIS3 in annual mean or summer temperature from the highly sensitive northern/northeastern Atlantic region (Fig. 1a): Irminger Sea core SO82-5 (summer SST derived from planktic foraminiferal assemblages using SIMMAX modern analog technique transfer function [van Kreveld et al., 2000]), northeast Atlantic (eastern Rockall Trough) core MD95-2006 (summer SST derived from planktic foraminiferal assemblage counts using Artifical Neural Network technique [Dickson et al., 2008]), Iberian margin core MD95-2040 (summer SST derived from planktic foraminiferal assemblages using SIMMAX modern analog technique [de Abreu et al., 2003]), and Iberian margin core MD01-2444 (annual mean SST based on alkenone unsaturation index $U^{k'}_{37}$ [Martrat et al., 2007]). All SST records cover the entire MIS3, except for the record of MD95-2006, which only covers the interval 56-40 ka B.P.

Estimating the magnitude of AMOC variations using reconstructed SST changes further requires linearity of the AMOC-SST relationship (i.e., the SST sensitivity must be independent of the AMOC

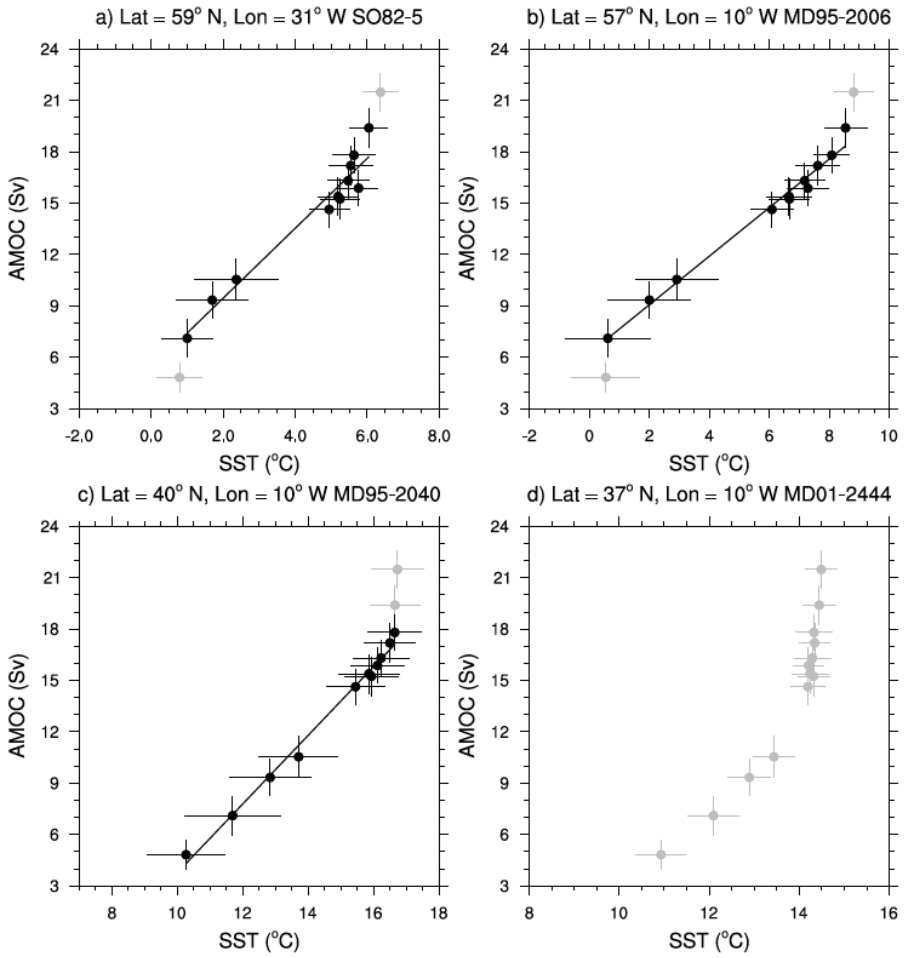

Figure 2. Annual mean AMOC strength versus annual mean or summer (JJA) SST at the four selected sediment core locations (Fig. 1) as given by the set of equilibrium states of the MIS3 freshwater hosing/extraction experiments along with linear regression lines. States marked by gray pionts were excluded from the linear regression analysis. (a) Summer SST in the Irminger Sea (SO82-5), (b) summer SST in the Northeast Atlantic (MD95-2006), (c) summer SST at the Iberian margin (MD95-2040), and (d) annual mean SST at the Iberian margin (MD01-2444). Due to its highly non-linear behaviour the AMOC-SST relationship at site MD01-2444 was not considered in the estimation of MIS3 AMOC variation. SSTs are taken from the nearest single grid point to the corresponding core location. All values are based on 100-year means. Bars show the standard deviations calculated from annual or summer, respectively, values over 100 model years.

state [cf. Heslop and Paul, 2012]). Figure 2 shows the modeled AMOC-SST relationships at the four core locations. Considering the low amount of data points, linearity is judged by visual inspection only. For extremely strong AMOC states (>19-20 Sv) linearity of the AMOC-SST relation visibly disappears at all cores locations, whereas linearity disappears for very weak AMOC (<5 Sv) at core location

SO82-5 and MD95-2006. In between, the AMOC-SST relationship is sufficiently linear, except for site MD01-2444, which shows a highly non-linear behavior throughout. We therefore decided to remove the temperature record of MD01-2444 as well as the extreme AMOC states (colored in gray, Fig. 2) from the linear regression analysis such that only the linear AMOC-SST regimes at the three remaining sites (SO82-5, MD95-2006, and MD95-2040) are considered. This implies that the following estimation of stadial-interstadial AMOC changes requires that interstadial AMOC strengths was lower than ~19 Sv during MIS3.

For each record (SO82-5, MD95-2006, and MD95-2040), we estimated a mean stadial SST and a mean interstadial SST by taking all stadial and interstadial states in the time interval 50 ka to 30 ka B.P. into account (for the MD95-2006 record, the shorter interval 50-40 ka B.P. was used which still provides five D-O stadial-interstadial transitions). Uncertainties in these temperature estimates were taken into account by calculating the standard deviations of the sets of individual stadial and interstadial temperature estimates for each record. The calculated differences between mean interstadial and mean stadial SSTs along with 1σ-uncertainties for each record are listed in Table 1. Note that we excluded Heinrich stadials [Hemming, 2004] from our estimates of mean stadial temperatures due to their infrequent occurrence and hence poor statistics (only Heinrich events 4 and 5 occur in the interval 50-30 ka B.P.).

Using the linearized AMOC-SST relationships (i.e. regression of AMOC on SST) from the CCSM3 experiments at the locations of the three sediment core sites SO82-5, MD95-2006, and MD95-2040 (Fig. 2), we estimate the magnitude of AMOC changes associated with stadial-interstadial SST differences derived from the proxy records. Table 1 summarizes the calculated regression slopes and resulting estimates for AMOC changes along with 1σ-uncertainties following from Gaussian uncertainty propagation. All three estimates are around 9-10 Sv. Calculating a weighted mean from the three AMOC estimates and their 1σ-uncertainties yields a 9.2 ± 1.2 Sv difference of the AMOC strength between interstadial and (non-Heinrich) stadial states during MIS3. The high non-linearity of the AMOC to the freshwater forcing [Xiao Zhang et al., 2014] further implies that the stadial AMOC was likely weaker than 11 Sv, while the interstadial AMOC was likely stronger than 14 Sv, according to the CCSM3 results.

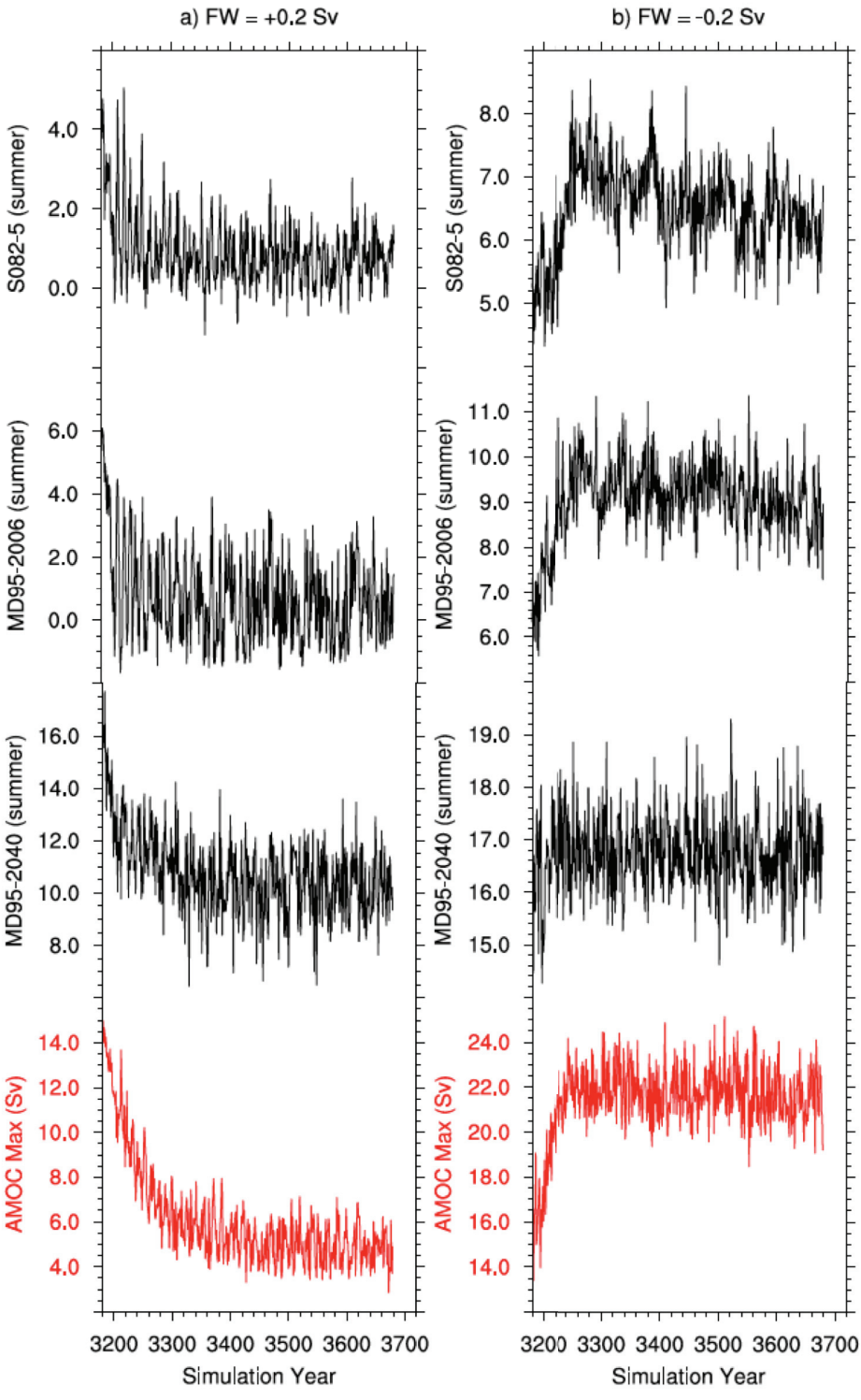

Figure 3. Timeseries of summer (JJA) SST at the three selected sediment core locations (see Table 1) along with annual mean AMOC strength (red) in (a) the +0.2 Sv freshwater hosing run, and (b) the -0.2 Sv freshwater extraction run. Both experiments start at model year 3170 (from the equilibrated MIS3 baseline run) and are integrated for 500 years each with continuous positive/negative freshwater forcing. Core numbers are indicated on the left.

Our estimates are based on AMOC-SST regression analyses of (quasi-)equilibrium climate states. However, D-O stadials and interstadials are transient phenomena and sometimes do not persist longer than a few hundred years [cf. Dickson et al., 2008]. It is therefore instructive to examine the timescale of SST adjustment (i.e. transient behaviour) to AMOC changes at the core sites. Figure 3 shows the SST and AMOC spin-up timeseries for the two experiments with extreme forcing, i.e. +0.2 Sv (Fig. 3a) and -0.2 Sv (Fig. 3b) freshwater forcing. All timeseries demonstrate a rapid adjustment of SST to AMOC changes at the core sites on a shorter-than-century timescale. The rapid SST response at the core locations lends support to our equilibrium-climate approach to estimate stadial-interstadial AMOC variations using North Atlantic records rather than records from southern latitudes where temperature adjustment to AMOC change may take much longer [e.g. Schmittner et al., 2003; Knutti et al., 2004].

Keeping atmospheric greenhouse gas concentrations fixed in our simulations, our approach of SST-based estimates of AMOC variability neglects potential feedbacks associated with changes in

Sediment core number and location	Estimated SST difference between interstadial and stadial states from the sediment core (°C)	Modelled slope of AMOC-SST regression (Sv/°C)	Estimated AMOC difference between interstadial and stadial states (Sv)
SO82-5 (59°N, 31°W; Irminger Sea)	4.5 ± 1.3 (summer)	2.0 ± 0.16	9.3 ± 2.7
MD95-2006 (57°N, 10°W; Northeast Atlantic)	6.3 ± 1.0 (summer)	1.4 ± 0.06	8.9 ± 1.5
MD95-2040 (40°N, 10°W; Iberian margin)	5.3 ± 1.6 (summer)	2.0 ± 0.06	10.6 ± 3.2

Table 1. Estimated summer SST differences between MIS3 interstadial and (non-Heinrich) stadial states at the three selected North Atlantic core locations from paleothermometry, slope of least-squares linear regression of AMOC on summer SST as derived from the equilibrium states of the set of MIS3 freshwater hosing/extraction model experiments (Fig. 2), and estimated AMOC variations with uncertainties (1σ) following from Gaussian uncertainty propagation.

atmospheric greenhouse gas concentrations and hence longwave radiative forcing caused by ocean circulation changes [e.g. Schmittner and Galbraith, 2008]. However, the small CO_2 variations associated with non-Heinrich stadials and the following D-O warming events are ~5 ppm or less [Ahn and Brook, 2014] and have no noticeable effect (i.e., much lower than 1 K) on northeast Atlantic SST [Van Meerbeeck et al. ,2009]. It is therefore reasonable to assume that the first-order effect of MIS3

millennial-scale AMOC variability on North Atlantic temperatures is directly due to changes in the large-scale oceanic heat transport.

6. Conclusions

We have investigated the ocean temperature response to variations in AMOC strength by performing a set of freshwater hosing/extraction experiments under MIS3 (38 ka B.P.) glacial boundary conditions using the comprehensive coupled climate model CCSM3. The main target of this study was to provide a global spatial fingerprint of ocean temperature response to D-O-related AMOC changes and, further, to estimate the differences in AMOC strength between MIS3 stadial and interstadial states by combining temperature reconstructions with model simulations. The simulations suggest the highest SST sensitivity to AMOC changes in the northeastern North Atlantic, especially in summer. Due to the high sensitivity and a rapid adjustment time, SST reconstructions from this region turn out to be particularly suitable for estimating past AMOC changes. Significant temperature responses are also found at subsurface levels. However, the subsurface temperature fingerprint could not be exploited for our purpose of estimating MIS3 AMOC variability due to a lack of high-resolution D-O-resolving subsurface temperature records.

From three North Atlantic SST records we could estimate a stadial-interstadial AMOC strength difference of 9.2 ± 1.2 Sv (Heinrich stadials excluded), provided that interstadial AMOC strengths was below ~19 Sv during MIS3. Moreover, the CCSM3 results suggest that the stadial AMOC was weaker than 11 Sv, while the interstadial AMOC was stronger than 14 Sv. These estimates are based on one CGCM only. Besides the need for more high-resolution surface and subsurface proxy records for the MIS3 interval, more MIS3 simulations using state-of-the-art CGCMs are needed to better constrain this estimate. So far, only few CGCM simulations of MIS3 climate exist [Merkel et al., 2010; Singarayer and Valdes, 2010; Brandefelt et al., 2011; Gong et al., 2013; Mohtadi et al., 2014]. Sophisticated data assimilation techniques could provide absolute numbers for AMOC strength [cf. Kurahashi-Nakamura et al., 2014], but for MIS3, this would require a much larger glacial proxy database.

Acknowledgement

This study was funded by the DFG-Research Center / Cluster of Excellence “The Ocean in the Earth System”. The CCSM3 climate model experiments were run on the SGI Altix Supercomputer of the “Norddeutscher Verbund für Hoch- und Höchstleistungsrechnen” (HLRN). We are grateful to the two anonymous reviewers for their constructive comments and suggestions.

References

Ahn, J., and E.J. Brook, (2007), Atmospheric CO_2 and climate from 65 to 39 ka B.P., Geophys. Res. Lett., 34, L10703.

Ahn, J., and E.J. Brook, (2014), Siple Dome ice reveals two modes of millennial CO2 change during the last ice age, Nature Communications, 5:3723, doi:10.1038/ncomms4723.

Álvarez-Solas, J., et al., (2011), Heinrich event 1: an example of dynamical ice-sheet reaction to oceanic changes, Clim. Past, 7, 1297–1306.

Bereiter et al., (2012), Mode change of millennial CO_2 variability during the last glacial cycle associated with a bipolar marine carbon seesaw, Proc. Natl. Acad. Sci. U. S. A., 109, 9755–9760.

Berger, A., (1978), Long term variations of daily insolation and Quaternary climatic changes, J. Atmos. Sci., 35(2), 2362–2367.

Bond, G., et al. (1993), Correlations between climate records from North Atlantic sediments and Greenland ice, Nature, 365,143–147.

Brandefelt, J., et al., (2011), A coupled climate model simulation of Marine Isotope Stage 3 stadial climate, Clim. Past, 7, 649–670.

Broecker et al., (1992), Evidence for massive discharges of icebergs into the North Atlantic ocean during the last glacial period, Nature, 360, 245-249.

Broecker, W.S., (2000), Abrupt climate change: causal constraints provided by the paleoclimate record, Earth Sci. Rev., 51, 137–154.

Cessi, P., K. Bryan, and R. Zhang, (2004), Global seiching of thermocline waters between the Atlantic and the Indian–Pacific Ocean Basins, Geophys. Res. Lett. 31, L04302.

Collins et al., (2006), The Community Climate System Model Version 3 (CCSM3), J. Climate, 19, 2122–2143.

Crowley, T.J., (1992), North Atlantic Deep Water cools the southern hemisphere, Paleoceanogr., 7, 489–497.

Dansgaard W. et al., (1993) Evidence for general instability of past climate from a 250-kyr ice-core record, Nature, 364,218–220.

Davis, J.C., (1986), Statistics and Data Analysis in Geology, 2nd ed. x + 646 pp. New York, Chichester, Brisbane, Toronto, Singapore: John Wiley. ISBN 0-471-83743-1.

de Abreu et al., (2003), Millenial-scale oceanic climate variability off the Western Iberian margin during the last two glacial periods, Marine Geology, 196(1-2), 1-20.

Dokken, T. M., and E. Jansen, (1999), Rapid changes in the mechanism of ocean convection during the last glacial period, Nature, 401, 458–461.

Dickson et al., (2008), Centennial-scale evolution of Dansgaard-Oeschger events in the northeast Atlantic Ocean between 39.5 and 56.5 ka B.P., Paleoceanography, 23(3), PA3206.

Elliot, M.L., L. Labeyrie, and J.C. Duplessy, (2002), Changes in North Atlantic deep-water formation associated with the Dansgaard-Oeschger temperature oscillations (60–10 ka), Quat. Sci. Rev., 21(10), 1153–1165.

EPICA Community Members, (2006), One-to-one coupling of glacial climate variability in Greenland and Antarctica, Nature, 444, 195–198.

Flückiger, J., et al., (2004), N_2O and CH_4 variations during the last glacial epoch: Insight into global processes, Global Biogeochem. Cycles, 18, doi: 10.1029/2003GB002122.

Ganachaud, A., and C. Wunsch, (2000), Improved estimates of global ocean circulation, heat transport and mixing from hydrographic data, Nature, 408, 453–457.

Gebbie, G., P. Huybers, (2006), Meridional circulation during the Last Glacial Maximum explored through a combination of South Atlantic delta-18O observations and a geostrophic inverse model, Geochem. Geophys. Geosys., 7, Q11N07, doi:10.1029/2006GC001383.

Gong, X., G. Knorr, and G. Lohmann, (2013), Dependence of abrupt Atlantic meridional ocean circulation changes on climate background states, Geophys. Res. Lett., 40, 3691–3704.

Goodman, P.J., (2001), Thermohaline adjustment and advection in an OGCM, J. Phys.Oceanogr. 31, 1477–1497. doi:10.1175/1520-0485(2001) 031.

Grousset, F.E., et al., (1993), Patterns of ice-rafted detritus in the glacial North Atlantic, Paleoceanography, 8(2), 175-192, doi:10.1029/92PA02923.

Handiani, D., et al., (2013), Tropical vegetation response to Heinrich Event 1 as simulated with the UVic ESCM and CCSM3, Clim. Past, 9, 1683-1696, doi:10.5194/cp-9-1683-2013.

Hemming, S.R., (2004), Heinrich events: massive late Peistocene detrius layers of the North Atlantic and their global climate imprint, Rev. Geophys., 42:RG1005, doi:10.1029/2003RG000128.

Heslop, D. and A. Paul, (2012), Fingerprinting of the Atlantic Meridional Overturing Circulation in climate models to aid in the design of proxy investigations, Clim. Dyn., 38:1047-1064, doi: 10.1007/s00382-011-1042-0.

Huang, R.X., M.A. Cane, N. Naik, and P. Goodman, (2000), Global adjustment of the thermocline in response to deepwater formation. Geophys. Res. Lett. 27 (6), 759–762.

Johns, W. E., et al., (2011), Continuous, array-based estimates of Atlantic Ocean heat transport at 26.5°N, J. Climate, 24, 2429–2449.

Keigwin, L.D. and E. A. Boyle, (1999), Surface and deep ocean variability in the northern Sargasso Sea during marine isotope stage 3, Paleoceanography, 14, doi: 10.1029/1998PA900026.

Knutti, R., J. Flückiger, T. F. Stocker, and A. Timmermann, (2004), Strong hemispheric coupling of glacial climate through freshwater discharge and ocean circulation, Nature, 430(7002), 851–856.

Kurahashi-Nakamura, T., Losch, M., and A. Paul, (2014), Can sparse proxy data constrain the strength of the Atlantic meridional overturning circulation?, Geosci. Model Dev., 7, 419-432.

LeGrand, P. and C. Wunsch, (1995), Constraints from paleo-tracer data on the North Atlantic circulation during the last glacial maximum, Paleoceanography, 10, 1011–1045.

Levis, S., et al., (2004), The community land model's dynamic global vegetation model (CLM-DGVM): technical description and user's guide, NCAR Technical Note NCAR/TN-459+STR, National Center for Atmospheric Research, Boulder, CO, 50 pp.

Li , C. C., (1964), Introduction to experimental statistics, New York: McGraw-Hill, 1964.

Lohmann, G., (2003), Atmospheric and oceanic freshwater transport during weak Atlantic overturning circulation, Tellus 55, 438–449.

Lopes dos Santos, R.A. et al., (2010), Glacial interglacial variability in Atlantic meridional overturning circulation and thermocline adjustments in the tropical North Atlantic. Earth Planet. Sci. Lett., 300, 407-414.

Lynch-Stieglitz et al., (2007), Atlantic Meridional Overturning Circulation During the Last Glacial Maximum, Science, 316, 66-69.

Marcott, et al., (2011), Ice-shelf collapse from subsurface warming as trigger for Heinrich events, Proc. Natl. Acad. Sci., doi:10.1073/pnas.1104772108.

Martrat et al., (2007), Four climate cycles of recurring deep and surface water destabilizations on the Iberian Margin, Science, 317(5837), 502-507.

McManus, J.F., et al., (2004), Collapse and rapid resumption of Atlantic meridional circulation linked to deglacial climate changes, Nature, 428, 834-837.

Merkel, U., M. Prange, and M. Schulz, (2010), ENSO variability and teleconnections during glacial climates, Quat. Sci. Rev., 29, 86-100.

Mohtadi M, et al., (2014), North Atlantic forcing of tropical Indian Ocean climate, Nature, 509(7498), 76–80.

Oleson, K. W., et al. (2008), Improvements to the Community Land Model and their impact on the hydrological cycle, J. Geophys. Res., 113, G01021, doi:10.1029/2007JG000563.

Peltier, W. R. (2004), Global glacial isostasy and the surface of the ice-age Earth: The ICE-5G (VM2) model and GRACE, Annu. Rev. Earth Planet. Sci., 32, 111–149.

Peltier, W. R., and G. Vettoretti (2014), Dansgaard-Oeschger oscillations predicted in a comprehensive model of glacial climate: A “kicked” salt oscillator in the Atlantic, Geophys. Res. Lett., 41, 7306–7313, doi:10.1002/2014GL061413.

Prange, M., and R. Gerdes, (2006), The role of surface freshwater flux boundary conditions in Arctic Ocean modelling, Ocean Modelling, 13, 25-43.

Prange, M., G. Lohmann, V. Romanova, and M. Butzin, (2004), Modelling tempo-spatial signatures of Heinrich Events: influence of the climatic background state, Quat. Sci. Rev., 23, 521–527.

Rahmstorf, S., (2002), Ocean circulation and climate during the past 120,000 years, Nature, 419, 207–214.

Rasmussen, T. L., and E. Thomsen, (2004), The role of the North Atlantic Drift in the millennial timescale glacial climate fluc-tuations, Palaeogeogr. Palaeoclimatol. Palaeoecol.,210,101–116.

Ritz et al., (2013), Estimated strength of the Atlantic overturning circulation during the last deglaciation, Nature Geosci., 6, 208–212.

Rühlemann, C. et al., (2004), Intermediate depth warming in the tropical Atlantic related to weakened thermohaline circulation: Combining paleoclimate and modeling data for the last deglaciation, Paleoceanography, 19, PA1025, doi:10.1029/2003PA000948.

Sarnthein, M., et al. (2001), Fundamental modes and abrupt changes in North Atlantic circulation and climate over the last 60 ky—Concepts, reconstructions and numerical modeling, The Northern North Atlantic: A Changing Environment, edited by P. Schäfer et al., pp. 365–410, Springer-Verlag, New York.

Schmidt et al., (2012), Impact of Abrupt Deglacial Climate Change on Tropical Atlantic subsurface temperatures, Proc. Natl. Acad. Sci., 109, 14348-14352.

Schmittner, A., and E. D. Galbraith, (2008), Glacial greenhouse gas fluctuations controlled by ocean circulation changes, Nature, 456, 373-376, doi:10.1038/nature07531.

Schmittner, A., Saenko, O. A. and Weaver, A. J., (2003), Coupling of the hemispheres in observations and simulations of glacial climate change, Quat. Sci. Rev., 22, 659-671.

Shaffer, G., S.O. Malskaer and C.J. Bjerrum, (2004), Ocean subsurface warming as a mechanism for coupling Dansgaard-Oeschger climate cycles and ice-rafting events, Geophys. Res. Lett., 31, L24202, doi:10.1029/2004GL020968.

Singarayer, J.S. And P.J. Valdes, (2010), High-latitude climate sensitivity to ice-sheet forcing over the last 120 kyr., Quaternary Science Reviews, 29, 43–55.

Smith, R. D., S. Kortas, and B. Meltz, (1995), Curvilinear coordinates for global ocean models, Tech. Rep. LA-UR-95-1146, Los Alamos National Laboratory, 50 pp.

Spahni, R., et al., (2005), Atmospheric methane and nitrous oxide of the late Pleistocene from Antarctic ice cores, Science, 310, 1317–1321.

Stocker, T. F., and S. J. Johnsen, (2003), A minimum thermodynamic model for the bipolar seesaw, Paleoceanography, 18(4), 1087.

van Kreveld et al., (2000), Potential links between surging ice sheets, circulation changes, and the Dansgaard-Oeschger cycles in the Irminger Sea, 60-18 kyr, Paleoceanography, 15(4), 425-442.

Van Meerbeeck, C. J., H. Renssen and D. M. Roche, (2009), How did Marine Isotope Stage 3 and Last Glacial Maximum climates differ? – Perspectives from equilibrium simulations, Clim. Past, 5, 33–51.

Winguth, A., D. Archer, E. Maier-Reimer, and U. Mikolajewicz, (2000), Paleonutrient data analysis of the glacial Atlantic using an adjoint ocean general circulation model, in Inverse Methods in Global Biogeochemical Cycles, Geophys. Monogr. Ser., vol. 114, edited by P. Kasibhatla et al., pp. 171–183, AGU, Washington, D. C.

Yeager, S.G., et al., (2006), The low-resolution CCSM3, J. Clim., 19, 2545–2566.
Zarriess, M., et al., (2011), Bipolar seesaw in the northeastern tropical Atlantic during Heinrich stadials. Geophysical Research Letters, 38, L04706.

Zarriess, M., H. Johnstone, M. Prange, S. Steph, J. Groeneveld, S. Mulitza, and A. Mackensen, (2011), Bipolar seesaw in the northeastern tropical Atlantic during Heinrich stadials, Geophysical Research Letters, 38, L04706, doi:10.1029/2010GL046070.

Zhang, Xiao, et al., (2014), Instability of the Atlantic overturning circulation during Marine Isotope Stage 3, Geophys. Res. Lett., 41, 4285–4293.

Zhang, Xu, et al., (2014), Abrupt glacial climate shifts controlled by ice sheet changes, Nature, 512, 290-294, doi:10.1038/nature13592.

Zhang, X., et al., (2012), Changes in equatorial Pacific thermocline depth in response to Panamanian seaway closure: Insights from a multi-model study, Earth Planet. Sci. Lett., 317–318, 76–84.

Chapter 4

Changes in equatorial Pacific thermocline depth in response to Panamanian Seaway closure: Insights from a multi-model study

Xiao Zhang, Matthias Prange, Silke Steph, Martin Butzin, Uta Krebs, Daniel J. Lunt, Kerim H. Nisancioglu, Wonsun Park, Andreas Schmittner, Birgit Schneider, Michael Schulz

Author affiliations:

Xiao Zhang: MARUM – Center for Marine Environmental Sciences, University of Bremen, D-28334 Bremen, Germany

Matthias Prange: MARUM – Center for Marine Environmental Sciences, University of Bremen, D-28334 Bremen, Germany

Silke Steph: Dept. of Geosciences, University of Bremen, D-28334 Bremen, Germany

Martin Butzin: MARUM – Center for Marine Environmental Sciences, University of Bremen, D-28334 Bremen, Germany

Uta Krebs: Institute for Geosciences, Dept. of Geology, Kiel University, D-24118 Kiel, Germany

Daniel J. Lunt: School of Geographical Sciences, University of Bristol, Bristol BS8 1SS, UK

Kerim H. Nisancioglu: Bjerknes Centre for Climate Research, Allegaten 55, NO-5007 Bergen, Norway

Wonsun Park: IFM-GEOMAR, Leibniz-Institut fuer Meereswissenschaften, D-24105 Kiel, Germany

Andreas Schmittner: College of Oceanic and Atmospheric Sciences, Oregon State University, Corvallis, OR 97331, USA

Birgit Schneider: Institute for Geosciences, Dept. of Geology, Kiel University, D-24118 Kiel, Germany

Michael Schulz: MARUM – Center for Marine Environmental Sciences, University of Bremen, D-28334 Bremen, Germany

April 2011

Abstract

The early Pliocene warm phase was characterized by high sea surface temperatures in the eastern equatorial Pacific. A new hypothesis suggests that the progressive closure of the Panamanian seaway contributed substantially to the termination of this state. According to this hypothesis, intensification of the Atlantic meridional overturning circulation (AMOC) – induced by the closure of the gateway – was the principal cause of equatorial Pacific thermocline shoaling during the Pliocene. In this study, twelve Panama seaway sensitivity experiments from eight ocean/climate models of different complexity are analyzed to examine the effect of an open gateway on AMOC strength and thermocline depth. All models show an eastward Panamanian net throughflow, leading to a reduction in AMOC strength compared to the corresponding closed-Panama case. In those models that do not include a dynamic atmosphere, deepening of the equatorial Pacific thermocline appears to scale almost linearly with the throughflow-induced reduction in AMOC strength. Models with dynamic atmosphere do not follow this simple relation. There are indications that in four out of five models equatorial wind-stress anomalies amplify the tropical Pacific thermocline deepening. In summary, the models provide strong support for the hypothesized relationship between Panama closure and equatorial Pacific thermocline shoaling that might have set the stage for the turnaround from a warm zonally symmetric to the modern equatorial Pacific cold tongue state.

1 Introduction

During the warm early Pliocene, ~5.5 to 4 Ma ago, sea surface temperatures in the eastern equatorial Pacific were similar to those of the western tropical Pacific warm pool (Ravelo et al. 2004, Wara et al. 2005, Fedorov et al. 2006, Lawrence et al. 2006). The absence of the eastern equatorial Pacific cold tongue was linked to a weak Walker Circulation, a deep thermocline and low biogenic productivity in the tropical region (Barreiro et al. 2006, Fedorov et al. 2006, Dekens et al. 2007). It has been suggested that this warm equatorial state was responsible for a 3-4°C warmer-than-present global mean surface temperature and the absence of major ice sheets in the Northern Hemisphere via processes and teleconnections similar to those that are at work during El Niño states (e.g. Cane and Molnar 2001, Molnar and Cane 2002, Barreiro et al. 2006, Huybers and Molnar 2007, Chiang 2009, Vizcaino et al. 2010), although other studies have disputed this (Lunt et al. 2008b, Haywood et al. 2007). Recent studies suggested mechanisms that might have contributed to maintaining the "permanent El Niño-like" climate state, involving a higher frequency of tropical cyclones in the early Pliocene (Fedorov et al. 2010) or a dynamical state approaching "equatorial superrotation" with westerly surface wind anomalies over the equatorial Pacific (Tziperman and Farrell 2009). However, causes or preconditions for the termination of the equatorial Pacific zonally symmetric state remain obscure. In particular, the original hypothesis by Cane and Molnar (2001), which suggests a key role for the northward displacement and uplift of New Guinea and Halmahera in triggering the climatic switch in the equatorial Pacific, could not be corroborated by climate model experiments thus far (Jochum et al. 2009).

A new hypothesis brings the Pliocene closure of the Panamanian seaway into play. Analyzing oxygen isotope and Mg/Ca temperature records from shallow- and deep-dwelling planktonic foraminifers, Steph et al. (2010) reconstructed the Pliocene evolution of the thermocline in the eastern equatorial Pacific and found that gradual shoaling of the thermocline between 4.8 and 4 Ma ago occurred synchronously with the progressive closure of the Panamanian seaway and an increase in the Atlantic meridional overturning circulation (AMOC). Based on these findings along with simulation results from the coupled climate model ECBILT-CLIO, Steph et al. (2010) suggested the following chain of events: The early Pliocene shoaling of the Panamanian seaway caused an intensification of the AMOC driven by enhanced North Atlantic Deepwater (NADW) formation. Enhanced NADW production resulted in an increased volume of the "cold water sphere" and hence to upward thermocline shifts in the global ocean transmitted by baroclinic oceanic adjustment processes (Huang et al. 2000, Goodman 2001, Cessi et al. 2004, Timmermann et al. 2005, Haarsma et al. 2008, Lopes dos Santos 2010). In the eastern equatorial Pacific, the thermocline shoaling preconditioned the turnaround from a warm to an equatorial cold tongue state, before intensified trade winds (probably related to high-latitude glaciation)

could bring cold waters to the surface after ~3.6 Ma, setting the stage for the modern El Niño/Southern Oscillation system as evidenced by fossil corals from the Philippines (Watanabe et al. 2011).
In this study, we shall further test the hypothesized relationship between Panama closure, AMOC strength and equatorial Pacific thermocline depth. How robust are the model results presented by Steph et al. (2010) among different models? How strong is the influence of changes in AMOC strength on tropical Pacific thermocline depth? How may wind-stress feedbacks affect the Pacific thermocline? To address these questions, we analyze and compare climate model results from twelve different Panamanian seaway-closure simulations.

2 Model simulations and analysis

A total of twelve experiments with eight different models is analyzed in this study. In contrast to coordinated model intercomparison projects, the model experiments were set up independently, such that differences in boundary conditions, Panama seaway depth, etc. exist. Table 1 provides an overview of the different models and setups. Five models include a dynamic atmosphere, thus allowing for, e.g., wind-stress feedbacks (HadCM3, CCSM2, CCSM3, KCM and ECBILT-CLIO). The other three models (UVIC, BREMIC/LSG, MIT) apply prescribed modern wind fields to force the ocean. All use present-day or pre-industrial boundary conditions, except for the HadCM3 experiment in which mid-Pliocene boundary conditions are applied. The mid-Pliocene boundary conditions include reduced ice-sheet sizes, Pliocene vegetation distribution and enhanced atmospheric CO_2 concentration (400 ppmv). As a result, the global mean surface temperature is ca. 3°C warmer compared to pre-industrial conditions (Lunt et al. 2008a).
Applying different seaway depths and vertical diffusivities, Schneider and Schmittner (2006) performed a series of sensitivity experiments with the UVIC model. These experiments are referred to as UVIC3sh, UVIC3in, UVIC6sh and UVIC6in, where “3”, “6”, “sh” and “in” stand for low vertical diffusivity (0.3 $cm^2\ s^{-1}$ in the upper ocean), high vertical diffusivity (0.6 $cm^2\ s^{-1}$ in the upper ocean), shallow seaway (130 m) and intermediate-depth seaway (700 m). This allows us to examine the effects of both vertical mixing and Panamanian sill depth on the behavior of the Pacific equatorial thermocline in one and the same model. We note that the UVIC simulations with a 2000 m deep Panamanian gateway performed by Schneider and Schmittner (2006) were not included in this paper, as the results of these simulations are nearly identical to the UVIC runs with a 700 m deep seaway.
Four previously unpublished Panama experiments have been conducted and are included in this study. ECBILT-CLIO was used in the first new experiment. Apart from a shallower Panamanian sill depth (415 m), the experimental design is identical to that described by Prange and Schulz (2004) who applied a 700 m deep seaway in their original study. In the second previously unpublished

experiment, we employed the global ocean model BREMIC/LSG coupled to a simplified energy balance model. The closed-Panama control run with modern boundary conditions is described in Butzin et al. (2005, 2011). In the corresponding open-Panama experiment, the model has been integrated into a new equilibrium after implementing a 500 m deep seaway by replacing three land grid

Model name	Atmosphere component	AMOC (Sv); closed/open seaway	Seaway depth (m)	Net eastward flow through seaway (Sv)	Remark	Reference for model	Reference for open-Panama experiment
UVIC 3sh	Energy-moisture balance model	13/11	130	5	Vert. diffusivity: 0.3–1.3 $cm^2 s^{-1}$	Weaver et al. (2001)	Schneider and Schmittner (2006)
UVIC 3in	Energy-moisture balance model	13/5	700	10	Vert. diffusivity: 0.3–1.3 $cm^2 s^{-1}$	Weaver et al. (2001)	Schneider and Schmittner (2006)
UVIC 6sh	Energy-moisture balance model	18/17	130	7	Vert. diffusivity: 0.6–1.6 $cm^2 s^{-1}$	Weaver et al. (2001)	Schneider and Schmittner (2006)
UVIC 6in	Energy-moisture balance model	18/13	700	16	Vert. diffusivity: 0.6–1.6 $cm^2 s^{-1}$	Weaver et al. (2001)	Schneider and Schmittner (2006)
BREMIC/LSG	Simplified energy balance model	18/10	500	14		Maier-Reimer et al. (1993), Prange et al. (2003)	This study
MIT (OGCM)	Mixed boundary conditions	31/28	1000	16	No Arctic Ocean	Marshall et al. (1997)	Nisancioglu et al. (2003)
HadCM3	General circulation model	20/10	370	8	Mid-Pliocene boundary conditions	Gordon et al. (2000)	Lunt et al. (2008a)
CCSM2	General circulation model	14/12	800	12		Kiehl and Gent (2004), Prange (2008)	Steph et al. (2006a)
CCSM3	General circulation model	16/8	1475	11		Collins et al. (2006), Yeager et al., (2006)	This study
KCM	General circulation model	14/11	1200	13		Park et al. (2009)	This study
EC415 (ECBILT-CLIO)	Quasi-geostrophic circulation model	27/19	415	11		Goosse and Fichefet (1999), Opsteegh et al. (1998)	This study
EC700 (ECBILT-CLIO)	Quasi-geostrophic circulation model	27/15	700	14		Goosse and Fichefet (1999), Opsteegh et al. (1998)	Prange and Schulz (2004)

Table 1. Overview of the model simulations analyzed in this paper. “AMOC” refers to the North Atlantic overturning streamfunction maximum. Four different experiments were performed with the UVIC model which differ in Panamanian seaway depth and vertical mixing. These experiments are denoted by “3”, “6”, “sh” and “in” which stands for low vertical diffusivity (0.3 $cm^2 s^{-1}$ in the upper ocean), high vertical diffusivity (0.6 $cm^2 s^{-1}$ in the upper ocean), shallow seaway (130 m) and intermediate depth seaway (700 m). With ECBILT-CLIO, two experiments with different seaway depths were carried out, denoted by EC415 and EC700, which stands for 415 m and 700 m depth, respectively.

cells by ocean cells. The third new experiment employed the comprehensive Community Climate System Model version 3 (CCSM3) in its low-resolution version (Collins et al. 2006, Yeager et al. 2006). The resolution of the atmospheric component is T31 (~3.75° transform grid) with 26 levels, while the ocean component has a nominal resolution of 3° with 25 levels in the vertical (higher meridional resolution of 0.9° around the equator). Along with a 1000-year-integrated control run with present-day boundary conditions, we performed another 1000-year integration with a 1500 m deep Panamanian seaway by replacing three land grid cells by ocean grid cells between North and South America. Both runs were initialized with present-day observational data. Last but not least, the Kiel Climate Model, KCM (Park et al. 2009), was used in the fourth previously unpublished experiment. In the simulations described here, the atmospheric resolution is T31 with 19 levels. The horizontal ocean resolution is

based on a 2° Mercator mesh and is on average 1.3°, with enhanced meridional resolution of 0.5° close to the equator, and with 31 levels in the vertical. In the open-Panama run, the seaway is 1200 m deep and four grid cells wide. Control and sensitivity runs were integrated for 1000 years.
All results presented in this paper refer to long-term annually averaged quantities from equilibrated model runs. In order to analyze the effect of an open Panamanian seaway on the Pacific equatorial thermocline in a specific model, we calculated the depth of the 20°C isotherm (referred to as Z20) in the experiment with open gateway and compare it to the corresponding model run with closed gateway. We note that the thermocline is generally defined as the depth at which the vertical temperature gradient is at maximum. In numerical ocean models, however, the search for this maximum would always result in thermocline depths that correspond exactly to depths of grid points. Hence changes, which are smaller than the vertical grid spacing would not be observed when using the maximum temperature gradient for thermocline depth calculations. By contrast, the depth of an isotherm is not bound to the grid spacing; an isotherm can well reside between two grid points in the vertical and its depth can easily be found by linear interpolation of the gridded temperature field. Z20 is a commonly used quantity to specify the depth of the Pacific equatorial thermocline, since it closely matches the depth of the maximum vertical temperature gradient under modern climate conditions in that region (e.g. McPhaden and Yu 1999, Harrison and Vecchi 2001, Fedorov and Philander 2001, Timmermann et al. 2007, Steph et al. 2010). It should be noted that even though the HadCM3 experiment has a higher global mean temperature due to Pliocene boundary conditions, Z20 still matches the depth of the maximum vertical temperature gradient in the equatorial Pacific.

3 Results and discussion

All models simulate an eastward net volume transport through the Panamanian gateway (i.e. from the Pacific to the Atlantic). The invasion of relatively low-saline Pacific water into the Atlantic results in a weakening of NADW formation and hence in a reduction of the AMOC.

Figure 1 displays the effect of an open Panama gateway on the depth of the Pacific tropical thermocline (Z20). The models show a general deepening of the equatorial thermocline when the seaway is open, except for the shallow-gateway UVIC runs and the MIT model. Z20 changes (i.e. differences between model runs with open Panama gateway minus corresponding model runs with closed isthmus) averaged over the Niño-3 region (150°W-90°W, 5°N-5°S) are plotted against AMOC changes in Figure 2.
We first consider only those models that do not include wind-stress feedbacks. The graph shows that models, which exhibit equatorial thermocline shoaling in response to an open Panamanian seaway

(UVIC3sh, UVIC6sh, MIT), simulate only minor changes in the AMOC. In these models, the removal of Pacific thermocline water by the upper-ocean outflow from the Pacific to the Atlantic leads to Pacific thermocline shoaling (cf. Figure 6 in Sarnthein et al. 2009). In models that simulate larger AMOC changes, Z20 increases in response to an open seaway (UVIC3in, UVIC6in, BREMIC/LSG). In these cases, the effect of a weakened AMOC overcompensates the effect of Pacific thermocline water removal through the gateway, i.e. reduced formation of deepwater in the northern North Atlantic leads to a decrease in the volume of the "cold-water sphere" and, hence, to downward thermocline-shifts in the global ocean (Huang et al. 2000, Goodman 2001, Cessi et al. 2004, Timmermann et al. 2005, Haarsma et al. 2008, Lopes dos Santos 2010). We find that the change in Z20 scales almost linearly with the change in AMOC as indicated by the regression line in Figure 2, i.e. the greater the reduction in AMOC strength, the stronger the deepening of the Pacific equatorial thermocline. This result strongly supports the hypothesis of Steph et al. (2010) which states that the Pliocene shoaling of the equatorial Pacific thermocline was the result of a global oceanic adjustment in response to AMOC amplification, which, in turn, was induced by the gradual closing of the Panamanian seaway.

The models with dynamic atmosphere (CCSM2, CCSM3, HadCM3, KCM and ECBILT-CLIO), however, do not fit to this linear regression. In CCSM2, CCSM3, HadCM3 and KCM, the Z20 differences lie above the regression line calculated from the models without wind-stress feedback, whereas the Z20 response in ECBILT-CLIO is relatively small given the large AMOC change (Figure 2). We note that basically the same picture emerges when plotting Z20 changes against percentage AMOC changes instead of absolute AMOC changes (not shown). These findings suggest a substantial modification of the AMOC-Z20 relationship through dynamical processes in the atmosphere and air-sea coupling.

In order to further elucidate these processes, we plotted changes in equatorial zonal wind stress along with changes in Z20 for CCSM2, CCSM3, HadCM3, KCM and ECBILT-CLIO (EC415 and EC700) in Figure 3. In all models, weakening of the AMOC induced by an open Panamanian seaway causes cooling of the Northern Hemisphere and warming of the Southern Hemisphere which, in turn, leads to a southward shift of the Intertropical Convergence Zone (cf. Steph et al. 2006a, Lunt et al. 2008a, Steph et al. 2010) and associated wind anomalies over the equatorial Pacific that are mostly easterly. On timescales longer than that of equatorial adjustment, generally stronger easterlies result in an increase in the mean depth of the equatorial Pacific thermocline (Vecchi et al. 2006, Vecchi and Soden 2007). We propose that this wind-stress effect is likely to be responsible for the relatively large central Pacific thermocline responses in CCSM2, HadCM3 and KCM (Figure 2). Only in the easternmost region of the equatorial Pacific, the stronger easterlies tend to shoal the thermocline in these models. In ECBILT-CLIO, however, the largest easterly wind-stress anomalies are found west of

150°W (Figure 3). Such easterly wind-stress anomalies over the western Pacific tend to shoal the equatorial thermocline in the central and eastern Pacific (Timmermann et al. 2007). Consequently, the wind-stress response weakens rather than amplifies changes in the depth of the equatorial thermocline in ECBILT-CLIO. In CCSM3, a westerly wind-stress anomaly west of 135°W tends to move surface water into the Niño-3 region, leading to a substantial deepening of the thermocline in that area. Nevertheless, it is worth noting that even those models that simulate an equatorial Pacific thermocline deepening in the Niño-3 region in response to an open Panama gateway, do not necessarily capture the thermocline deepening at the sites of the sediment cores from which Steph et al. (2010) inferred their hypothesis (Figure 1).

The UVIC sensitivity experiments (Schneider and Schmittner 2006) further reveal the important effect of vertical diffusivity on the Panamanian throughflow, the sensitivity of the AMOC, and the equatorial Pacific thermocline. In both the shallow-gateway experiments (UVIC3sh, UVIC6sh) and the intermediate-depth runs (UVIC3in, UVIC6in), stronger vertical mixing leads to a stronger eastward throughflow (Table 1). This finding is consistent with the reasoning of Nof and Van Gorder (2003) who showed that eastward flow through the Panamanian gateway depends on diapycnal mixing and/or NADW formation, with NADW formation in turn being dependent on diapycnal mixing (e.g. Schneider and Schmittner 2006). The UVIC runs further show that the gateway-induced AMOC changes are stronger in the low-diffusivity runs than in the high-diffusivity experiments (despite smaller Panamanian throughflow). This finding is consistent with earlier studies that suggested enhanced stability of the AMOC to North Atlantic surface salinity perturbations with increasing vertical mixing (Schmittner and Weaver 2001, Prange et al. 2003, Nof et al. 2007). As a result, the UVIC low-diffusivity experiments (UVIC3sh, UVIC3in) exhibit a larger Z20 response than the corresponding high-diffusivity cases (UVIC6sh, UVIC6in).

4 Summary and conclusions

The major findings of our multi-model study can be summarized as follows:

(1) All model experiments with an open Panama gateway show an eastward Panamanian net throughflow, leading to a reduction in NADW formation and hence AMOC strength compared to the corresponding closed-Panama case.

(2) In the absence of wind-stress feedbacks, deepening of the equatorial Pacific thermocline induced by an open Panamanian seaway scales almost linearly with the throughflow-induced reduction in AMOC strength, i.e. a weaker (stronger) AMOC is associated with a deeper (shallower) equatorial Pacific thermocline.

(3) There are strong indications that wind-stress effects may amplify (CCSM2, CCSM3, HadCM3, KCM) or weaken (ECBILT-CLIO) this thermocline deepening substantially, depending on the longitudinal shape of the equatorial zonal wind anomaly. We note, however, that with its highly simplified atmospheric component (quasi-geostrophic approximation), ECBILT-CLIO has to be considered less reliable in simulating tropical dynamics than the comprehensive models CCSM2, CCSM3, HadCM3 and KCM. Moreover, besides tropical air-sea momentum fluxes, tropical and extra-tropical surface heat and freshwater fluxes cannot be ruled out as drivers for equatorial thermocline changes.
(4) The simulated volume flux of the Panamanian throughflow and the gateway's impact on the AMOC and the depth of the equatorial Pacific thermocline depend sensitively on the parameterization of poorly constrained parameters like vertical diffusivity.
Taken together, the model results strongly support the hypothesis by Steph et al. (2010), which states that intensification of the AMOC – induced by the progressive closure of the Panamanian seaway – played a key role in the Pliocene shoaling of the equatorial Pacific thermocline. This thermocline shoaling might have preconditioned the turnaround from a warm eastern equatorial Pacific to the modern equatorial cold tongue state. The relationship between AMOC and equatorial Pacific thermocline may also be relevant for the assessment of future changes in tropical climate dynamics. The fate of the AMOC under anthropogenic warming may be crucial for the future development of the Pacific equatorial thermocline and hence the characteristics of the El Niño/Southern Oscillation.

Acknowledgements
We thank Ralf Tiedemann, Axel Timmermann and Ute Merkel for stimulating discussions. This work has received funding through the DFG Research Center/Excellence Cluster "The Ocean in the Earth System". M.B. is funded through the DFG Research Unit "Understanding Cenozoic Climate Cooling". The CCSM3 climate model experiments were run on the SGI Altix Supercomputer of the "Norddeutscher Verbund für Hoch- und Höchstleistungsrechnen" (HLRN).

References

Barreiro, M., G. Philander, R. Pacanowski, and A. V. Fedorov (2006), Simulations of warm tropical conditions with application to Middle Pliocene atmospheres, Clim. Dyn., 26, 349–365, doi:10.1007/s00382-005-0086-4.

Butzin, M., M. Prange, and G. Lohmann (2005), Radiocarbon simulations for the glacial ocean: the effects of wind stress, Southern Ocean sea ice and Heinrich events. Earth and Planetary Science Letters, 235, 45-61.

Butzin, M., G. Lohmann, and T. Bickert (2011), Miocene ocean circulation inferred from marine carbon cycle modeling combined with benthic isotope records. Paleoceanogr., 26, PA1203, doi:10.1029/2009PA001901.

Cane, M., and P. Molnar (2001), Closing of the Indonesian seaway as a precursor to east African aridification around 3–4 million years ago. Nature, 411, 157-162.

Cannariato, K. G., and A. C. Ravelo (1997), Pliocene-Pleistocene evolution of eastern tropical Pacific surface water circulation and thermocline depth. Paleoceanogr., 12(6), 805–820, doi:10.1029/97PA02514.

Cessi, P., K. Bryan, and R. Zhang (2004), Global seiching of thermocline waters between the Atlantic and the Indian-Pacific Ocean Basins. Geophys. Res. Lett., Vol. 31, L04302, doi:10.1029/2003GL019091.

Chiang, J. C. H. (2009), The Tropics in Paleoclimate, Annu. Rev. Earth Planet. Sci., 37, 263–297. doi:10.1146/annurev.earth.031208.100217.

Collins, D. W., M. L. Blackmon, G. B. Bonan, J. J. Hack, T. B. Henderson, J. T. Kiehl, W. G. Large, and D. S. McKenna (2006), The Community Climate System Model Version 3 (CCSM3), J. Climate, 19, 2122-2143.

Dekens, P. S., A. C. Ravelo, and M. D. McCarthy (2007), Warm upwelling regions in the Pliocene warm period, Paleoceanography, 22, PA3211, doi:10.1029/2006PA001394.

Fedorov, A.V. and S. G. Philander (2001), A stability analysis of the tropical ocean-atmosphere interactions: Bridging Measurements of, and Theory for El Niño, J. Climate, 14, 3086-3101, doi: 10.1175/1520-0442(2001)014.

Fedorov, A.V., P. S. Dekens, M. McCarthy, A. C. Ravelo, P. B. deMenocal, M. Barreiro, R. C. Pacanowski and S. G. Philander (2006), The Pliocene Paradox (Mechanisms for a Permanent El Niño), Science, 312, 1485 – 1489, doi:10.1126/science.1122666.

Fedorov, A.V., C. M. Brierley, and K. Emanuel (2010), Tropical cyclones and permanent El Niño in the early Pliocene epoch, Nature, 463, 1066-1070, doi:10.1038/nature08831.

Goodman, P.J. (2001), Thermohaline adjustment and advection in an OGCM, J. Physical Oceanography, 31, 1477-1497, doi: 10.1175/1520-0485(2001)031.

Goosse H., and Fichefet T. (1999) Importance of the ice–ocean interactions for the global ocean circulation: a model study, J. Geophys. Res., 104(C10), 23,337–23,355, doi:10.1029/1999JC900215.

Gordon, C., C. Cooper, C.A. Senior, H. Banks, J.M. Gregory, T.C. Johns, J.F.B. Mitchell and R.A. Wood, (2000), The simulation of SST, sea ice extents and ocean heat transports in a version of the Hadley Centre coupled model without flux adjustments. Climate Dynamics, 16, 147-168.

Haarsma, R. J., Campos, E., Hazeleger, W., Severijns, C. (2008), Influence of the meridional overturning circulation on tropical Atlantic climate and variability. J. Climate, 21, 1403–1416.

Harrison, D.E. and G. A. Vecchi (2001), El Niño and La Niña: Equatorial Pacific surface temperature and thermocline variability, 1986-98, Geophys. Res. Lett., 28 ,1051-1054.

Haywood, A. M., P. J. Valdes, and V. L. Peck (2007), A permanent El Nino-like state during the Pliocene?, Paleoceanogr., 22, PA1213, doi:10.1029/2006PA001323.

Huang, R. X., M. A. Cane, N. Naik, and P. Goodman (2000), Global adjustment of the thermocline in response to deepwater formation, Geophys. Res. Lett., 27(6), 759–762.

Huybers, P., and P. Molnar (2007), Tropical cooling and the onset of North American glaciation, Clim. Past, 3, 549-557.

Jochum, M., B. Fox-Kemper, P. H. Molnar, and C. Shields (2009), Differences in the Indonesian seaway in a coupled climate model and their relevance to Pliocene climate and El Niño. Paleoceanogr., 24, PA1212, doi:10.1029/2008PA001678.

Kiehl, J. T., and P. R. Gent (2004), The Community Climate System Model, Version 2, J. Climate, 17, 3666-3682.

Lawrence, K.T., Z. H. Liu, and T. D. Herbert (2006), Evolution of the eastern tropical Pacific through Plio-Pleistocene glaciation, Science, 312, 79–83, doi:10.1126/science.1120395.

Lopes dos Santos, R. A., M. Prange, I. S. Castañeda, E. Schefuß, S. Mulitza, M. Schulz, E. M. Niedermeyer, J. S. Sinninghe Damsté, and S. Schouten (2010), Glacial-interglacial variability in Atlantic meridional overturning circulation and thermocline adjustments in the tropical North Atlantic. Earth Planet. Sci. Lett., 300, 407-414.

Lunt, D. J., P. J. Valdes, A. Haywood and I. C. Rutt (2008a), Closure of the Panama Seaway during the Pliocene: Implications for climate and Northern Hemisphere glaciation, Clim. Dyn., 30, 1–18, doi:10.1007/s00382-007-0265-6.

Lunt, D. J., G. L. Foster, A. M. Haywood, E. J. Stone (2008b), Late Pliocene Greenland glaciation controlled by a decline in atmospheric CO2 levels. Nature, 454, 1102-1105.

Maier-Reimer, E., U. Mikolajewicz, and K. Hasselmann, Mean circulation of the Hamburg LSG OGCM and its sensitivity to the thermohaline surface forcing, (1993), J. Phys. Oceanogr., 23, 731– 757

Marshall, J., A. Adcroft, C. Hill, L. Perelman, and C. Heisey, (1997), A finite-volume, incompressible Navier-Stokes model for studies of the ocean on parallel computers. J. Geophys. Res., 102(C3), 5753–5766.

McPhaden, M. J., and X. Yu (1999), Equatorial waves and the 1997–98 El Niño, Geophys. Res. Lett., 26(19), 2961–2964, doi: 10.1029/1999GL004901.

Molnar, P., and M. A. Cane (2002), El Niño's tropical climate and teleconnections as a blueprint for pre-Ice-Age climates, Paleoceanography, 17(2), doi:10.1029/2001PA000663.

Nisancioglu, K. H., M. E. Raymo, and P. H. Stone (2003), Reorganization of Miocene deep water circulation in response to the shoaling of the Central American Seaway, Paleoceanography, 18(1), 1006, doi:10.1029/2002PA000767.

Nof, D., and S. Van Gorder (2003), Did an open Panama Isthmus correspond to an invasion of Pacific water into the Atlantic? J. Phys. Oceanogr., 33, 1324–1336. doi: 10.1175/1520-0485(2003)033.

Nof, D., S. Van Gorder, and A.M. De Boer (2007), Does the Atlantic meridional overturning cell really have more than one stable steady state? Deep-Sea Res. I, 54 (11), 2005-2021.

Opsteegh, J.D. R.J. Haarsma, and F.M. Selten, (1998), ECBilt: A dynamic alternative to mixed boundary conditions in ocean models. Tellus, 50A, 348-367.

Park, W., Keenlyside, N., Latif, M., Stroeh, A., Redler, R., Roeckner, E. and Madec, G. (2009), Tropical Pacific climate and its response to global warming in the Kiel Climate Model. J. Climate, 22, 71–92. doi:10.1175/2008JCLI2261.1

Prange, M., G. Lohmann, and A. Paul, (2003), Influence of vertical mixing on the thermohaline hysteresis: Analyses of an OGCM. Journal of Physical Oceanography, 33(8), 1707-1721.

Prange, M., and M. Schulz (2004), A coastal upwelling seesaw in the Atlantic Ocean as a result of the closure of the Central American Seaway. Geophys. Res. Lett., 31, L17207, doi:10.1029/2004GL020073.

Prange, M., (2008), The low-resolution CCSM2 revisited: new adjustments and a present-day control run. Ocean Science, 4, 151-181.

Ravelo, A. C., D.H. Andreasen, M. Lyle, A. O. Lyle, and M. W. Wara (2004), Regional climate shifts caused by gradual global cooling in the Pliocene epoch, Nature, 429, 263–267, doi:10.1038/nature02567.

Sarnthein, M., G. Bartoli, M. Prange, A. Schmittner, B. Schneider, M. Weinelt, N. Andersen, and D. Garbe-Schönberg (2009), Mid-Pliocene shifts in ocean overturning circulation and the onset of Quaternary-style climates. Clim. Past, 5, 269-283.

Schmittner, A., and A. J. Weaver (2001), Dependence of multiple climate states on ocean mixing parameters. Geoph. Res. Lett., 28, 1027-1030.

Schneider, B., and A. Schmittner (2006), Simulating the impact of the Panamanian seaway closure on ocean circulation, marine productivity and nutrient cycling, Earth Planet. Sci. Lett., 246, 367–380, doi:10.1016/j.epsl.2006.04.028.

Steph, S., R. Tiedemann, M. Prange, J. Groeneveld, D. Nürnberg, L. Reuning, M. Schulz, and G. Haug (2006a), Changes in Caribbean surface hydrography during the Pliocene shoaling of the Central American Seaway. Paleoceanography, 21, PA4221, doi:10.1029/2004PA001092.

Steph, S., R. Tiedemann, J. Groeneveld, A. Sturm, and D. Nürnberg (2006b), Pliocene changes in tropical East Pacific upper ocean stratification: Response to tropical gateways?, Proc. Ocean Drill. Program Sci. Results, 202, 1-51.

Steph, S., R. Tiedemann, M. Prange, J. Groeneveld, M. Schulz, A. Timmermann, D. Nürnberg, C. Rühlemann, C. Saukel, and G. H. Haug (2010), Early Pliocene increase in thermohaline overturning: A precondition for the development of the modern equatorial Pacific cold tongue, Paleoceanography, 25, PA2202, doi:10.1029/2008PA001645.

Timmermann, A., S.-I. An, U. Krebs, and H. Goosse (2005), ENSO suppression due to weakening of the North Atlantic thermohaline circulation, J. Climate, 18, 3122–3139, doi: 10.1175/JCLI3495.1

Timmermann, A., Y. Okumura, S.-I. An, A. Clement, B. Dong, E. Guilyardi, A. Hu, J. H. Jungclaus, M. Renold, T. F. Stocker, R. J. Stouffer, R. Sutton, S.-P. Xie, and J. Yin, (2007), The influence of a weakening of the Atlantic Meridional Overturning Circulation on ENSO, J. Clim., 20, 4899–4919, doi: 10.1175/JCLI4283.1

Tziperman, E., and B. Farrell (2009), Pliocene equatorial temperature: Lessons from atmospheric superrotation, Paleoceanogr., PA1101, doi:10.1029/2008PA001652.

Vecchi, G. A., B. J. Soden, A. T. Wittenberg, I. M. Held, A. Leetmaa, and M. J. Harrison (2006), Weakening of tropical Pacific atmospheric circulation due to anthropogenic forcing. Nature, 441, 73-76.

Vecchi, G. A., and B. J. Soden, (2007), Global Warming and the Weakening of the Tropical Circulation, J. Clim., 20, 4316–4340, doi: 10.1175/JCLI4258.1.

Vizcaíno, M., S. Rupper, and J. C. H. Chiang (2010), Permanent El Niño and the onset of Northern Hemisphere
glaciations: Mechanism and comparison with other hypotheses, Paleoceanography, 25, PA2205, doi:10.1029/2009PA001733.

Wara, M. W., A. C. Ravelo, and M. L. Delaney (2005), Permanent El Niño-Like Conditions During the Pliocene Warm Period, Science, 309, 758-761, doi: 10.1126/science.1112596.

Watanabe, T., et al. (2011), Permanent El Nino during the Pliocene warm period not supported by coral evidence. Nature, 471, 209-211.

Weaver, A. J., and Coauthors, (2001), The UVic Earth System Climate Model: Model description, climatology and application to past, present and future climates. Atmos.–Ocean, 39, 361–428.

Yeager, S.G., Shields, C.A., Large, W.G., and Hack, J.J., (2006), The low-resolution CCSM3. J. Clim. 19, 2545–2566.

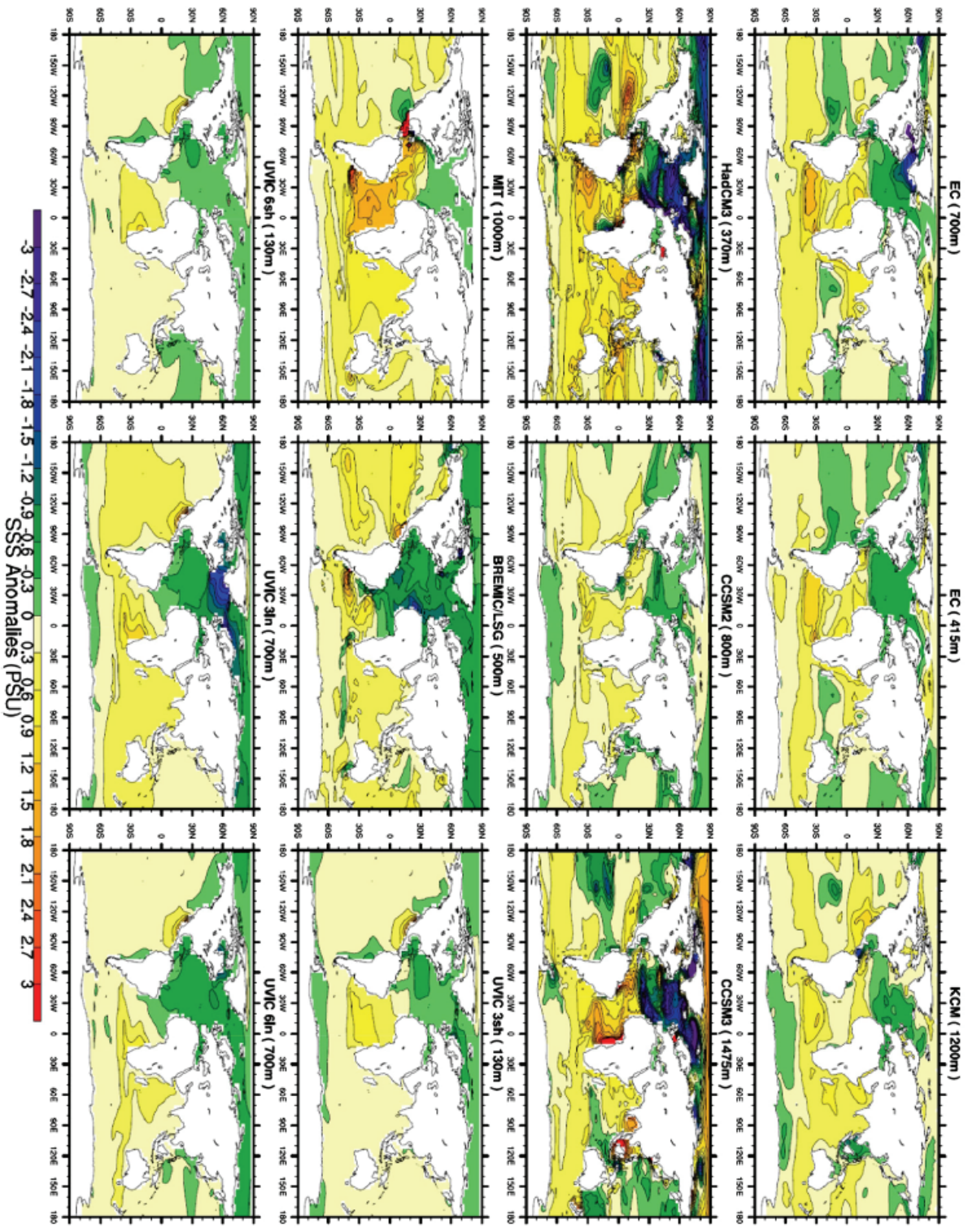

Fig. 1. Effect of an open Panamanian seaway on global sea surface salinity (SSS): Difference in SSS (psu) between runs with open and closed Panama gateway (i.e. open minus closed) in the various models. The depth of the seaway in the different experiments is given in parentheses.

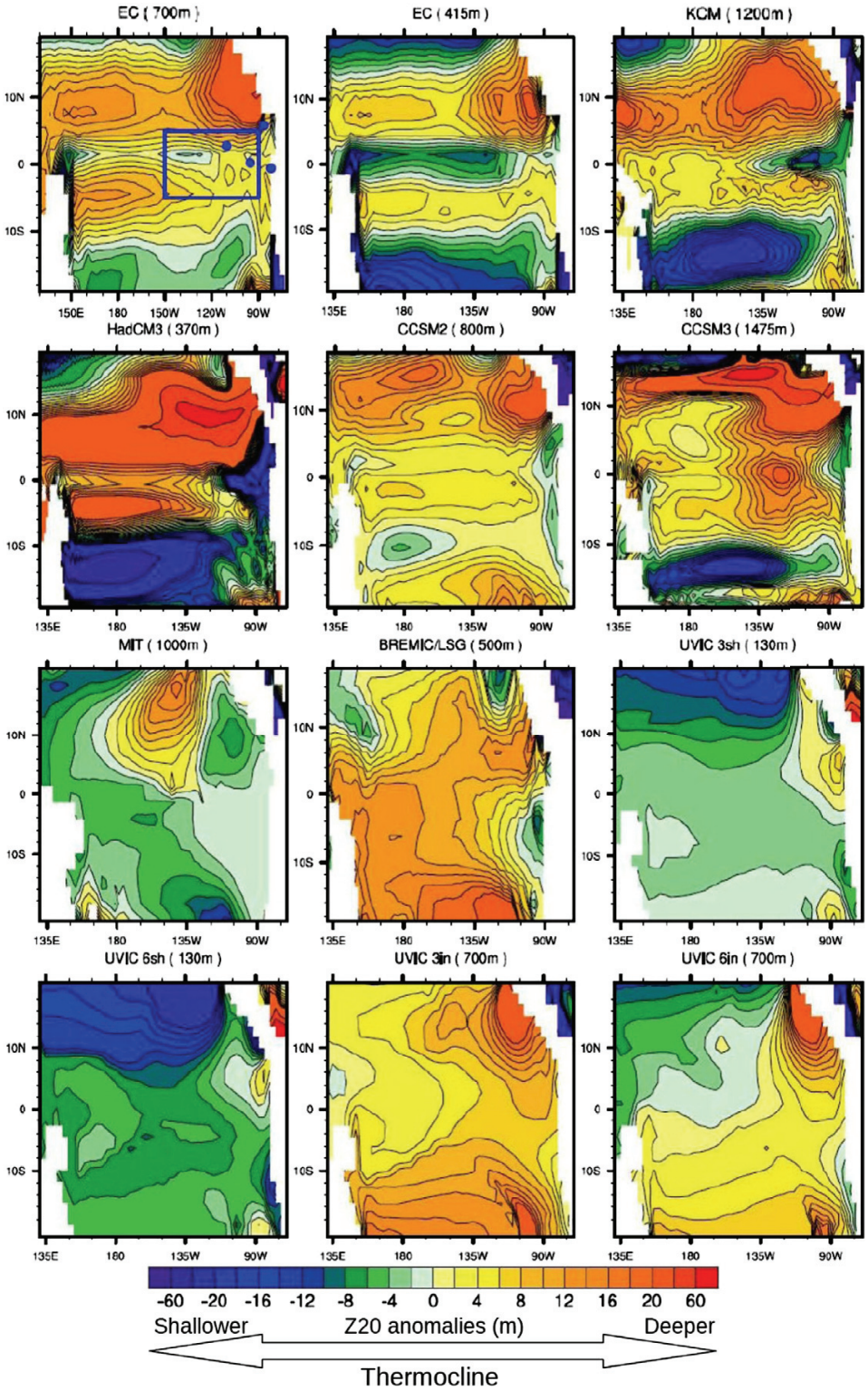

Fig. 2. Effect of an open Panamanian seaway on the equatorial Pacific thermocline: Difference in the depth of the 20 °C isotherm (Z20) between runs with open and closed Panama gateway (i.e. open minus closed) in the various models. The blue box marks the Niño-3 region. The blue dots indicate the locations of sediment cores from which Pliocene tropical thermocline shoaling has been inferred (Cannariato and Ravelo, 1997, Steph et al., 2006b, Steph et al., 2010 and Wara et al., 2005). The depth of the seaway in the different experiments is given in parentheses.

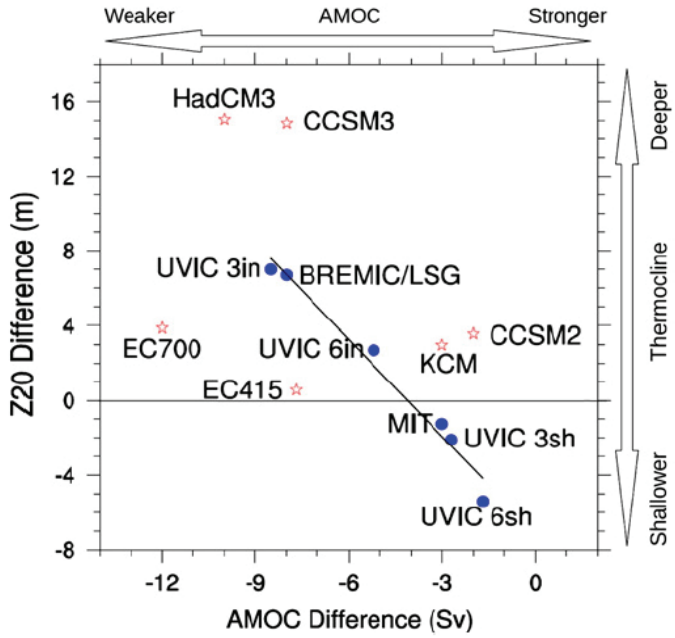

Fig. 3. Effect of an open Panamanian seaway on the eastern equatorial Pacific thermocline and AMOC strength. “Z20 difference” refers to the difference in the depth of the 20 °C isotherm in the Niño-3 region (i.e. averaged over the region 150°W–90°W, 5°N–5°S) between runs with open and closed Panama gateway (i.e. open minus closed), while “AMOC difference” refers to the change in the North Atlantic overturning streamfunction maximum (open minus closed) in the various models. The dots mark models without wind-stress feedback, whereas models that include a dynamic atmosphere are marked by stars. The regression line has been calculated by only taking the models without wind-stress feedback into account.

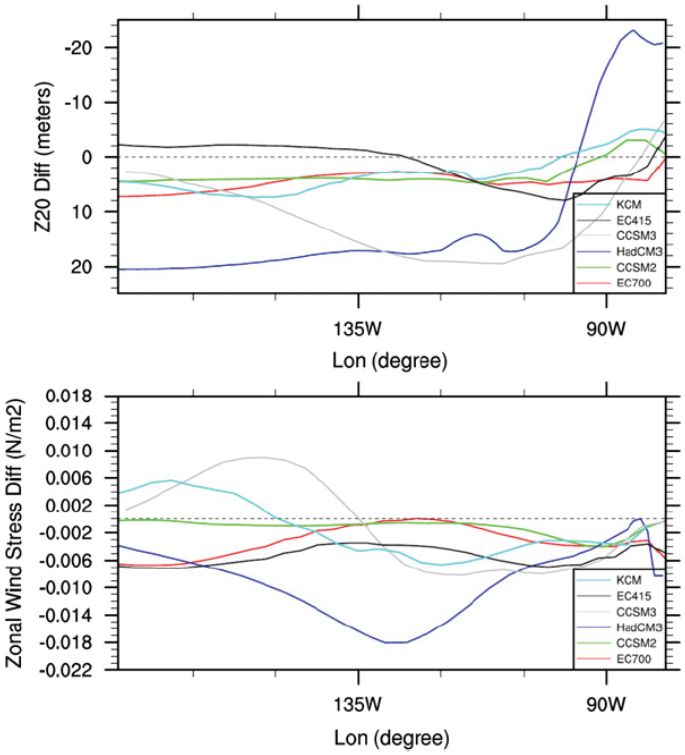

Fig. 4. Effect of an open Panamanian seaway on equatorial Pacific thermocline depth and zonal wind-stress (both averaged over 5°N–5°S) in models that include a dynamic atmosphere. “Z20 diff” refers to the difference in the depth of the 20 °C isotherm between runs with open and closed Panama gateway (i.e. open minus closed), while “Zonal Wind Stress Diff” refers to the change in equatorial Pacific zonal wind-stress (open minus closed) in the various models.

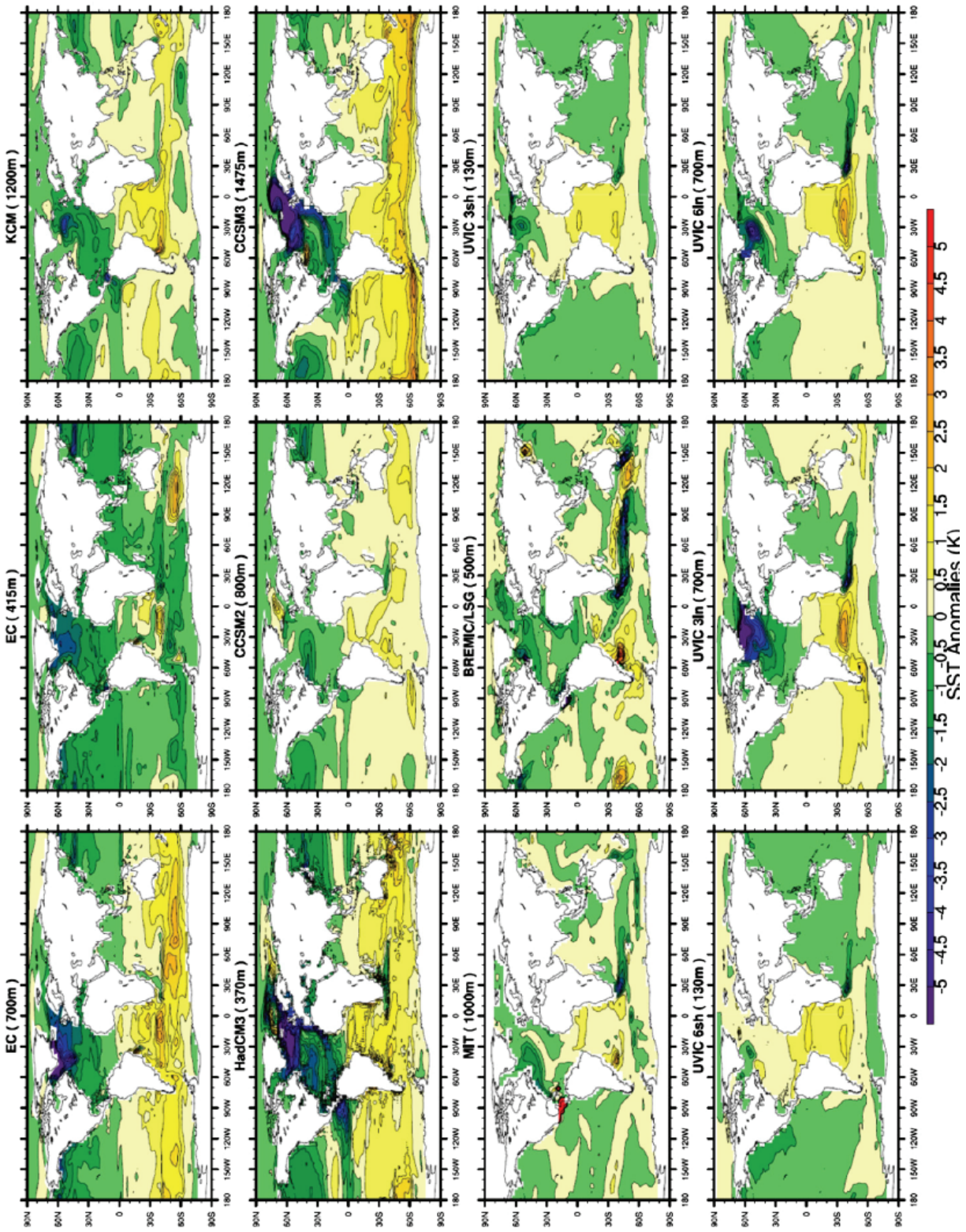
EC (700m)
EC (415m)
KCM (1200m)
HadCM3 (370m)
CCSM2 (800m)
CCSM3 (1475m)
MIT (1000m)
BREMC/LSG (500m)
UVIC 3sh (130m)
UVIC 6sh (130m)
UVIC 3ln (700m)
UVIC 6ln (700m)
SST Anomalies (K)
-5 -4.5 -4 -3.5 -3 -2.5 -2 -1.5 -1 -0.5 0 0.5 1 1.5 2 2.5 3 3.5 4 4.5 5

Fig. 5. Effect of an open Panamanian seaway on global sea surface temperature (SST): Difference in SST (K) between runs with open and closed Panama gateway (i.e. open minus closed) in the various models. The depth of the seaway in the different experiments is given in parentheses.

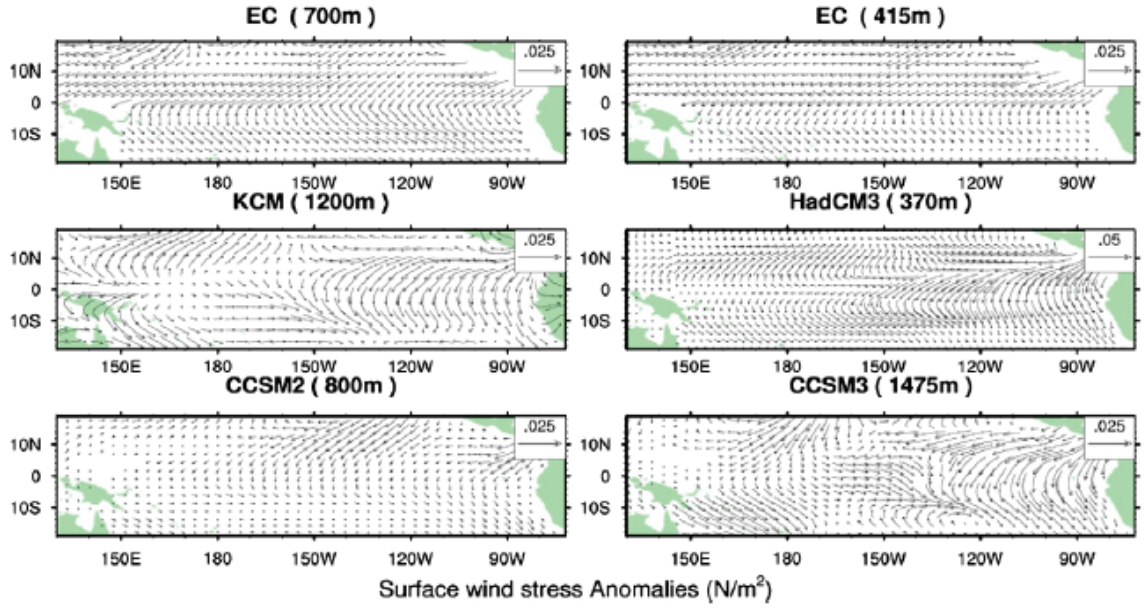

Fig. 6. Effect of an open Panamanian seaway on tropical Pacific surface wind stress: Difference in surface wind stress (N/m^2) between runs with open and closed Panama gateway (i.e. open minus closed) in the various models that include a dynamic atmosphere. Note the different reference scale of HadCM3 experiment. The depth of the seaway in the different experiments is given in parentheses.

5. Summaries and Outlook

5.1 Summaries

This thesis focused on AMOC stability and climate responses to an altered AMOC through two approaches: 1) freshwater forcing experiments in a state-of-the-art climate model with MIS3 background climate and 2) compare results from different climate models simulating Panamanian Seaway's final closure during the early Pliocene, which might affect the AMOC strength and changed global ocean circulation pattern. The first important objective is to study the AMOC stability property in a colder background climate compare to present day (38 ka BP), since it was suggested that the AMOC might in a more sensitive mode and have multiple equilibrium during cold stadial, which has never showen in a state-of-the-art climate model. The second objective is to obtain a picture of global climate footprint as response to freshwater forcing at the Nordic Seas. In such way, it is possible to provide preferable locations for the AMOC reconstruction. More importantly, combning model simulations and proxy records, insterstadial-stadial AMOC strength change was estimated. Questions proposed in Chapter 1 are answered as below:

1) Is the AMOC in a multiple equilibrium state or a monostable state if we apply glacial boundary conditions in a state-of-the-art coupled model through freshwater hosing/extraction experiments?

According our CCSM3 freshwater hosing/extraction experiment results, the AMOC is in a monostable mode during MIS3. The AMOC maximum showed a linear relationship to the freshwater forcing at the Nordic Seas (Chapter 2). Larger positive freshwater injection caused a stronger deduction of the AMOC and larger negative freshwater flux resulted in a more strengthened AMOC. The AMOC strength changes occurred rapidly (less than 200 model years) within a range between +0.02 Sv and -0.02 Sv amount of freshwater input and there was obvious threshold behaviour of Northern Hemisphere sea ice cover as response to freshwater perturbations. Consisting with previous model studies, most of state-of-the-art climate model showed a monostable AMOC in hosing experiments whereas most of the simpler models showed a bistable or multiple stable AMOC.

2) How does global climate system response to North Atlantic freshwater perturbation in such model setups? Is glacial background climate able to improve the model results compare to observations?

As it was shown in chapter 2, the AMOC maximum responsed almost linearly to freshwater flux and a larger freshwater flux into the North Atlantic generally caused a stronger global climate response. Summarizing all the twelve freshwater tests, global climate was clearly in two different states. One is a cold stadial state with profound extension of Northern Hemisphere sea ice and particular low surface temperature at the North Atlantic. The other is a mild interstadial climate state with much less sea ice and mild surface temperature. The relative unstable MIS3 baseline state showed an abrupt deduction of the AMOC strength when freshwater injection exceeded a threshold (+0.02 Sv). As response to a weakened AMOC, equator-to-pole heat transport was reduced as well and global surface temperature showed a clear bipolar seesaw pattern, which was shown in both observations and model simulations (e.g. Broecker 1998; Stocker 1998; Stocker and Johnson 2003). Deep convection was also shut down when the freshwater exceeded +0.02 Sv and there was a great expansion of the sea ice cover at the Nordic Seas during winter. Greenland temperature reduction in our simulation is consist with observations during the D-O events and we suggest that Greenland surface temperature is primarily controlled by Nordic Sea ice cover since an increasing of freshwater injection did not cause a further cooling at Greenland. Lastly, we also observed other climate responses e.g. a southward shift of the ITCZ and a strong subsurface warming in the North Atlantic, which were shown in many other hosing experiments (e.g. Broccoli et al. 2006; Stouffer et al. 2006).

3) By applying statistical test, is it possible to locate areas, which are sensitive or even have linear temperature responses to the AMOC strength variation, since such information is helpful for the AMOC reconstruction? Are these statistical results consistent with observations?

Based on simulation and statistical results, the following surface areas showed strongest linear relation between the AMOC strength change and temperature variation: North Atlantic and southern Indian Ocean. This high temperature sensitivity to the AMOC change was also suggested by very recent studies. On the other hand, most of the tropical areas did not show a linear regression. Southern Atlantic and tropical Indian Ocean showed high linear relationship between ocean temperature and the AMOC strength variations in the shallow layers in the ocean. This linear regression spread to global ocean except mid-latitude Pacific at around 600m depth. And there was strong subsurface warming in the North Atlantic as proxy records and model simulations suggested.

4) Is it possible to estimate the AMOC strength variations between cold stadial and warm interstadial based on the simulations? Was the AMOC greatly deducted during the Heinrich statial compare to interstadial?

By combining proxy records and model simulations, the estimated change in the AMOC strength between interstadial and stadial state is 10.4 +(-) 1.6 Sv in this study. Though the estimated error is much smaller than previous study, more proxy records as well as model-data assimulation have the potential to improve this estimation. With regard to AMOC deduction during the HE stadial, the estimation error is quite large since proxy records are quite limited. The possibility of an active AMOC cannot be ruled out based on this estimation.

5) How does the AMOC response to closure of the Panamanian Seaway?

All the models in the model comparison study showed an eastward Panamanian through flow that leads to a reduction of the AMOC in the open Seaway circumstance (Steph et al. 2010) due to freshwater transport from the Pacific to the Atlantic.

6) Does the Pacific thermocline show shoaling or deepening as response to the Seaway closure? Is this shoaling/deepening model dependent? How does wind system involved in this process?

A stronger AMOC was shown when the Seaway is closed and such increased circulation could cause a shoaling of global thermocline and a northward shift of the ITCZ in all the models a result of oceanic adjustment (Lunt et al. 2008; Steph et al. 2006; Steph et al. 2010). Wind stress feedback amplified the change in thermocline depth in the Pacific when a dynamic atmosphere component was included in the model; whereas models without a dynamic atmosphere showed an almost linear response of thermocline shoaling to the strengthening of the AMOC.

5.2 Outlook

5.2.1 The AMOC stability during pre-industrial and MIS3

Our results strongly support the conclusion that the MIS3 baseline AMOC is possiblely monostable. However, as it is shown in Chapter 2, the AMOC requires almost 1500 model years to reach an equilibrium state. Such long integration was not performed under pre-industrial climate and freshwater tests are also not presented. In this sense, it is difficult to compare the AMOC stability in a colder climate to present day. The AMOC related study should involve its predictability and its possible variations in the future. Hence, it would be ideal to perform pre-industrial control and freshwater

hosing/extraction tests in CCSM3 with the same integration time so that the results would be comparable and provide proper predictive information. Furthermore, the reanalysis and atmosphere data from present day show a negative value of Fov (net freshwater import by the overturning circulation in the Atlantic, e.g. Doblas-Reyes et al. 2009), indicating multiple equilibria of the AMOC, which is controversy with most of the coupled model studies (e.g. Drijfhout et al. 2011). This could either due to observation flaws or model deficiencies. Thus, more observations, especially from the Southern Hemisphere can provide useful information to determine the AMOC stability in the future, since a strong coupling of surface temperature at the North Atlantic and the Southern Ocean as well as coupling of deep water formation between these two sides is shown.

5.2.2 The driving process of the AMOC

It is still not clear whether surface wind or thermohaline process is the dominant driver of the AMOC. The AMOC is considered mainly thermohaline driven in this study since the model was forced with freshwater forcing in ocean surface. In other circumstances, if the AMOC is wind dominated, its strength should be quite sensitive to wind stress at the Southern Ocean. Sijp and England (2009) showed an AMOC that strongly affected by the Southern Ocean winds whereas Rahmstorf and England (1997) argued the effect of the wind field to the AMOC is only moderate. Hence, it is preferable that we further perform sensitivity tests forced by both wind observations and fixed surface wind field with long model integration time. Such sensitivity tests can provide information about how strongly surface wind can affect the AMOC.

5.2.3 Boundary conditions in the model

The relation between the HEs and the AMOC strength was intensively studied in climate models; however, there is no firm coherent change in the AMOC during the D-O cycles. Though Clark et al. (2007) proposed that AMOC changes produced the D-O cycle during MIS3, it is still difficult to distinguish the AMOC deduction during the HE stadials and non-HE stadials. Due to the fact that D-O events were more profound during the early stage of MIS3 than the late stage and also background climate has a great potential to affect the AMOC stability in the model. It would be helpful to perform both baseline and freshwater forcing model simulations during the early, middle and late stage of MIS3. In such a way, it is possible to study boundary condition effects within MIS3 e.g. solar forcing and therefore distinguish the AMOC behaviour during the HE cycles and non-HE cycles.

5.2.4 Threshold of the system

Our simulations showed threshold behaviour in the AMOC strength, the Northern Hemisphere ice cover and Greenland temperature as response to freshwater flux between +0.01 Sv and +0.02 Sv. If computational resource allows, it would be interesting to narrow down the threshold region, e.g. performing experiments with +0.015 Sv freshwater injection, since it could provide information for the AMOC reconstruction. In the mean time, such experiments care able to investigate the existence of hysteresis behaviour in the AMOC in CCSM3.

References:

Arz, H.W., J. Patzold, and G. Wefer, (1998), Correlated millennial-scale changes in surface hydrography and terrigenous sediment yield inferred from last-Glacial marine deposits off Northeastern Brazil, Quat. Res., 50, 157–166.

Broccoli, A. J., K. A. Dahl, and R. J. Stouffer, (2006), Response of the ITCZ to Northern Hemisphere cooling, Geophys, Res. Lett., 33, L01702, doi:10.1029/2005GL024546.

Broecker, W. S., (1998), Paleocean circulation during the last deglaciation: A bipolar seesaw?, Paleoceanography, 13, 119–121.

Clark, P.U., S.W. Hostetler, N.G. Pisias, A. Schmittner, and K.J. Meissner, (2007), Mechanisms for a ~7-kyr climate and sea-level oscillation during marine isotope stage 3. In: Ocean Circulation: Mechanisms and Impacts, Geophys. Monogr. Ser., 173, 209–246, AGU, Washington, D. C.

Doblas-Reyes, F. J., A. Weisheimer, M. Deque, N. Keenlyside, M. McVean, J. M. Murphy, P. Rogel, D. Smith, and T. N. Palmer, (2009), Addressing model uncertainty in seasonal and annual dynamical ensemble forecasts, Q. J. R. Meteorol. Soc., 135(643), 1538–1559, doi:10.1002/qj.464.

Drijfhout, S. S., S. L. Weber, and E. van der Swaluw, (2011), The stability of the MOC as diagnosed from model projections for pre-industrial, present and future climates, Clim. Dyn., doi:10.1007/s00382-010-0930-z.

Lunt, D. J., P. J. Valdes, A. Haywood, and I. C. Rutt, (2008), Closure of the Panama Seaway during the Pliocene: Implications for climate and Northern Hemisphere glaciation, Clim. Dyn., 30, 1 – 18, doi:10.1007/s00382-007-0265-6.

Rahmstorf, S. and M. H. England, (1997), The influence of southern hemisphere winds on North Atlantic deep water flow, J. Phys. Oceanogr., 27, 2040-2054.

Porter, S. C., and Z. S. An, (1995), Correlation between climate events in the North Atlantic and China during the last glaciation, Nature, 375, 305–308.

Rohling, E.J., A. Hayes, D. Kroon, S. De Rijk, and W. J. Zachariasse, (1998), Abrupt cold spells in the NW Mediterranean, Paleoceanography ("Currents"), 13, 316-322.

Sijp, Willem P., Matthew and H. England, (2009), Southern Hemisphere Westerly Wind Control over the Ocean's Thermohaline Circulation, J. Climate, 22, 1277–1286.

Steph, S., R. Tiedemann, J. Groeneveld, A. Sturm, and D. Nürnberg, (2006), Pliocene changes in tropical East Pacific upper ocean stratification: response to tropical gateways? Proc. Ocean Drill. Program Part B Sci. Results, 202, 1–51.

Steph, S., R. Tiedemann, M. Prange, J. Groeneveld, M. Schulz, A. Timmermann, D. Nürnberg, C. Rühlemann, C. Saukel, and G.H. Haug, (2010), Early Pliocene increase in thermohaline overturning: a precondition for the development of the modern equatorial Pacific cold tongue, Paleoceanography 25, PA2202, doi:10.1029/2008PA001645.

Stocker, T. F., (1998), The seesaw effect, Science, 282,61–62.

Stocker, T. F., and S. J. Johnsen, (2003), A minimum thermodynamic model for the bipolar seesaw, Paleoceanography, 18(4), 1087,doi:10.1029/2003PA000920.